PHYSICAL AND CHEMICAL PERFORMANCE TESTING OF ONTARIO ASPHALT PAVEMENTS

by

IMAD UBAID

A thesis submitted to the Department of Chemistry

In conformity with the requirements for

the degree of Masters of Science

Queen's University

Kingston, Ontario, Canada

(September 2016)

Abstract

Thermal and fatigue cracking are the two of the major pavement distress phenomena that contribute significantly towards increased premature pavement failures in Ontario. This in turn puts a massive burden on the provincial budgets as the government spends huge sums of money on the repair and rehabilitation of roads every year. Governments therefore need to rethink and re-evaluate their current measures in order to prevent it in future. The main objectives of this study include: the investigation of fatigue distress of 11 contract samples at 10^{o}C, 15^{o}C, 20^{o}C and 25^{o}C and the use of crack-tip-opening-displacement (CTOD) requirements at temperatures other than 15^{o}C; investigation of thermal and fatigue distress of the comparative analysis of 8 Ministry of Transportation (MTO) recovered and straight asphalt samples through double-edge-notched-tension test (DENT) and extended bending beam rheometry (EBBR); chemical testing of all samples though X-ray Fluorescence (XRF) and Fourier transform infrared analysis (FTIR); Dynamic Shear Rheometer (DSR) higher and intermediate temperature grading; and the case study of a local Kingston road. Majority of 11 contract samples showed satisfactory performance at all temperatures except one sample. Study of CTOD at various temperatures found a strong correlation between the two variables. All recovered samples showed poor performance in terms of their ability to resist thermal and fatigue distress relative to their corresponding straight asphalt as evident in DENT test and EBBR results. XRF and FTIR testing of all samples showed the addition of waste engine oil (WEO) to be the root cause of pavement failures. DSR high temperature grading showed superior performance of recovered binders relative to straight asphalt. The local Kingston road showed extensive signs of damage due to thermal and fatigue distress as evident from DENT test, EBBR results and pictures taken in the field. In the light of these facts, the use of waste engine oil and recycled asphalt in pavements should be avoided as

these have been shown to cause premature failure in pavements. The DENT test existing CTOD requirements should be implemented at other temperatures in order to prevent the occurrences of premature pavement failures in future.

Acknowledgements

First and foremost, I would like to offer my great thanks and gratitude to God Almighty for all his blessings that he bestowed on me and my family.

I would like to offer my sincere thanks and gratitude to my supervisor Dr. Simon A.M. Hesp for his continued support and guidance throughout the period of my degree. I think it was a rewarding opportunity of my career to work under his guidance. He continued to be a source of great inspiration and knowledge throughout this period of study. His advice, guidance and tips during my thesis writing and especially regarding my future career prospects have helped me significantly towards my professional development. I would also like to offer special thanks to my supervisory committee members Dr. Donal Macartney and Dr. Guojun Liu for their constructive feedback regarding my thesis and my research work.

Sincere thanks and gratitude goes to my colleague and my great friend Yamnath Gotame for his continued support and help throughout this degree. I would also like to thank my former colleagues Migle Paliukaite, David Sowah Kuma and Ben Rudson for their assistance and support during our training in laboratory equipment, procedures and protocols. I would like to offer special thanks to Dr. Herbert Shurvell for his assistance and guidance during X-ray fluorescence (XRF) testing of my samples.

Special thanks goes to all faculty members and staff in the Chemistry Department for their assistance during this study period.

In the end, I would like to thank my parents Mr. Ubaid-us-Salam and Mrs. Nuzhat Bajwa for their continued support throughout this period. In fact, special thanks and gratitude goes to my mother for her immense support and encouragement towards the completion of my degree in

spite of her hardships and pain that she endured during her entire cancer treatment process. It was her support and encouragement that motivated me to continuously work hard throughout this study period.

Table of Contents

List of Figures

List of Tables

List of Abbreviations

AASHTO	American Association of State and Highway Transportation Officials
ASTM	American Society for Testing and Materials
BBR	Bending Beam Rheometer
CTOD	Critical Crack Tip Opening Displacement
C-SHRP	Canadian Strategic Highway Research Program
DENT	Double-Edge-Notched Tension
DSR	Dynamic Shear Rheometer
DTT	Direct Tension Test
EBBR	Extended Bending Beam Rheometer
EWF	Essential Work of Fracture
FTIR	Fourier Transform Infrared
GPa	Giga Pascal
G*	Complex Shear Modulus
HMA	Hot Mix Asphalt
kPa	Kilo Pascal
keV	Kilo Electrovolt
mN	Mili Newton
MTO	Ministry of Transportation of Ontario
PAV	Pressure Aging Vessel
PCC	Portland cement concrete
PG	Performance Grade
PI	Penetration Index

PIB	Polyisobutylene
RAP	Recycled Asphalt Pavement
RTFO	Rolling Thin Film Oven
SBS	Styrene Butadiene Styrene
Superpave	Superior Performing Pavements
SHRP	Strategic Highway Research Program
T_g	Glass transition temperature
Wt	Total Work of Fracture
W_e	Essenital work of Fracture
WEO	Waste Engine Oil
W_p	Plastic Work of Fracture
XRF	X-Ray Fluorescence

Chapter 1

Introduction

1.1 Overview

Thermal and fatigue cracking are two of the major pavement distresses that have contributed significantly to the increase in premature pavement failures seen in Ontario in recent years. Thermal cracking occurs as a result of varying factors and causes [31]. These factors include: the stiffness of asphalt could be too high for a given climatic zone, traffic loading and subsequent excessive flexing of the surface in thin asphalt pavements can contribute to transverse cracking, asphalt cement content can be too low allowing oxygen and water to readily enter the pavement, and a range of other less important factors [16-27,31]. When the surface temperature falls in winter, the asphalt mixture attempts to contract. This contraction is somewhat allowed across the pavement but rather prevented along the length of the pavement due to the presence of restraints in that direction [31]. If the total thermal stress resulting from all contributing factors is taken into account, it occurs in both longitudinal and transverse directions. If this stress reaches a certain critical limit, the pavement suffers in the form of cracks appearing in weak areas such as joints, shoulders or segregated spots. These occur due to inadequate movement as the granular base is frozen during cold weather. When the first snow melts, these small visible cracks transform to form larger cracks as the base moves to facilitate the opening of the damaged pavement. These cracks can occur across or along the pavement or can be present in both directions based on how thick the pavement is, how much care was taken

to prevent segregation during construction, improper drainage, the absolute minimum temperature reached and the age of the pavement itself [9, 28-30, 31].

Small weak spots and areas of stress concentration that are related to longitudinal cracks can give rise to the growth of transverse cracks in subsequent winters [31]. The formation of cracks continues until thermal stresses no longer exceed the tensile strength of the mixture. Eventually, there is a limiting value, which the pure thermal stress cannot exceed. It is based on the strength of the pavement material, the friction with the granular base and the level to which the asphalt cement is under-designed for a particular climatic condition. In the long run, the pavement needs reconstruction and repair as the chemical and physical aging of the cement increases the rate of thermal and fatigue cracking.

Due to concern about the competition from the Portland cement concrete (PCC), "asphalt producers are driven to use low cost modification technologies for their products." [31] These modification technologies are often implemented without the use of performance-based field trials and specifications. In the absence of these protocols, these measures present a potential liability in the long run. In 1987, the Superpave™ binder specification system was introduced as a part of Strategic Highway Research Program (SHRP). These new protocols aimed at specifying asphalt binders with a 98% reliability that the "road surface would not crack." [31] However, it has been widely recognized that with only a few exceptions, the vast majority of binders that are graded under the Superpave pavement specification system, failed prematurely [1-14, 31].

The problems with Superpave were recognized in its early stages of development, when the two Canadian Strategic Highway Research Program (C-SHRP) trials in Hearst, Ontario, and Lamont, Alberta, showed cracking severities that differed by a factor of 20 and 30, respectively, for asphalt cements of nearly the same low temperature grade [1, 4-6, 9 ,11, 31]. As a result, the Ontario Ministry of Transportation (MTO) initiated a program for the development of improved low temperature and fatigue specification tests. As a result of this effort, the double-edge-notched tension-test (DENT) and extended bending beam rheometer test (EBBR) were developed as an improvement over previously used direct tension test (DTT) and bending beam rheometer (BBR) test [31]. Testing of asphalt samples in their ductile state added reproducibility to the DENT test. By adding additional conditioning times of 24 and 72 hours to the original BBR test, the ability of the binders to resist thermal and fatigue stresses after appropriate cold conditioning was better assessed.

The aim of this thesis is to investigate the ductility and the ability of 10 Ministry of Transportation of Ontario (MTO) samples through DENT test at 10, 15, 20 and 25 degrees Celsius. Apart from these 10 MTO samples, this study seeks to investigate the root causes of premature failures through DENT testing and EBBR analysis of 8 MTO recovered and tank asphalt binder samples. In addition to these investigations, previous case study of premature failure involving local road in Kingston Ontario, has also been included as a part of this thesis.

1.2 Asphalt and its Origins

Asphalt has many names. These names are based on the nature of its application, source, location and a particular time in history. It is known as bitumen in Europe, "*Until the start of the 20th century, it was termed as Asphaltium.* [32] *The term was derived from Ancient Greece "Asphaltos"."* [32] It can be a solid or semi-solid at room temperature or it can be liquefied by heating or by emulsifying it in petroleum solvents. It can act as an effective adhesive and a waterproofing agent and has as such been known to man for a very long time [33]. Asphalt is primarily used in road construction as a binder mixed with aggregate particles to give asphalt concrete. Its secondary use is for bituminous waterproofing products for production of roofing felt and for the sealing of flat roofs [34].

Asphalt in nature is found in naturally occurring asphalt lakes, hardened after exposure to the elements. These lakes are left behind by surface accumulation of petroleum forced upward by geological deposits [33]. These asphalt lakes can be found on the island of Trinidad off the northern cost of Venezuella and at the La Brea 'Tar" Pits near Los Angeles. Another natural source of asphalt includes porous rocks such as sandstone or limestone impregnated with asphalt. The asphalt from this source is called rock asphalt. Naturally occurring asphalt has been used as a road-construction and waterproofing material for thousands of years by many known civilizations. These include ancient Babylonians, Egyptians, Greeks and Romans. Despite its extensive use in history, its

current application as a major ingredient in paving material did not start until the development of modern petroleum refining techniques in the early 1900s

1.3 Pavement

A pavement can be classified into two categories; a rigid and a flexible pavement. Rigid pavements are the pavements that primarily consist of Portland cement concrete (PCC). They do not necessarily have a base and sub-base course [35]. On the contrary; the flexible pavement has asphalt as its primary building material. A flexible pavement contains a thin wearing surface of asphalt constructed over a base course and a sub-base course. These layers are made up of gravel or stone and reside on a compacted subgrade. The following Figure 1 further illustrates a difference between two pavements.

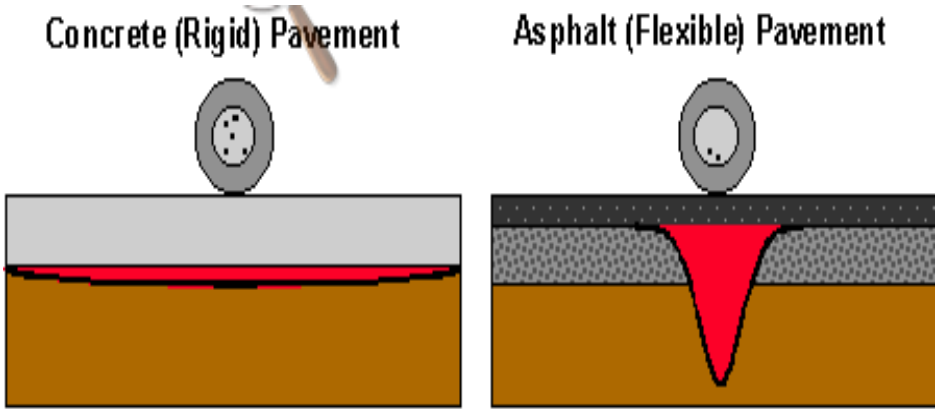

Figure 1. Differences between Rigid and Flexible Pavements [35].

Hot Mix Asphalt (HMA) pavements are flexible as mentioned above, as the overall pavement structure deflects under loading [36]. This pavement structure consists of

several layers of material. Each of these layers gets the load from its top layer, distributes it, and then transmits it to the bottom layer.

HMA pavement consists of many layers as illustrated in Figure 2 [37]. The bottom layer is the existing soil or subgrade. The subgrade is also called the base lift. The layer on the top of the subgrade is an aggregate base course which is sometimes stabilized with asphalt, cement or fly-ash. The layer on the top of the aggregate base course is the asphalt pavement layer. The wearing course or the top layer of the pavement is "responsible for smooth driving experience and adequate skid resistance." The wearing course is made with a smaller sized aggregate then the asphalt base course, which is responsible for the tight and closed surface texture in order to prevent the penetration of moisture and other weather elements into the pavement structure.

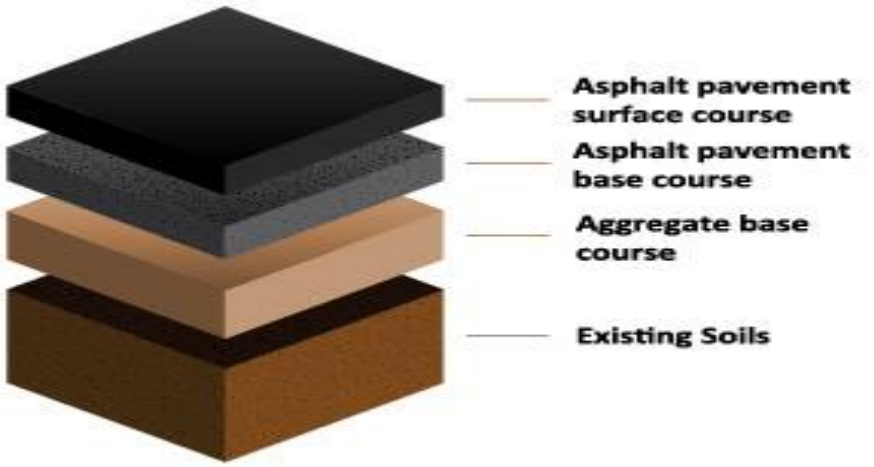

Figure 2. Layers of Hot Mix Asphalt Pavement [37].

1.4 Sources and Nature

As described above, as far as the nature and sources of asphalt cements are concerned, it can be broken down to two categories.

1.4.1 Natural Asphalt

Natural asphalt can be found in nature in its pure form in asphalt lakes or as rock asphalt (i.e. porous rock impregnated with asphalt such as sandstone or limestone) [33]. The examples of lake asphalt include Trinidad Lake Asphalt "on Trinidad off the cost of Venezuela and from the La Brea Tar Pits close to Los Angeles." The lake asphalt exists in an emulsified form i.e. it contains approximately 40% asphalt, 30% water and 30% mineral matter [38]. Its refining involves heating it to a liquid consistency. As a result, the heavy material settles down whereas the light fraction goes to the top, where it is driven off. The resulting asphalt is harder than the manufactured one with a penetration index of 2 since it contains 40% mineral matter.

1.4.2 Petroleum Asphalt

The present and most abundant source of asphalt is petroleum refining. It is a more viscous portion of some crude oils. These crude oils "vary in their consistency and color from burgundy wine to material as black and viscous as asphalt itself" [38]. These crude oils can be classified into two categories

- **Paraffin**

These crudes primarily contain paraffin wax after the fractional distillation of more volatile components.

- Mixed Base Crudes include the mixture of both the waxes and the asphalt [38].

Parafin wax based crude oil consists of gasoline, kerosene, diesel Oil, lubrication oils and asphalt cement [38].

1.5 Composition

Asphalt comes from the fractional distillation of certain crude oils, a product that was formed naturally from organic matter over millions of years under different degrees of temperature and pressure [33]. About 90-95 percent by weight of asphalt contains hydrocarbons. The remaining 5-10% consists of heteroatoms and trace metals. The heteroatoms include oxygen, nitrogen and sulfur. These elements replace carbon atoms in the asphalt molecular structure. They are a cause of many unique chemical and physical properties of asphalt. The type and composition of heteroatoms in asphalt is based on the crude source and the exposure to aging. Metals such as vanadium, nickel and iron are found in concentrations of less than 1% in asphalt. The presence of these metals in asphalt gives some indication of asphalt crude source.

The chemical structure of asphalt is highly complex. In case of a possible chemical analysis, the resulting data would be too overwhelming to make a correlation with the rheological properties of asphalt [39]. It is possible to separate the asphalt into two broad categories known as asphaltenes and maltenes. The maltenes can be further broken down

into saturates, aromatics and resins. Chromatographic techniques are used widely to define the asphalt structure. This procedure initially involves the precipitation of asphaltenes using n-heptane followed by the chromatographic separation of resins, aromatics and saturates. Asphaltenes are insoluble in n-heptane. These are complex and highly polar aromatic materials consisting primarily of hydrogen and carbon along with some oxygen, nitrogen and sulfur. As a result of employing several techniques to determine the molecular weight, the values found fall within the range of 300-600,000 g/mol. Asphaltenes have a significant contribution to the rheological properties of asphalt about 5 to 25% by the weight of the material. With an increase in the asphaltene content, asphalt becomes increasingly harder with lower penetration, higher softening point and thus higher viscosity.

Resins are n-heptane soluble compounds [39]. They also contain carbon, hydrogen, some oxygen, nitrogen and sulfur. They are dark brown in color solid, semi-solid and are highly adhesive in nature. These are dispersing agents or peptizers for asphaltenes. The proportion of resin to asphaltenes determines a solution type (sol) or gelatinous (gel) type asphalt. Separated resin fractions have a molecular weight ranging from 500 to 50,000 g/mol.

Aromatics are the lowest molecular weight naphthenic aromatic compounds in asphalt [39]. They make up a major portion of the dispersion medium for peptised asphaltenes. About 40 to 65% of asphalt consists of aromatics. These are dark brown viscous liquids with an average molecular weight in the range of 300 to 2,000 g/mol. They are comprised

of non-polar carbon chains, in which the unsaturated ring system exists predominantly. They have a strong ability to dissolve other high molecular weight hydrocarbons.

Saturates contain straight and branch chain hydrocarbons with alkyl naphthenes and alkyl aromatics [39]. They have similar molecular weights as aromatics. Asphalt is traditionally considered as a colloidal system, which contains high molecular weight asphaltenes micelles dissolved in a lower molecular weight maltenes. These micelles consist of an insoluble asphaltene core surrounded by a corona of high molecular weight aromatic resins, which act as a stabilising solvating layer. In the occurrence of sufficient amount of resins and aromatics with a good solvating power, the asphaltenes are fully dispersed and the resulting micelles have a good mobility within asphalt. These are called "sol–type" asphalts. In the absence of sufficient amount of resins and aromatics, The asphaltenes can link together, thereby forming an open packed structure of linked micelles in which the : internal voids are filled with the intermicellar fluid of mixed composition. These are called gel-type asphalts. The Figure 3 and 4 show the structure of sol- and gel-type asphalt respectively.

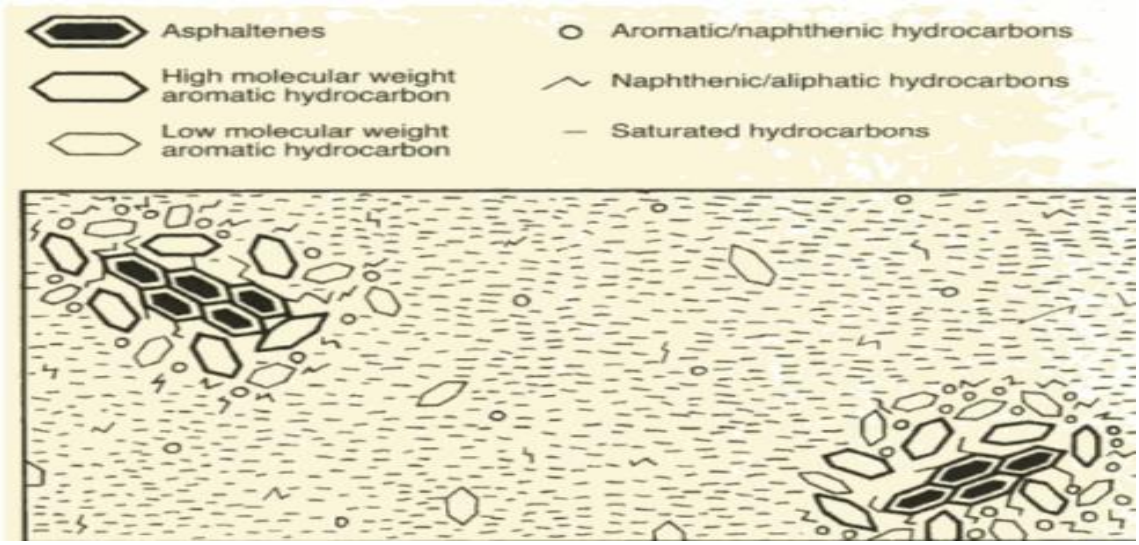

Figure-3 Representation of a Sol type Asphalt [39].

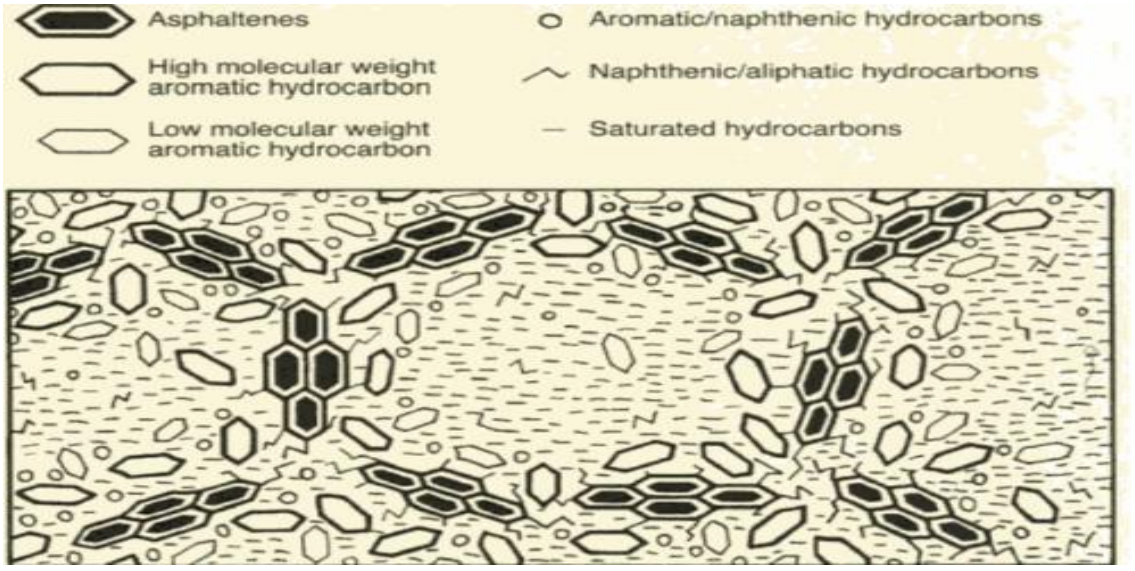

Figure 4. Representation of a Gel type Asphalt [39].

1.6 Properties

1.6.1 Chemical Properties

By systematically blending all the fractions separated from the asphalt, it has been found that the composition has an effect on the rheology [39]. By keeping the asphaltene level constant, it has been observed that an increase in the aromatic content at a constant saturates to resin ratio has a negligible effect on rheology except for a minute reduction in shear susceptibility. Under a constant asphaltenes and resins to aromatic ratio, an increase in saturates content increases the softness of asphalt. With the addition of resins under constant asphaltene levels, asphalt becomes harder and the penetration index and the shear susceptibility decreases. It has also been increasingly observed that asphalt properties mainly depend on the composition of the asphaltenes within the asphalt cement. With an increase in the concentration of asphaltenes, the asphalt binder becomes more viscous.

1.6.2 Physical Properties

Physical properties of asphalt include durability, temperature susceptibility, viscoelasticity and aging susceptibility.

1. **Durability:** It is a measure of how asphalt binder alters its properties in response to aging i.e. it has been observed that in general the asphalt binder loses its viscous nature and becomes increasingly elastic, stiff and brittle with aging [40].
2. **Temperature Susceptibility:** The asphalt properties are highly sensitive to variations in temperature. Asphalt becomes increasing stiff as the temperature drops where as it

becomes softer as the temperature increases. The degree of this susceptibility is based on the asphalt crude source [41].

3. **Viscoelasticity:** Asphalt is a highly viscoelastic material. It acts as a viscous liquid at high temperatures and behaves like an elastic solid at low temperatures. At intermediate temperatures, asphalt displays both these properties [41]. Apart from temperature susceptibility, asphalt properties are also dependent on the rate of loading and the loading time. At a slow loading rate, asphalt demonstrates viscous flow. At a high loading rate, it behaves like an elastic solid.
4. **Aging:** Asphalt properties also change with aging. The primary source of aging in asphalt cement is oxidation [41]. Upon reaction with oxygen, asphalt structure and properties can change significantly. It makes asphalt stiffer and as a result brittle. At high temperatures, there is a high likelihood of oxidation hardening to occur. Significant amount of hardening occurs during Hot Mix Asphalt (HMA) production. Therefore this susceptibility should be kept in mind when designing the asphalt pavement.

1.7 Performance Grading System

Asphalt binders are currently graded according to Superior Performance Pavement (Superpave) (Superior Performing Pavements) performance specification protocols [33]. This system was developed in the late 1980s as a result of joint efforts of US highway agencies as a part of the Strategic Highway Research Program. This grading system uses consistent physical performance property requirements to grade all binders. However, the difference occurs in the grades. The Superpave system uses maximum and minimum

temperatures at which these performance requirements must be met. The asphalt pavements are graded according to their respective geographical area and their climatic conditions. For instance, an asphalt binder of grade 70-28 has a maximum temperature of 70 degrees Celsius which the pavement will likely reach. Similarly -28^{o}C is the minimum temperature, which the pavement will likely reach. In other words, the pavement will be sufficiently stiff to resist rutting up to 70 degree Celsius whereas, it will be sufficiently soft to resist low temperature cracking down to the minimum limit of -28 degree Celsius. Researchers use the Superpave software called LTPP long term pavement performance binder selection software to obtain high and low temperature grades for binders needed in a particular location. This software contains a database of weather information from 6092 reporting weather stations across the United States and Canada. During the period of operation of these weather stations, the hottest seven day period was identified, and an average maximum air temperature was determined[33]. Similarly, the coldest seven day period was identified and subsequently the minimum average air temperature was determined. Now the maximum pavement temperature is the temperature 20 mm below the pavement surface and the lowest pavement temperature is the temperature at the pavement surface.

1.8 Scope and Objectives

The majority of roads in Ontario fail prematurely. Thermal and fatigue stresses are one of the major root causes of these premature failures. In the last 12 years, the Ontario government aims to spend $ 160 billion in the reconstruction and rehabilitation of public infrastructure including Ontario roads [42].

The government and the industry need to rethink and revisit their strategies and implement corrective actions and revised asphalt performance testing protocols in order to reduce these costs.

The main of objective of this study was to:

1- Measure the ductility and the ability of 10 MTO samples through double-edge notched tension (DENT) test at 5,10,15,20 and 25 degrees Celsius. The main purpose here was to study different grades at 15 degree Celsius and then at different temperatures at the same CTOD (crack tip opening displacement) requirements.
2- Measure the ductility and the ability of an additional 8 MTO recovered and tank asphalt binder contract samples through DENT testing.
3- Measure the ability of the 8 MTO contract samples to resist thermal and fatigue stress through (BBR) test and to relate these findings with the DENT test results.
4- Chemical testing of all contract samples through X-ray fluorescence (XRF) and Fourier transform infrared (FTIR) analysis and compare these results with the physical property tests of the samples mentioned above.

In addition to the above objectives, the high and intermediate temperature grading of all samples through dynamic shear rheometer (DSR) analysis were included. A detailed discussion and the results from the previous case study will be included as well. This case study involves the detailed study of the root causes behind the premature failure of local road in Kingston, Ontario.

Chapter 2

Background

2.1 Reversible or Physical Hardening

Physical hardening in asphalt and other amorphous polymers occurs due to the readjustment or reorganization of molecules to reach at an ideal thermodynamic state under specific conditions [42].

This phenomenon in asphalts and other amorphous polymers was first reported by Struik 1978. It is essentially a reversible process that takes place at low temperatures [43]. It produces time-dependent isothermal changes in specific volume and as a result, changes in mechanical properties. The effect is reversible once the material is heated back to the room temperature.

This transition takes place due to the isothermal reduction in free volume at temperatures near glass transition temperature (T_g) [43]. This transition as a result increases stiffness and significant reduction in stress relaxation capacity of asphalt. Figure 5 illustrates in detail the physical hardening process.

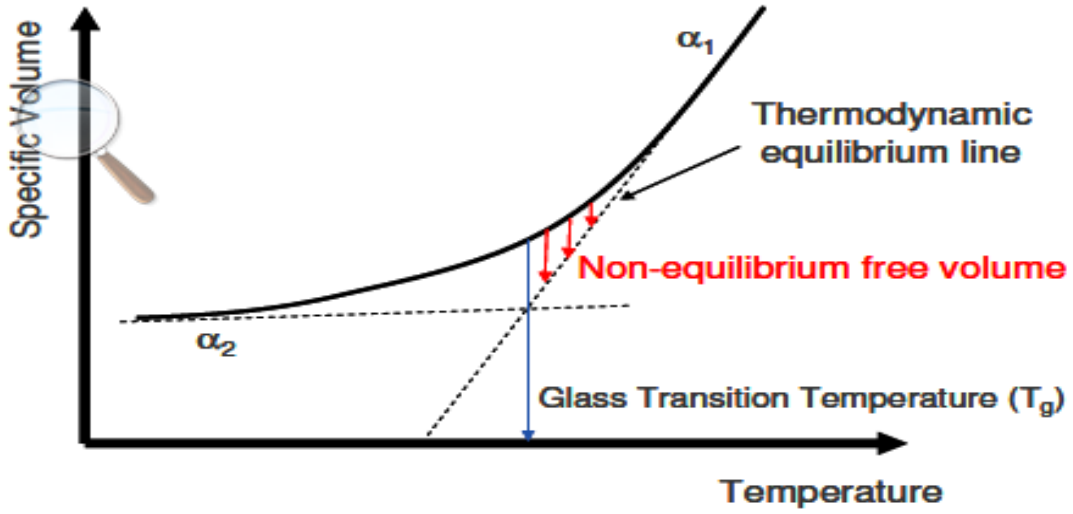

Figure-5. Physical Hardening and its Relation to Free Volume [43]**.**

According to the free volume theory as proposed by Stuik, the material's total volume contains a fraction that constitutes the volume of molecules and their vibrational motion and fraction containing a free volume due to packing irregularities [42-46]. When asphalt binders are cooled from higher temperatures above T_g, the reduction in free volume due to the molecular organization is rapid then the molecular changes due to the vibrational motion of molecules. This transition follows a linear trend above the T_g as illustrated in Figure 6 above. Upon approaching the T_g, The transition due to the molecular adjustment becomes slower, whereas the free volume reduction due to the vibration motion becomes prominent. If the material is left under these isothermal conditions for an extended period of time, then the molecular organization does occur and as a result produces significant changes in the mechanical properties. This transition is called the physical hardening.

Under these conditions, asphalt binders are in metastable condition. The first order properties under this transition remain unchanged [42-46]. However, second order properties such as coefficient of thermal expansion and heat capacity are impacted significantly. According to recent studies, the rate of physical hardening depends on the chemical composition such as the length of molecular chains and the wax content. It has been found in recent studies that physical hardening in asphalt occurs even above the T_g relative to other amorphous polymers. This transition in asphalt can be attributed to an additional mechanism i.e., the partial crystallization of some fraction of asphalt binder due to the high wax content.

2.2 Failure Modes in Asphalt

Asphalt pavements fail as a result of both structural and environmental factors. The structural factor involves the failure of the pavement due to the repeated traffic loadings over a period of time [47[. When a wheel applies the load to the pavement, vertical compressive and shears stresses "are transmitted within the asphalt layer." and the horizontal tensile stress at the bottom part of the asphalt layer [47,41]. The asphalt pavement should be sufficiently strong to withstand compressive and shear stresses to prevent the damage due to rutting. Similarly, the pavement should also have sufficient tensile strength to overcome the tensile stresses at the base of the asphalt pavement occurring due to the fatigue cracking after repeated loadings. Damage occurring in asphalt as a result of environmental factors include frost heave i.e. "the upward of movement of the subgrade" occurring due to the "expansion of an accumulated soil moisture as it freezes, thaw weakening, i.e., a week subgrade condition occurring due to

the soil saturation as “ice within the soil melts”, physical or low temperature hardening and the infiltration of the moisture within the pavement structure. The prevention of damage occurring from all these factors demands continuous, consistent and ongoing maintenance and repair of these roads. These prevention practices, whether major or minor, increase the life of the pavement significantly as illustrated in the following Figure 6.

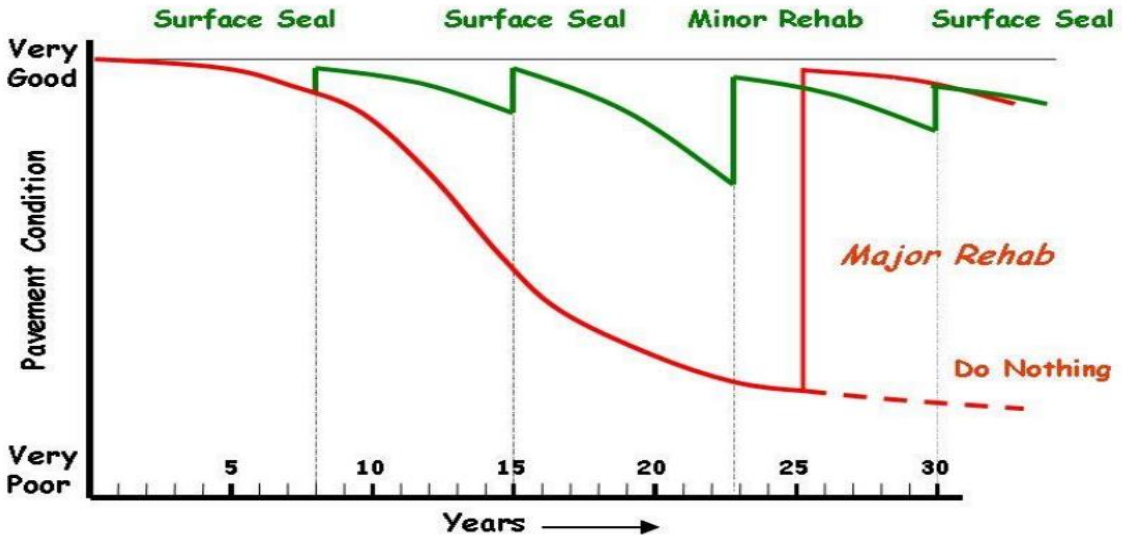

Figure 6. Graph of Pavement Condition vs Pavement life in terms of number years. Comparison of pavement performance in terms of major and minor rehabilitation vs “Do Nothing Approach.” [47]

Failure in asphalt pavements occur as a result of [41]

- Fatigue Cracking
- Rutting or Permanent Deformation
- Thermal or Low Temperature Cracking
- Buildup or Infiltration of Moisture.

2.2.1 Rutting or Permanent Deformation

Rutting or permanent deformation can be described by a "surface cross section", which "is no longer in its designed position." [41] Rutting is caused by accumulated small unrecoverable deformations occurring due to repeated loadings. Rutting mainly occurs as a result of two principal factors.

The first factor involves the permanent deformation due to a weak subgrade. In this case, the subgrade is not strong enough to withstand repeated applied stress. Stiffer paving materials can provide partial resistance to this type of deformation [41]. However, this type of deformation is essentially a structural problem rather than a material issue.[41] The pavement does not possess enough strength or thickness to resist the applied stress It can also be caused due to the weakening of the underlying layer as a result of the infiltration of moisture. The following Figure 7 illustrates this phenomenon in detail.

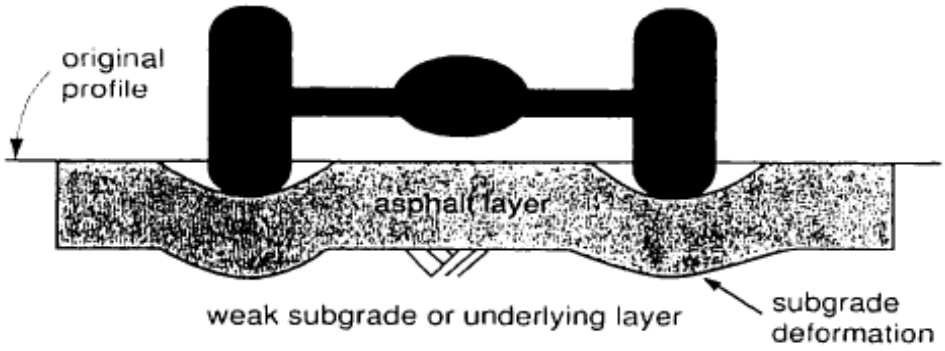

Figure 7. Permanent Deformation due to Weak Subgrade [41]**.**

The second case of rutting involves deformation due to the weak asphalt layer [41]. In this case, the asphalt layer does not have sufficient shear strength to withstand applied

stress due to the repeated heavy loading. This type of deformation results in the formation of rut or groove that can be best described by " a downward and lateral movement of the asphalt mixture." It can be a cause of weak asphalt surface course or weak underlying asphalt layer. This usually happens during summer time and high pavement temperatures. Figure 8 illustrates this phenomenon.

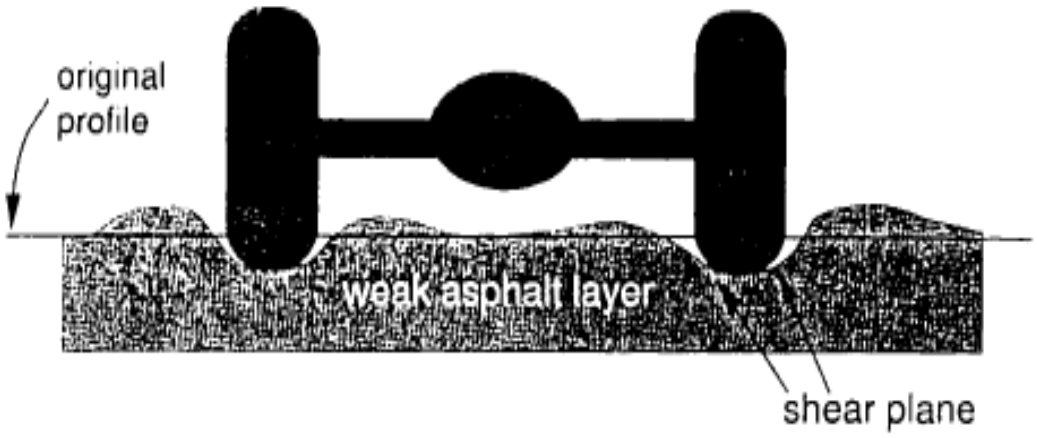

Figure 8. Permanent Deformation from Weak Asphalt Layer [41]**.**

In order to prevent this, the asphalt binder should be selected such that it is stiff enough at high temperatures to act as an elastic band which returns to its original position once the load is removed [41]. It can also be prevented by selecting the aggregate material that is cubical i.e. it has a high internal friction. It has a rough surface texture and is "graded to develop particle to particle contact."

2.2.2 Fatigue Cracking

Fatigue cracking occurs when pavement is excessively stressed from repeated heavy loading, which results in the formation of cracks [41]. Its early indication appears in the form of intermittent longitudinal cracks. These initial cracks eventually combine to form bigger cracks. Alligator cracking is an advanced stage of fatigue cracking, which can be described by transverse cracks joining the longitudinal cracks. The extreme case involves the occurrence of potholes in which, "pavement pieces become dislodged by traffic." Figures 9 and 10 show a schematic of alligator cracks and potholes respectively.

Figure 9. Alligator Cracking [48]**.**

Figure 10. Potholes [49]**.**

A variety of factors contribute to fatigue cracking. The occurrence of repeated heavy traffic loads is one of these factors. Thin pavements with weak underlying layers are more vulnerable to high traffic loads due to the higher deflection [41]. This defection causes horizontal tensile strass at the bottom of the asphalt layer, which eventually contributes to fatigue cracking. Other factors include poor construction, poor drainage and under designed pavements. If fatigue cracking occurs at the end of the design period or completion of the number of design loads, it is considered an indication for restoration or rehabilitation. However, if this phenomenon occurs earlier in the design period, then it is considered a design flaw such as underestimation of design loads. The prevention of fatigue cracking involves [41]:

- Correct or Adequate determination of number design loads during the pavements service life.
- Use of thicker pavements.
- Prevention of the infiltration of moisture into the subgrade.

- Use of moisture resistant pavement materials.
- Use of HMA strong enough to resist usual deflections.

2.2.3 Thermal or Low Temperature Cracking

Thermal cracking occurs due to poor environmental conditions [41]. It can be recognized by transverse cracks at a consistent spacing along the pavement as can be observed by the following Figure 11.

Figure-11. Transverse Cracking [50].

These cracks occur due to the pavement shrinkage in winter. This shrinkage generates tensile stresses within the asphalt layer and when these stresses exceed the tensile strength of the material, the asphalt layer cracks [41]. The process initiated from single low temperature cycle. However it later develops under repeated subsequent low temperature cycles. In general, hard asphalts are more sensitive to this phenomenon where as soft binders with appropriate air-void content are less sensitive and more resistant to thermal cracking.

2.2.4 Moisture Damage

Moisture susceptibility in asphalt pavements happens because of the weakening of the adhesive bond between asphalt binder and the aggregate. If this weakness is critical, the result is stripping. Asphalt binder and aggregate adhesive interaction can be explained in terms of four mechanisms. The first one involves mechanical principal [51]. Asphalt binder settles into the surface irregularities and the pores of the aggregate. Once this binder cools down and hardens, it forms a mechanical lock. The presence of the residual moisture on the aggregate can have serious impact on this phenomenon as the moisture will decrease the amount of binder infiltration into aggregate and reduce the mechanical lock. The second mechanism involves chemical aspect. According to this principle, the adhesion occurs due to a chemical reaction between the binder and the aggregate. If the binder surface is acidic, then the resulting chemical bond will not be strong enough to withstand the effects of moisture. The third mechanism involves the surface chemistry at the aggregate-binder-water interface. At the wetting line (that is the edge of the drop as it spreads over a surface), the surface tension involving moisture and aggregate is greater than the tension involving binder and aggregate. When all 3 mediums are in contact, "water tends to displace asphalt binder." This results in an insufficient wetting of the aggregate surface by the asphalt binder. This as a result can lead to stripping. The fourth and the final mechanism of moisture susceptibility is the orientation of binder molecules in response to presence of ions on the aggregate surface. This as a result can produce weak attraction between the asphalt binder and the aggregate. If water is polar then the binder molecules, then it can easily displace the asphalt thereby essentially satisfying the

energy demands of the aggregate surface. The moisture susceptibility is controlled by variety of factors such as [51];

- **Binder properties:** Generally highly viscous binders with high asphaltene content are less susceptible to stripping and thus ideal for preventing stripping.
- **Aggregate Properties:** Hydrophobic aggregates are generally recommended to prevent the infiltration of moisture within the asphalt cement.
- **Air voids:** Aggregates with a porosity of less than or equal to 4% should be used. If this porosity is exceeded then the voids become interconnected and may allow easier moisture penetration.
- **Climate:** Wet climate, freeze thaw cycles and temperature fluctuations can result in the buildup of moisture within the asphalt pavement structure.

2.3 Viscoelastic Properties of Asphalt

Asphalt is viscoelastic in nature. This behavior of asphalt is based both on temperature and the rate of loading. It can be clearly demonstrated through the time-temperature superposition property of asphalt [52]. According to this property, the asphalt binder that was originally tested at a low temperature of the asphalt binder for 2 h, displays the same properties or results when tested at 10 C^{o} higher than the lowest temperature for 60 seconds in a Bending Beam Rheometer. The viscoelastic nature of asphalt under the different conditions of varying temperature and the rate of loading is discussed in detail below.

2.3.1 High Temperature or Slow Moving Conditions

Under the conditions of high temperature or slow moving, asphalt essentially behaves as a viscous fluid [33]. In this case, the asphalt binder and the aggregate both as a part of hot mix asphalt (HMA) bear the shearing stress as a result of loading. This type of behavior of asphalt can be illustrated by an analogy of the two adjacent layers of asphalt sliding past each other as demonstrated in the following Figure 12.

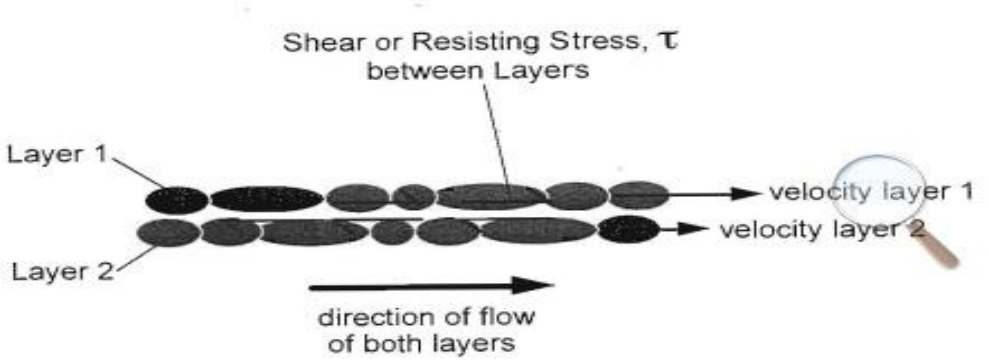

Figure-12. Demonstration of a viscous liquid flow [33].

As demonstrated in the above Figure 12, when "the top layer tries to pull the bottom layer along whereas the bottom layer tries to hold the top layer back" [33], as a result, a resisting force or friction is generated. This resistance is related to the shearing strain rate through the coefficient of viscosity. This relationship can be expressed by the following equation.

$$\tau = \mu \times \text{shearing strain rate} \quad [33]$$

In the above equation, τ is the resistance, μ is the viscosity and the shearing strain rate is the velocity at which two adjacent layers of liquid move relative to each other [33].From the above equation, the nature of the relationship between the shearing resistance and strain rate can be used to "explain differences in flow properties among various liquids." If this relationship is linear (i.e. the constant viscosity), then the fluid is said to be a Newtonian fluid. Over 60^{o}C, the asphalt binder acts as a Newtonian fluid. Some asphalt binders may demonstrate non-Newtonian behavior. There are cases of the non-linear relationship between the shear stress and shear strain. When the viscosity decreases with increasing shear strain then the fluid is said to be pseudo plastic or shear thinning. This type of behavior is shown by some modified asphalt binders. The second case involves an increase in viscosity with an increase in shear strain. Such flow behavior is said to be shear thickening or dilatant. It is demonstrated by clay slurries.

2.3.2 Low Temperature Behavior

At low temperatures, asphalt acts as an elastic solid. When the load is applied, it deforms and on the removal of the load, it quickly returns to its original shape [33]. However, when asphalt is excessively stressed, it becomes brittle and eventually breaks or crack. At low temperatures, internal stresses from repeated loads or temperature fluctuations, accumulate and eventually lead to the pavement failure.

2.3.3 Intermediate Temperature Behavior

At intermediate temperatures, asphalt behaves both as an elastic solid and a viscous liquid [33]. It is an ideal adhesive due to this behavior. When the asphalt mix is heated, the

binder acts as a lubricant allows the mixing of aggregate material, then coated and tightly compacted. Once cooled, the binder behaves as a strong glue to hold the aggregate particles in place. Under these conditions, when the load is applied, the asphalt and the aggregate immediately respond elastically followed by delayed viscous response of the binder itself.

2.3.4 Ageing

Asphalt consists of variety of organic compounds that can react with the oxygen in the environment [33]. This reaction as a result renders asphalt harder and increasingly brittle. This phenomenon is called oxidative hardening and is rather slow and takes place over the course of 7 to 8 years. That is why old asphalt pavements are more prone to cracking. Improperly compacted asphalt mixed with greater proportion of interconnected air voids experience more oxidative hardening. Other modes of hardening are volatilization and physical hardening. Volatilization takes place during hot mixing and construction and is more rapid then oxidative hardening. In this case, the hardening occurs due the loss of volatile components of asphalt. The third mode of ageing takes place at temperature below 0^{o}C. It occurs as the pavement experiences low temperatures for longer periods of time. In this case, the pavement continues to shrink and hardens.

2.4 Test Method Specifications

2.4.1 Conventional Testing Methods

2.4.1.1 Penetration Testing

Penetration testing is the earliest asphalt testing method [53]. The first penetration testing machine was invented in 1888 by HC Bowen of the Barber Asphalt Paving Company. Its basic principle was to "find the depth to which a truncated No. 2 sewing needle penetrated the asphalt binder under specific load, time and temperature conditions."

According to current American Society of Testing and Materials (ASTM) protocols, penetration testing is conducted under a following procedure as also illustrated in Figure 13 [53]:

- Sample specimens are prepared in sample containers as per (ASTM D5-97) and then placed in a water bath at a specified temperature of test for one to one and a half hour prior to the test.
- In order to test the sample, a needle loaded to 100g is brought close to sample surface and allowed to penetrate for 5 seconds. During the test, temperature is maintained at 25^{o}C. Penetration is measured in deci-millimeters.
- A total of at least 3 penetration measurements should be taken for one sample. With each new replica measurement, a clean needle should be used. The tip of the needle should be at least ten millimeters from the side of the sample container.

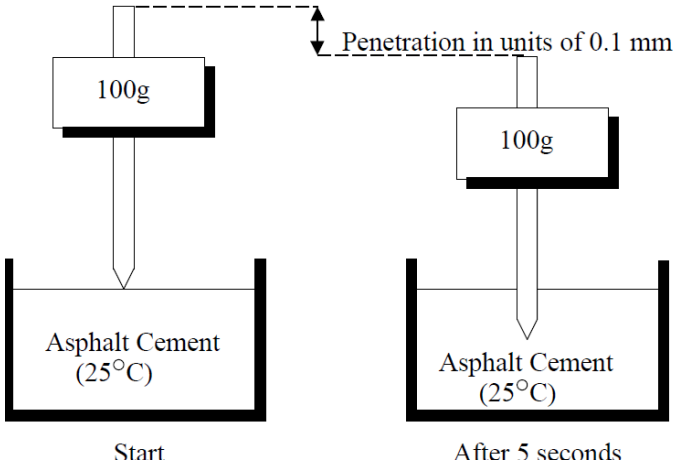

Figure 13. Penetration Testing Procedure [53].

This above testing procedure is performed under the assumption that "less viscous the asphalt, the deeper is the penetration over a period of 5 seconds." [54]. The resulting depth is roughly related with the binder's field performance. Asphalt binders with a higher penetration index are used for cold climates whereas the binders with a lower penetration index are used for hotter climates.

If the penetration of asphalt binders is considered over a range of temperatures, then the penetration can be related to the temperature variation by the following equation

$$\text{Log } P = AT + K$$

In the above equation,

P = Penetration number at a given temperature T [53]

A= measure of temperature susceptibility or temperature sensitivity [53]

K= constant

Penetration index (PI) is related to temperature susceptibility under the following equation [53]:

$$PI = \frac{20(1-25A)}{1+50A}$$

The value of temperature susceptibility or A can be found from the penetration determinations at two different temperatures [53]:

$$A = \frac{\log(pen\ at\ T_1) + \log(pen\ at\ T_2)}{T_{1-}T_2}$$

2.4.1.2 Ring and Ball Softening Point Test

The main aim for using this method is to find a defined softening point for asphalt and it does not have a defined melting point like water [55, 56]. As the temperature increase, asphalt changes from extremely brittle and thick to very soft liquid. This method continues to have significance in refining operations especially in the production of air blown asphalt. It gives an indirect measurement of viscosity. It is especially significant for roofing asphalt, as a high softening point shows that these materials will not flow in service. For typically paving grade asphalt, it is used in conjunction with the penetration test to determine the penetration index.

In this test, two asphalt horizontal disks, that are "cast in shouldered brass rings, are heated at a controlled rate in liquid bath while each disk supports a steel ball."[55] The softening point of asphalt is determined as an average of temperatures at which two disks are sufficiently softened to allow each ball covered in asphalt to fall a distance of 25 mm. The detailed procedure is illustrated in Figure 14.

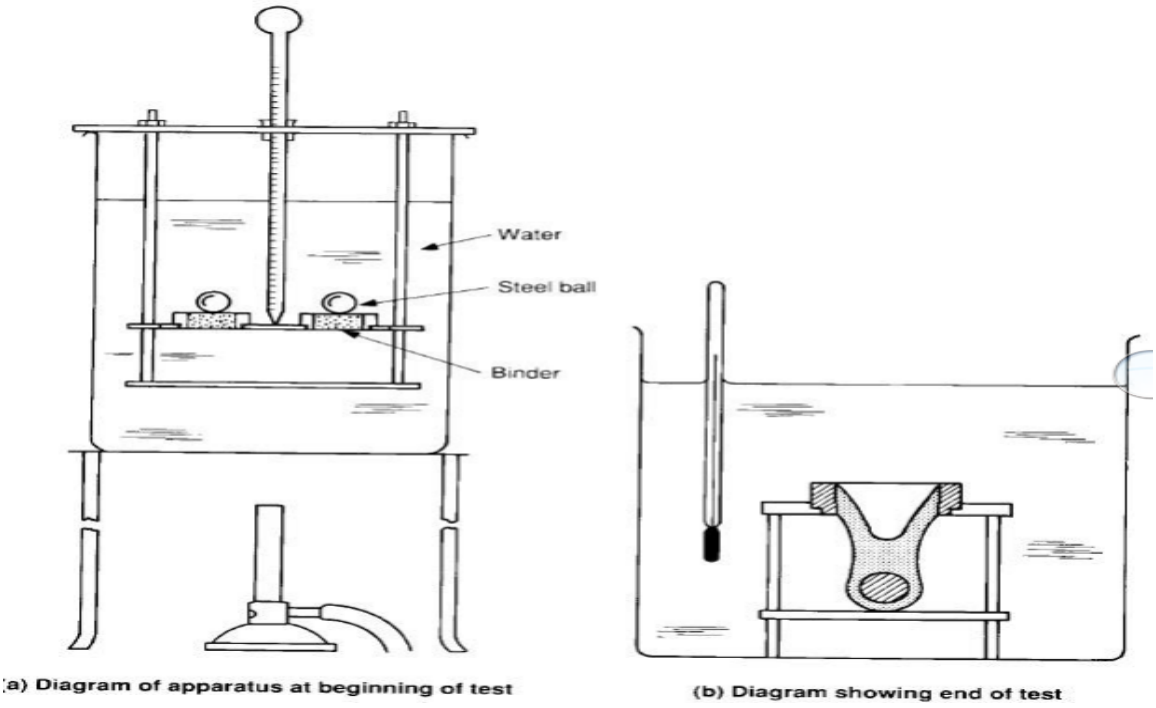

Figure 14. Ring and Ball Softening Point Test Procedure [55]**.**

2.4.1.3 Viscosity Test

Viscosity is a physical property that represents fluid's resistance to flow. This test measures an absolute viscosity of the fluid [57, 58]. It essentially measures the time it takes for the asphalt binder to travel up through the capillary tube by vacuum under strictly controlled conditions of vacuum and temperature.

This grading system was developed in early 1960s and it is an improvement over the penetration test.as it is largely empirical as compared to the viscosity test [59, 60]. This test can be performed on both the unaged sample (i.e. AC grading) and sample aged in Rolling Thin Film Oven or RTFO (i.e. AR grading). The AR grading represents the properties of a binder that has gone through a complete HMA manufacturing process.

The basic advantage of this test over penetration test is that it provides some measure of temperature susceptibility by testing the asphalt binder at three different temperatures of 25^{o}C, 60^{o}C (high temperature pavement) and finally 135^{o}C (pavement going through HMA manufacturing process).

2.4.2 Superpave Asphalt Specification Testing

2.4.2.1 Roling Thin Film Oven Test (RTFO)

The rolling thin film oven (RTFO) gives a short term aged asphalt binder for further physical testing [61]. The aim of this test is to simulate the short term aging that actual asphalt goes through during HMA manufacturing process and construction. Another purpose for this test is to determine a quantitative measure of the loss of volatiles during the aging process.

This quantitative measurement is essentially an indication of aging that a binder is exposed to during construction and manufacturing [33]. The RTFO process involves an electrically heated convection oven, which contains a circular vertical carriage that houses the sample bottles and "rotates about its center." During the operation, there is a continuous supply of hot air into the oven. This air jet blows into each sample bottle at the lowest position of their rotation. Prior to the placement of bottles in the oven, it must be pre-heated to 163^{o}C. The following Figure 15 contains schematic of RTFO equipment.

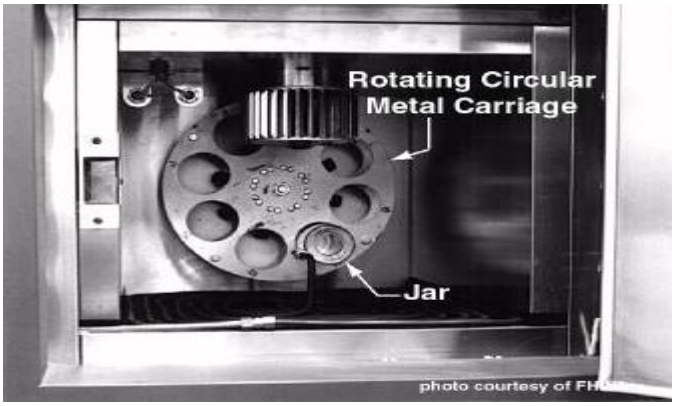

Figure-15. Rolling Thin Film Oven [61].

The first step in the RTFO process is the sample preparation [33]. Asphalt binders are heated until they become fluid. However care has to be taken not to heat in excess of 163^{o}C. After heating, binders are poured in RTFO bottles. The binder is poured such that there is 35 g of asphalt binder in all 8 RTFO bottles. The bottles are then placed in the RTFO bottle carriage. The carriage rotates at 15 revolutions per minute. The process continues at 163^{o}C for 85 minutes. After which, the samples are taken out and they can be used for further aging in Pressure aging Vessel (PAV), or tested in Bending Beam Rheometer (BBR) or Dynamic Shearing Rheometer (DSR).

For mass loss determination, two of the eight RTFO bottles are used. These bottles are weighed prior to and after the aging and the mass loss is determined from the following formula [33]:

$$\%\ Loss = \frac{Aged\ mass - Original\ mass}{Aged\ mass} \times 100$$

2.4.2.2 Pressure Aging Vessel (PAV)

Pressure aging vessel (PAV) takes the RTFO aged sample and provides a simulated long term aging environment for the sample [62]. In this equipment, the binder experiences heat and high pressures to simulate the aging during the service over the course of 7 to 10 years.

According to Superpave protocols, this procedure subjects the binder to high temperature and pressure for 20 hours [62]. PAV comprises PAV vessel and a forced draft oven [62, 33]. The air pressure in the oven is supplied and maintained by a compressed air gas cylinder equipped with a pressure regulator, release valve and slow-release bleed valve [33]. The equipment is designed to operate under a pressure of 2.10 MPa and either 90, 100 or 110^{o}C [62] . PAV also should have a digital continuous temperature and pressure monitor. The equipment can house 10 to 12 PAV pans placed in a sample rack. The Figure 16 below gives a schematic of the PAV equipment.

Figure 16. Pressure Aging Vessel [62].

After the RTFO aging process, the samples are poured immediately in the stainless steel PAV pans [33]. Each PAV pan is loaded with 50 g of asphalt binder and in total of 3 to 4 pans are used for one asphalt sample [62]. The sample pans are placed in PAV sample rack. The PAV oven is preheated to the desired temperature and once it is done, the sample rack is placed in the PAV vessel and then the lid is closed to prevent any heat loss. These samples then go through oxidative aging for 20 hrs at 2.10 MPa and 100 ^{o}C. At the end of 20 hours, the pressure is gradually lowered. After the pressure drops below 0.02 MPa, the lid is unscrewed and eventually opened. Sample rack is then taken out, pans are removed and heated at 163^{o}C for about 15 mins and the binder from all pans is transferred to a designated sample storage beaker and then later degassed in 15 KPa vacuum for nearly 30 minutes.

2.4.2.3 Dynamic Shear Rheometer (DSR)

Dynamic Shear Rheometer (DSR) characterizes the viscous and elastic behavior of asphalt binders [33, 63]. It measures the complex shear modulus (G*) (i.e. the total resistance of the material to deformation under the repeated pulses of shear stress) and phase angle (δ) (i.e., a lag between the applied shear stress and the shear strain. This is further illustrated in Figure 17.

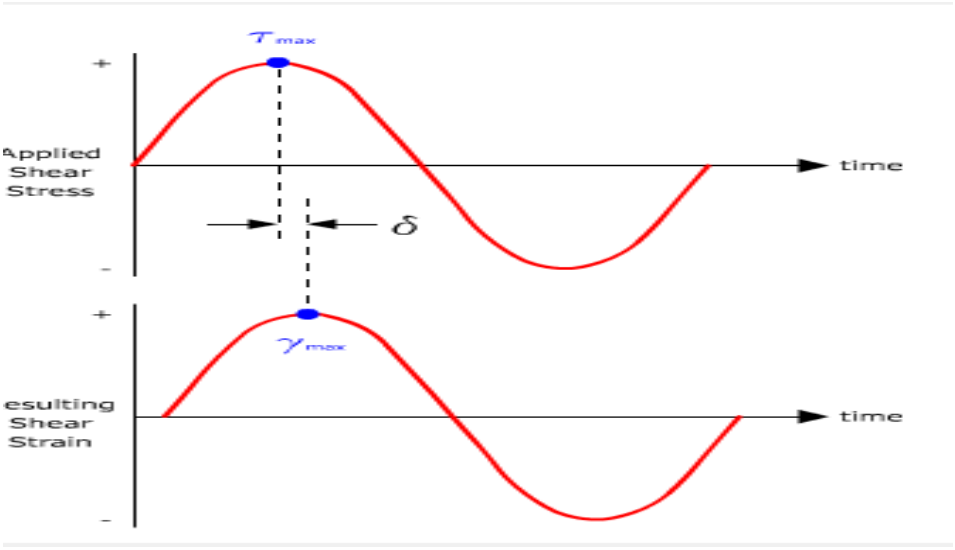

Figure 17. DSR curves showing both applied shear stress and resulting strain and a lag (δ) between them [63].

G* has two components: elastic and viscous. δ represents comparable amounts of elastic and viscous behavior at any given temperature [33,63]. The viscoelastic behavior of asphalt is dependent on temperature and rate of loading. At high temperatures, asphalt binder acts as a viscous liquid with no recoverable deformation. This is typically characterized by a δ value of 90^{o} and can be seen as a vertical line in the following Figure 18. At lower temperatures, asphalt behaves as an elastic solid with a recoverable deformation or a capacity rebound. This is typically characterized by a δ value of 0^{0} in the following Figure 18.

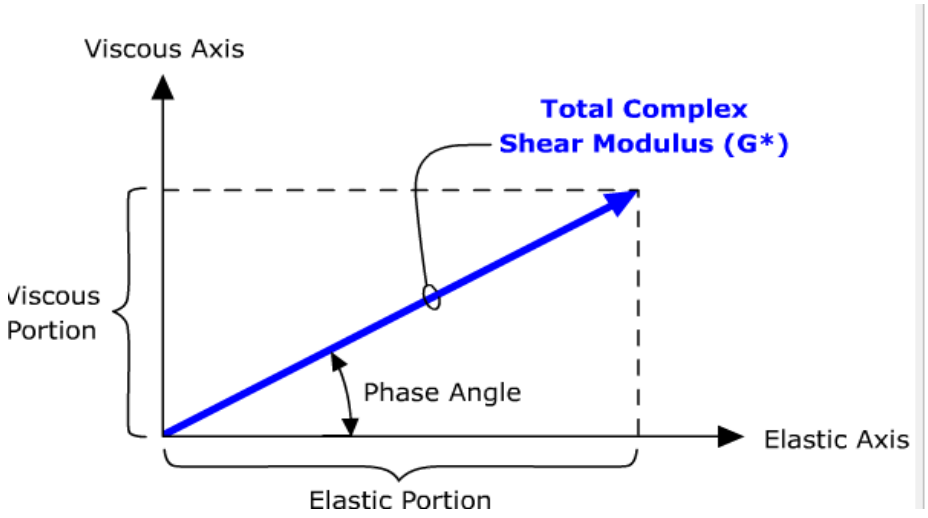

Figure 18. Viscoelastic nature of asphalt [63].

At higher temperature, rutting or permanent deformation is a greater concern [33,63]. Under these circumstances, asphalt should be sufficient to withstand the applied shear stresses as a result of repeated load and should be elastic. In this case, the elastic portion of complex modulus G*/sin δ should be maximized with a lower limit set to 1.1 KPa for unaged samples and 2.2 KPa for RTFO aged samples. At intermediate temperatures, the fatigue cracking is a major concern. It can be visualized as traffic cycle, where with each traffic cycle, load is being applied to deform the pavement surface. The part of this work done is elastic and the other part is viscous. The viscous portion should be minimized. Therefore, the pavement should be elastic and not excessively stiff. As a result, the viscous portion of complex modulus G*. sin δ should be minimized by setting a maximum limit of 5000 KPa. This is done for PAV aged samples. Figure 19 shows a schematic of DSR.

Figure 19. DSR and its components [63]**.**

This test involves a small sample that is sand witched between two parallel plates. The asphalt binder type determines the test temperature, the sample size and the plate diameter [33, 63]. Unaged and RTFO asphalt binder samples are tested at higher temperatures above 46^{o}C. Under these test conditions, 25 mm upper and bottom plates are used as shown in the above Figure 19. PAV aged asphalt binder samples are tested at intermediate temperature between 4^{o}C and 40^{o}C. Under these conditions, 8 mm upper and bottom plates are used as evident from Figure 19 above. A constant temperature is maintained for the test sample 'by heating or cooling the surrounding environmental chamber." [33]. The bottom plate remains fixed while the top plat swing back and forth at

10 radians /sec in a sinusoidal form [33, 63]. The equipment as a result measures the maximum applied stress, strain and the time lag. The instrument software then determines the complex shear modulus and the phase angle. The whole test procedure is automated.

The DSR testing is done under the following procedure [33, 63],

- The asphalt binder is heated until it is fluid enough to flow and pour.
- The binder is then poured into the silicon mould and cooled until it solidifies.
- Prior to the placement of the sample between the test plates, the test temperature, frequency (i.e. 10 radians per second) and loading ting time is selected based on the type of the asphalt binder (i.e. unaged, RTFO or PAV).
- The upper and bottom plates are preheated to the selected test temperature.
- The sample is then placed between the test plates.
- The test plates are brought sufficiently closer until the gap equals 1500 micro meters (for RTFO and unaged binder) and 2100 micrometers (for PAV aged sample).
- The sample is then trimmed around the edges.
- The gap between the test plates is selected at 1000 micrometers (for RTFO and Unaged asphalt binder) and 2000 micrometers (for PAV aged sample).
- The sample is then heated or cooled to the testing temperature.
- Once the binder sample is at the desired temperature, the test is started.
- Sample is conditioned for 10 cycles at the frequency of 10 radians per second.
- The measurements are then taken over the next ten cycles and the data is then reduced by the software to yield a value of complex modulus and phase angle.

The following Table 2.1 shows the performance specifications in term storage modulus limits for unaged, RTFO and PAV aged samples.

Table 2.1. DSR performance specification for different asphalt binder types [63]

Binder Type	Storage Modulus	Modulus Limits	Mode of Failure
Unaged	G*/Sinδ	Greater than or equal to 1.0 KPa	Rutting
RTFO	G*/Sin δ	Greater than or equal to 2.2 KPa	Rutting
PAV	G*.Sin δ	Less then or equal to 5000 MPa	Fatigue Cracking

2.4.2.4 Bending Beam Rheometer (BBR)

Bending Beam Rheometer (BBR) characterizes the low temperature behavior of asphalt binder. It measures the ability of the asphalt to resist low temperature cracking and how much the binder relaxes the load induced stresses [33]. The resistance to low temperature cracking comes in the form of creep stiffness and the relaxation ability of the asphalt can be quantified by measuring the m-value (i.e. the change in asphalt stiffness over time.). In theory, BBR test temperature should correspond to the lowest critical temperature of the asphalt pavement. However, it was observed, that when test was conducted at the temperature corresponding to the lowest temperature grade of the asphalt pavement, the procedure takes a long time (i.e. 2 hours) to finish [33, 64]. Therefore, by using the

principle of time-temperature superposition, it was decided that the test should be conducted at the temperature 10 degrees above the lowest temperature grade. This essentially produces same results at 60 seconds as compared to 2 hours testing time at the lowest critical temperature of asphalt. At low temperatures, asphalt binder acts as an elastic solid [33]. In order to truly simulate the thermal stresses that an asphalt pavement experiences in the field at low temperatures, the test takes in the asphalt binder that has previously gone through both RTFO and PAV aging processes BBR consists of a" loading frame, temperature controlled fluid bath, computer control and data acquisition system" . The following Figure 20 contains a schematic of BBR.

Figure-20. Bending Beam Rheometer [64].

The test essentially involves a small asphalt beam resting on two supports while the load is being applied at the midpoint by a blunt-nose shaft [33]. BBR loading system essentially consists of a loading cell that is mounted on a loading shaft, which is enclosed in an air bear to prevent the occurrence of friction during loading. Loading shaft also contains a transducer that monitors the variation in deflection. The following figure 21 shows a closer look at load being applied at the asphalt beam.

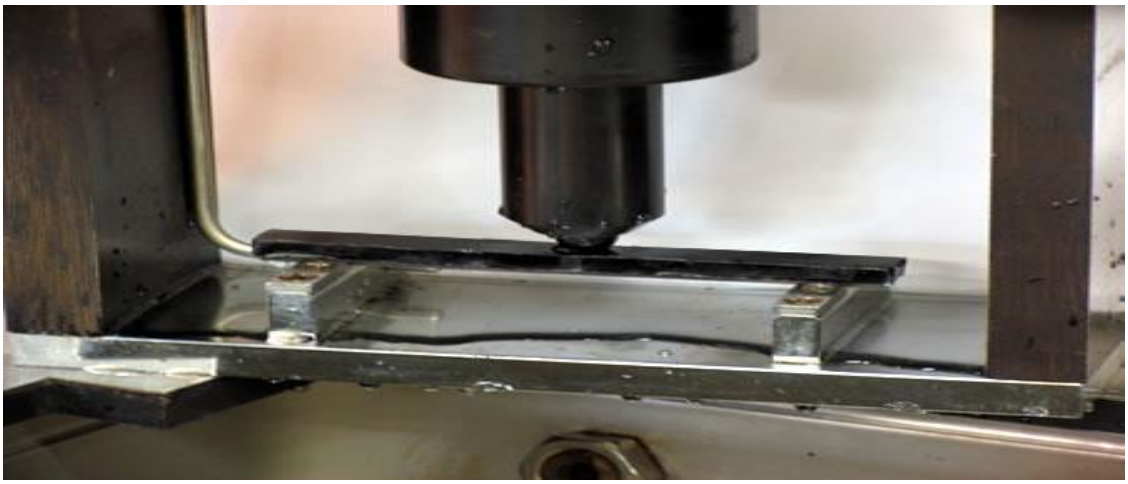

Figure-21. Closer look at the application of load on Asphalt beam [64].

This test utilizes the beam theory to determine creep stiffness under a creep load. The creep load in this case shows the accumulation of thermal stresses in asphalt in response to the temperature drop [33]. The instrument uses cooling liquids that will not freeze under temperatures below 0 ^{o}C. Liquids such as methanol, ethanol and ethylene glycol are normally used. The cooling liquid is circulated between the testing bath and the circulating bath, which maintains the liquid temperature to within 0.1^{o}C. For BBR testing, asphalt beams are prepared in silicon molds. Prior to pouring, asphalt binder PAV sample is heated at 163^{o}C for approximately 1 hour, until it is sufficiently fluid to flow. The asphalt is then poured into silicon molds "from one end to other in a continuous motion" [64]. Then the binder is allowed to cool for 30 to 45 minutes. Once sufficiently cooled, the excess binder is trimmed from the top edges with a hot knife then the molds are left at room temperature for 2 hours [33]. For demolding, the silicon molds are placed freezer at temperature below 0^{o}C for 4 or 5 seconds until the beams are firm solid. Then they are taken out of molds. Beams are then conditioned for 1 hour at temperatures below

0^oC. A set of 3 beams are tested at a temperature 10^oC above the asphalt cement lowest limiting temperature grade. The beams are then tested in BBR [64].

Prior to testing, BBR is first calibrated [64]. A thick rigid stainless steel reference beam is used to calibrate the load cell and the deflection transducer. The temperature transducer is calibrated using a thermometer. The equipment is supplied with thin stainless steel reference beam. It can be used periodically to check the overall system [33]. Prior to the starting of test, asphalt beam is placed on support and the test is started [64]. At first, BBR subjects the asphalt through some load conditioning steps [33]. Initially, a load of maximum 35 mN is applied to ensure beam's firm contact with supports. Then, a 250 mN load applied for 1 second. After which, the load is again reduced to 35mN. This load is applied for 20 seconds. Once the load conditioning is completed, a load of 250 mN is applied for 240 s. The instrument measures the deflection with time and as a result calculates the creep stiffness S(t) through the following formula:

$$S(t) = \frac{PL^3}{4bh^3\delta(t)}$$

In the above formula,

P= applied constant load (N)

L= distance between beam supports (102 mm)

h= beam thickness (6.25 mm)

S(t) =Creep stiffness at time "t".

δ(t)= Deflection at time (t).

The test output includes the creep stiffness at 60 sec, which has to be less than or equal to 300 MPa and the m-value, which should not exceed 0.3. The following Figure-22 shows a typical profile of load and stiffness with time [33].

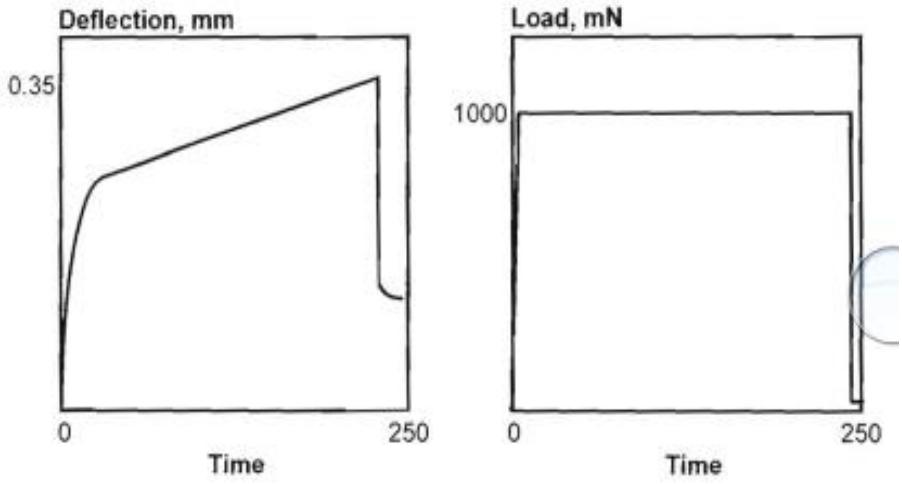

Figure-22. BBR stiffness and load output [33]**.**

The following Figure 23 further illustrates how the creep stiffness and m-values are calculated over time.

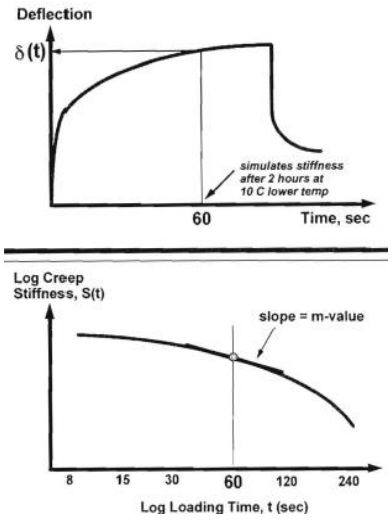

Figure-23. Creep Stiffness and m-value at 60 seconds [33]**.**

2.5 Modified Ministry of Transportation (MTO) Testing Methods

The current Superpave testing protocols fail to predict low temperature and fatigue cracking in asphalt pavements due to the inadequate conditioning time during the conventional BBR method and the prediction of only low strain properties through DSR. In response to these challenges, new and improved testing methods have been developed by Hesp Research Laboratory at Queens University Chemistry Department in collaboration with Ontario Ministry of Transportation (MTO). These tests are:

- LS 308 Extended Bending Beam Rheometry (EBBR)
- LS 299 Double Edge Notched Tension Test (DENT)

2.5.1 Extended Bending Beam Rheometer (EBBR) Protocol

Asphalt pavements cool for several weeks and months before their structure is affected by cold weather during the months of January, February and March [31]. It is during this period of extended conditioning that poor quality asphalt pavements consolidate their wax/asphaltene structure and thereby lose their ability to relax thermal stresses. Therefore, a 1 hour conditioning time that was specified in a conventional BBR method, is insufficient to truly simulate low temperature behavior of the binder as experienced by pavements in the field. As a result of this problem in the original BBR method, LS 308 extended BBR protocols were developed. As a part of these revised protocols, asphalt beams are conditioned and tested after 1 hr, 24 hrs and 72 h. According to these protocols, samples are conditioned at two temperatures that are 10 and 20^{o}C warmer then lowest temperature grade. The limiting temperatures correspond to the conditions where creep stiffness approaches 300 MPa and m-value reaches 0.3. As a part of this either duplicate or triplicate beams are used that go through same stages of conditioning and testing. The limiting grades are obtained through interpolation or extrapolation by plotting the grades on semi-logarithmic scale. A high degree of accuracy and confidence can be achieved through this method.

2.5.2 Double Edge Notched Tension Test (DENT)

Ductility tests were initially developed to replace the penetration tests in order to "provide a measure of strain tolerance in the non-linear regime." [31] According to the SHRP researchers, these tests gave unrealistically high levels of displacement. Therefore, Direct Tension Test (DTT) was developed. It measured a stress and strain on a dog bone

sample in a ductile to brittle and brittle region. Later, DTT was dropped because it failed to provide good reproducibility. As a part of MTO's efforts to improve and modify the previous Superpave protocols, DENT test was developed at Hesp Research Laboratory in the Department of Chemistry at Queen's University and in collaboration with MTO. The test is done after conditioning the sample for 3 hours at 15^{o}C to obtain the essential and plastic work of fracture and a critical crack tip opening displacement (CTOD).

Samples are prepared by pouring the binder in silicon molds. Samples of 3 different double edge notched shaped ligaments are prepared with ligament lengths of 5, 10 and 15 mm. They are then left to cool and solidify. Once sufficiently cooled, they are trimmed to remove the excess binder and then first conditioned for 10 to 15 minutes at room temperature and then for 3 hours in a testing bath [31]. They are then pulled apart at controlled rate until failure. The total energy of fracture (W_t) can be defined as an area under the load-displacement curve [7]. This total energy is the sum of essential work of fracture (W_e) and the plastic work of fracture (W_p) as can be seen in following equation:[31]

$$W_t = W_e + W_p$$

The essential work of fracture essentially generates new surfaces whereas "the plastic work is volume related and may involve single or perhaps various dissipation mechanisms [7].

The W_t and the other two work terms in the above equation can be converted into specific work of fracture by dividing them with the cross-sectional area of the beam (i.e. Length x width) [7]. Thus

$$Wt = w_e \times LB + \beta w_p L^2 B$$

Dividing by cross-sectional area (LB) on both sides, we get [7]:

$$Wt/(LB)= w_e+ \beta w_p L$$

$$w_t= w_e+ \beta w_p L$$

where

w_t= specific total work of fracture (J/m^2)

w_e= specific essential work of fracture (J/m^2)

w_p= plastic work of fracture (J/m^2)

B= sample thickness (m)

L= Ligament Length (m)

β= scaling factor that describes the shape of the plastic zone.

By plotting w_t vs ligament length L (m), we get the specific essential work of fracture (w_e) from the y-intersept and the plastic work βw_p from the slope of the graph.

The essential work of fracture can be used to determine critical crack tip opening displacement (CTOD) or δ_t. CTOD can be defined as a measure of strain tolerance in a ductile state under severe confinement [7]. Thus:

$$\delta_t.= w_e/\sigma_n$$

where σ_n represents a net-section stress, which is obtained by dividing the peak load for 5mm ligament by cross-sectional area [7].

Chapter 3

Materials and Experimental Methods

3.1 Materials

This thesis involves a detailed study and investigation of physical and chemical characteristics of 8 MTO samples and 10 contract samples. The details of these samples are provided in following tables.

Table 3.1 MTO Contract Samples

Samples	Highway	PG Grade
M1R	11	64-28
M2R	6	64-28
M3R	10	64-28
M4R	17	58-34
M5T	11	64-28
M6T	6	64-28
M7T	10	64-28
M8T	17	58-34

Table 3.2 Contract samples

Samples	Highway	PG Grade
D1	Hwy 401	PG 70-28
D2		PG 64-28D
D3		PG 64-28D
D4		PGAC 64-28D
D5	MTO	PG64-28 MD
D6	Hwy 28	PGAC 58-34P
D7		PG 58-34
D8	Hwy 417	PG 58-34 PMA
D9		PG 64-34MD
D10		PG 58-34
D11		PGAC 58-34P

3.2 Asphalt Binder Recovery

In this method, the asphalt binder was extracted from asphalt cores by using toluene. The properties of the recovered binder can vary significantly from its tank sample due to the exposure to contamination, aging and other changes as a result of its exposure to heat and the solvent. Care is taken to ensure that the procedure does not impact the properties of the binder relative to its original sample. The hot mix asphalt cores as received by Ontario Ministry of Transportation (MTO) were crushed into small chunks and collected

in two 1 Gallon tin cans. These crushed pieces were then soaked in toluene for a period of 24 hours. Dichloromethane is another solvent that can be used to extract the binder. However, in this case, Toluene was preferred as it is relatively safer to handle and easier to dispose of then Dichloromethane. After 24 hours, the asphalt mixture/ aggregate was washed with about 4 to 6 L of Toluene to obtain about 250 g of the asphalt binder. The extract (i.e the mixture containing binder in excess) was collected in 4 L empty glass bottles. The extract was then left for sedimentation for 5 hours. The binder recovery procedure was then carried out using a rotary evaporator (Rotovap) as shown in the following figure 24.

Figure 24. Rotary Evaporator [65] .

The procedure initial involves the condensation at 70-80^{o}C and an aspirator pressure of 180 mbar. The temperature is then later increased to 150^{o}C and 20-40 millibars. This procedure continued for one and half hour to ensure that no trace of solvent was left in the binder. This recovered binder was then used further testing and analysis.

3.3 Rotating Thin Film Oven (RTFO)

After the asphalt samples are received, they are subjected to ageing prior to testing and analysis. The ageing involves both RTFO and PAV ageing to simulate the pavement ageing during manufacturing and construction and in service respectively. The RTFO procedure was performed in a following sequence.

- The ageing temperature was set to 163^{o}C and the airflow to 4 L/min.
- Binder sample was heated in an oven until it was sufficiently fluid to pour. The heated sample was then sufficiently stirred to ensure homogeneity and the removal of air bubbles.
- About 35 g of binder was collected in each cylindrical RTFO bottle.
- The RTFO bottles were then placed on a rotating carriage in the oven. The carriage rotates at 15 revolutions per minute (rpm) for 85 minutes. During this time, the binder sample is constantly exposed to oxygen.
- After 85 minutes, the RTFO bottles are taken out of the oven and binder is transferred to PAV pans. Figure 25 shows the RTFO bottles before and after filling and after the RTFO ageing process.

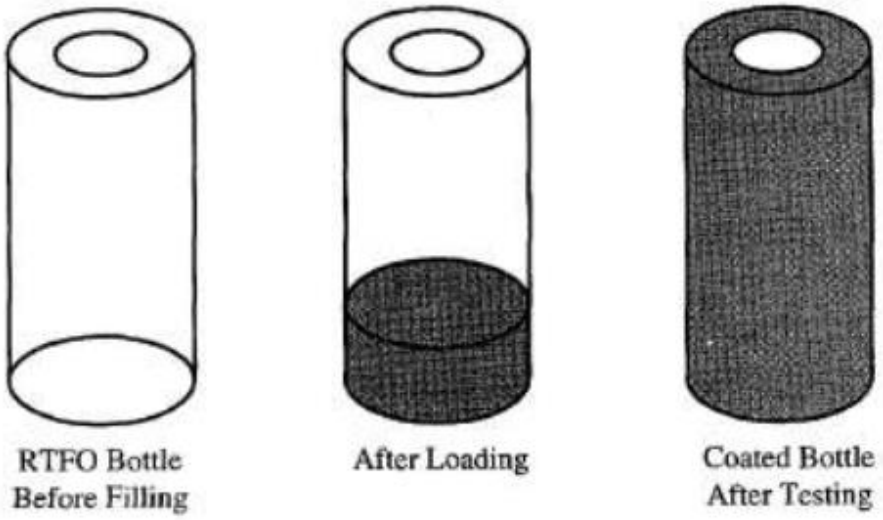

Figure 25. RTFO bottle before and after the RTFO ageing process [33].

3.4 Pressure Ageing Vessel (PAV)

The PAV procedure was conducted in a following sequence.

- Prior to aging, PAV oven was turned on and preheated to 100^{o}C.
- About 50g of RTFO aged asphalt binder was transferred to each thin stainless pan.
- The pans are then kept in a pan holder and then placed in PAV oven as shown in Figure 26.

Figure 26. Pressure Aging Vessel (PAV) and Pan Holder [65].

- The binder is aged for 20 hours at 100^{o}C and 2.1 MPa of airflow.
- At the end of aging process, pressure was gradually decreased to 0 MPa and the binder samples were transferred to a separate beaker for further testing.

3.5 Dynamic Shear Rheometer

The main purpose behind this testing procedure was to investigate the resistance of the original and recovered asphalt binder samples to rutting and fatigue cracking at higher and intermediate temperatures respectively. This test was performed on recovered, unaged, RTFO and PAV aged binder samples. The test was performed in a following sequence.

- The asphalt binder is heated until it is fluid enough to flow and pour.
- The binder is then poured into the silicon mould and cooled until it solidifies.

- Prior to the placement of the sample between the test plates, the test temperature, frequency (i.e., 10 radians per second) and loading ting time is selected based on the type of the asphalt binder (i.e. unaged, RTFO or PAV).
- The upper and bottom plates are preheated to the selected test temperature.
- The sample is then placed between the test plates.
- The test plates are brought sufficiently closer until the gap equals 1500 micrometers (for RTFO and unaged binder) and 2100 micrometers (for PAV aged sample).
- The sample is then trimmed around the edges.
- The gap between the test plates is selected at 1000 micrometers (for RTFO and Unaged asphalt binder) and 2000 micrometers (for PAV aged sample).
- The sample is then heated or cooled to the testing temperature.
- Once the binder sample is at the desired temperature, the test is started.
- Sample is conditioned for 10 cycles at the frequency of 10 radians per second.
- The measurements are then taken over the next ten cycles and the data is then reduced by the software to yield a value of complex modulus and phase angle.

3.6 Extended Bending Beam Rheometer (EBBR)

The extended BBR is used to characterize the low temperature behavior of asphalt cement. The test was performed in a following sequence.

- The asphalt sample was heated at 163^{o}C until it was sufficiently fluid to flow.
- The binder samples were then poured in silicon molds.
- Samples were then left to condition at room temperature for half an hour.

- After 30 minutes, the excess binder was trimmed along the edges of the mold using a heated knife.
- The sample beams were then placed in a sub-zero temperature for 5 seconds in order to further solidify so that they would be easier to take out for molds.
- Prior to testing, BBR is first calibrated. A thick rigid stainless steel reference beam is used to calibrate the load cell and the deflection transducer. The temperature transducer is calibrated using a thermometer. The equipment is supplied with thin stainless steel reference beam. It can be used periodically to check the overall system.
- Sample beams were then conditioned and tested after 1 hr, 24 hours and 72 hours. The conditioning temperatures are 10^{o}C and 20^{o}C higher than the low temperature grade of the binder.
- After 1 hr, sample beams were taken out of the conditioning bath and placed and left in a testing bath for 10 minutes.
- After 10 minutes, the sample beam was placed on beam supports and the test was initialized.
- At first, BBR subjects the asphalt through some load conditioning steps. Initially, a load of maximum 35 mN is applied to ensure beam's firm contact with supports. Then, a 250 mN load applied for 1 second. After which, the load is again reduced to 35mN. This load is applied for 20 seconds. Once the load conditioning is completed, a load of 250 to 300 mN is applied for 240 secs
- The instrument measures the asphalt beam deflection over time as a result gives creep stiffness and m-value at 60 secs in an output. The creep stiffness should not exceed 300 MPa and m-value should not be more then 0.3.

- Limiting grades can be obtained by interpolation or extrapolation plotting them on a semi-logarithmic scale.

3.7 Double Edge Notched Tension Test

Double Edge Notched Tension Test (DENT) provides a measure of strain tolerance in the area of high stress concentration in a non-linear regime. This test was performed in a following sequence.

- The DENT test equipment was turned on and the testing temperature was adjusted at 15^{o}C.
- The PAV aged asphalt binder residue was heated at 160^{o}C for one hour. Then, it was sufficiently stirred until it was fluid enough to pour.
- The asphalt binder was then poured into 3 silicon molds of ligament lengths 5, 10 and 15 mms between the stainless steel inserts as shown in Figure 27.

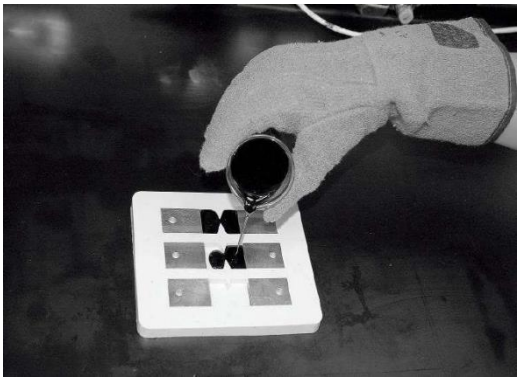

Figure 27. Sample Preparation for Dent Test [67].

- These asphalt beams are first conditioned for 20 minutes at room temperature and then for 3 hours in a testing bath at 15^{o}C.
- After 3 hours, sample beams are carefully taken out of molds in order to prevent any distortion of beams and thereby loaded onto pins as shown in Figure 28.

Figure 28. Dent Test Beams Loaded on Tesing Pins [68].

- The test is then initiated. All 3 ligaments are pulled apart at a constant speed of 50 mm/min until the fracture occurs.
- LS 299 Dent test protocols prescribe the use of duplicated beams for the same sample under the same testing conditions and parameters in order to ensure accuracy and reproducibility in the test results.
- The essential parameters such as essential work of fraction W_e, plastic work of fracture W_p and the critical crack tip opening displacement (CTOD) were determined with the help of instrument software and Excel spreadsheet.

3.8 X-Ray Fluorescence (XRF)

The X-ray Fluorescence (XRF) analysis was conducted on all straight and recovered asphalt samples to ascertain the existence of waste engine oil in asphalt pavements. This can be confirmed from the detection of zinc and molybdenum levels in asphalt samples [69].

The immediate benefit behind the addition of this modifier in asphalt cement is through a "partial precipitation of asphaltene fraction when the base asphalt is blended with this largely paraffinic material." [69]

Zinc is found in engine oil in the form of zinc dialkyldithiophosphate (ZDDTP). It is a "universal oxidant and an anti-wear additive."[70] Large amount of metals exist in engine oil as they catalyze the chemical oxidation process in asphalt thereby leading to poor field performance.

The process makes use of a handheld Bruker Instruments Tracer III XRF analyzer. It irradiates the material surface with the high energy X-rays [69]. It causes the ejection of inner K shell electrons from heavy elements. The resultant vacant spaces are re-occupied by the electrons from the outer L and M shells. The exit of electrons from the outer shells results in the emission of low energy X-rays that have a characteristic energy for the element being detected. This emitted radiation is then detected by the XRF analyzer and a plot of intensity vs X-ray energy is generated.

The asphalt samples were collected in Ziplock bags and placed on XRF scanner. The samples were then subsequently scanned for 20 seconds and the Zinc and Molybdenum levels in all asphalt samples were normalized to the levels in Safety-Kleen and Newalta engine oil residue.

3.9 Fourier Transform Infra-Red Spectroscopy (FTIR)

FTIR test was performed on all straight and recovered asphalt samples. For the purpose of analysis, a small amount of asphalt sample was taken using a heated spatula and then smeared on a preheated potassium bromide (KBr) disc. Prior to sample preparation, KBr disc was preheated at 140 ^{o}C for 3 minutes. The KBr disc coated with asphalt was then placed in the spectrometer and was scanned 16 times. Prior to each sample scan, FTIR spectrometer was calibrated by running a background scan. After the sample scan, a detailed data analysis was conducted by using Perkin Elmer Spectrum software. The software calculates an area under the peaks corresponding to the targeted functional groups [71]. These areas are then converted into the ratio of the peak area under functional to the area under CH_2 peak. The CH_2 functional group is used as an internal standard since it is highly inert to the oxidation processes as compared to the methyl (CH_3) group. These functional groups are typically targeted as they are found abundantly in asphalt and their content helps us identify major changes to the asphalt sample such as oxidation, polymer addition and the addition of recycled engine oil. These processed have been increasingly identified as the root cause of increased low temperature cracking and physical hardening in asphalt. These functional groups, their corresponding wavenumber

ranges and their significance in relation to above mentioned phenomena is given below [71].

- Carbonyl - 1760 cm^{-1} – 1665 cm^{-1}- increased content of this functional group represents a strong oxidation in asphalt sample. Its increased presence at the asphalt binder-aggregate interface makes the asphalt pavement highly prone to moisture damage.
- Sulfoxides-1070 cm^{-1} – 985 cm^{-1}- The presence of this functional is also an indication of oxidation process but is rather weaker indicator as compared to carbonyl group. The increased amount of Sulfoxides and Carbonyl also represent the existence of increased of asphaltenes insoluble in maltene content.
- Aromatics- 1650 cm^{-1} – 1535 cm^{-1}- Increased amount of aromatic content in asphalt is a positive indicator in relation to the pavement performance as it acts as a peptizer for the asphaltene content and thereby indicate possibility of a sol-type structure.
- Styrene- 710 cm^{-1} – 696 cm^{-1} and Butadiene- 983 cm^{-1} – 955 cm^{-1} are both positive indicators as their presence show the addition Styrene- Butadiene- Styrene (SBS) type polymer modifier, which is known to significantly enhance the pavement performance.
- Polyisobutylene – a strong indicator of the waste engine oil addition as it is a dispersant found in high concentrations in recycle engine oil.

Chapter 4

Results and Discussions

4.1 Double Edge Notched Tension Test (DENT)

The DENT test uses the essential work of fracture (EWF) method to determine the strain tolerance and the failure characteristics of the asphalt binder under a ductile state. It is "based on the energy analysis during yielding, necking and tearing processes that occur during the ductile failure." According to this method, the total work of fracture or total fracture energy (W_t) can be defined as an area under the load displacement curve. According to EWF method, this total fracture energy can be divided into the essential work of fracture (W_e) and the plastic work of fracture (W_p). The essential work represents the energy required for the fracture process. It is "surface related" [7] and is essentially a material property [72]. The plastic work of fracture on the other hand is "volume related" and "may involve single or various dissipation mechanisms" [7]. According to LS 299 protocol, test samples are first conditioned for 15 to 20 mins at room temperature and then in a testing bath at 15^{o}C for 3 hours. Then the sample specimens with ligament lengths of 5, 10 and 15 mm and the notches of 2.5, 5 and 7.5 mm are pulled apart at 50

mm/min until they fail. Then, a specific total work of fracture is determined from the area under the load displacement curve. This specific total work of fracture is then plotted against ligament lengths and is then extrapolated to a zero ligament length to obtain specific essential work of fracture. The slope from the same plot gives the specific plastic work of fracture times the shape factor β [73].

The shape factor is a scaling factor that describes the shape of the plastic zone [7]. The underlying assumptions behind EWF model are [7]:

- Load displacement diagrams for all ligaments from the same sample need to be similar in appearance.
- Ligaments need to be fully yielded before cracking starts
- The volume of the plastic zone is proportional to the square of the ligament length multiplied by the sample thickness

4.1.1 DENT Test Analysis of 8 Straight and Recovered Asphalt Samples

The following Figures 29 and 30 clearly show that sample specimens show similar pattern in terms of necking, yielding and tearing processes, as we proceed in the diagram from ligament to ligament; however, this same reproducibility is not apparent when the individual samples are compared.

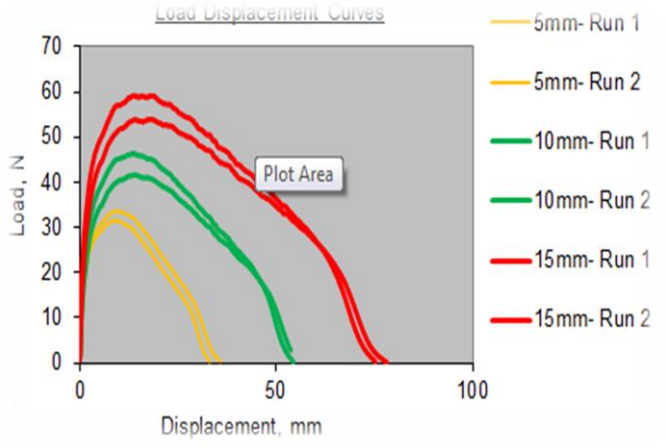

M1R Load Displacement Diagram

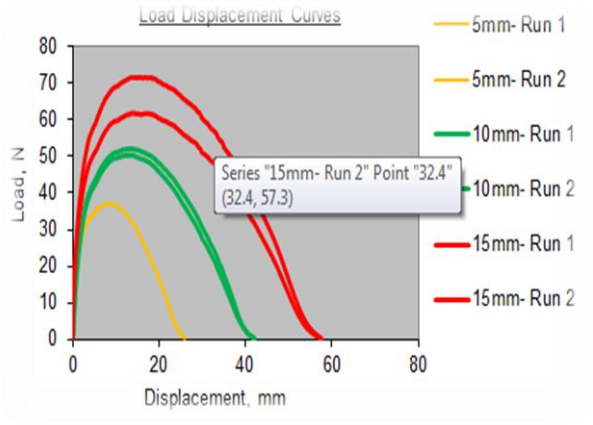

M2R Load Displacement Diagram

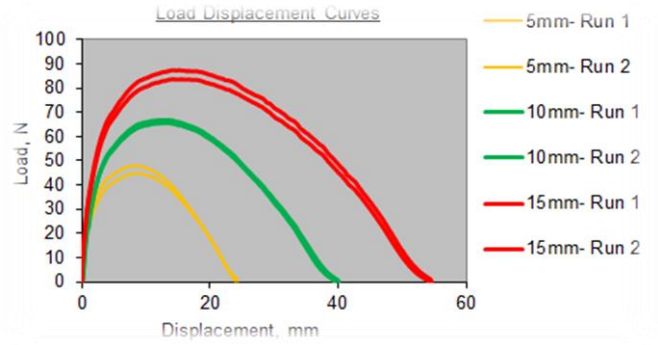

M3R Load Displacement Diagram

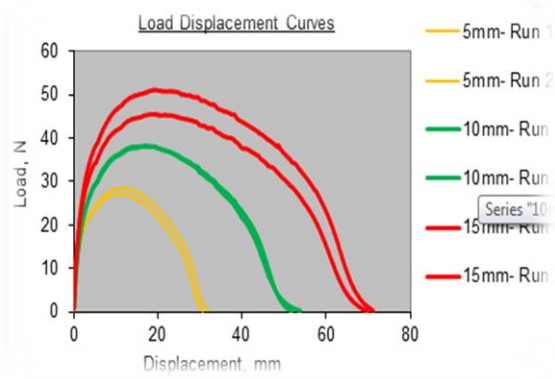

M4R Load Displacement Diagram

Figure 29. Load-Displacement Diagrams of recovered asphalt samples

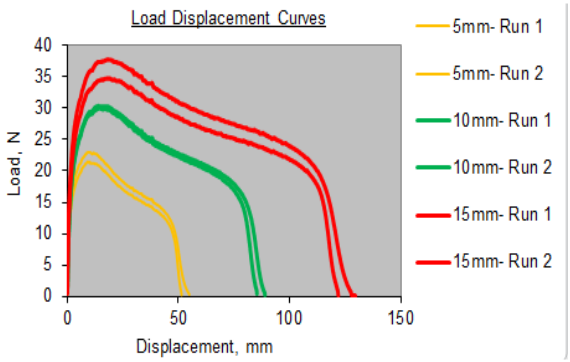

M5T Load Displacement Diagram

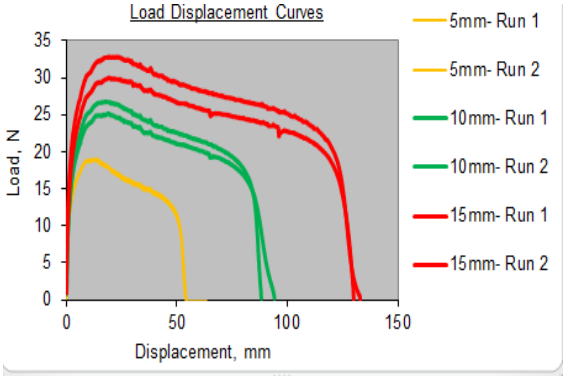

M6T Load Displacement Diagram

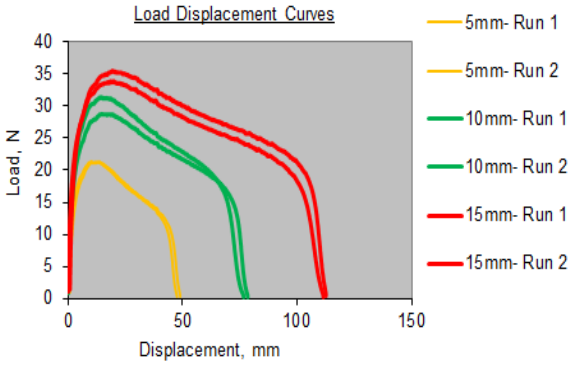

M7T Load Displacement Diagram

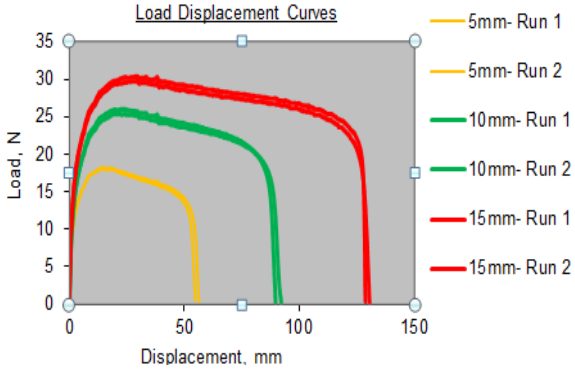

M8T Load Displacement Diagram

Figure 30. Load Displace Diagrams for straight tank samples

The apparent difference between the samples can be attributed to variety of factors such as source, composition and the way the samples were prepared [73]. It is also apparent from the above load displacement curves that all samples yielded fully prior to failure, which is evident from a sudden drop in load at the end of each test [7]. The EWF method gives a measure of energy required to pull apart tiny fibril of material when the binder is

subjected to high confinement [73]. It is a material property, which is independent of the geometry of the specimen as far as the performance grading of asphalt binder is concerned [71]. The plastic work of failure on the other hand is not a material property and is rather related to the mixture design, asphalt binder content and air voids. Asphalt mixtures rich in binder content generally have a higher plastic work of fracture and as a result exhibit high stain tolerance. Therefore, it is expected that both the essential and plastic work of fracture should be relatively high in order to provide a good resistance toward fatigue and low temperature cracking. The following Figures 31 and 32 contain the relative essential and plastic work of fracture of straight and recovered asphalt samples.

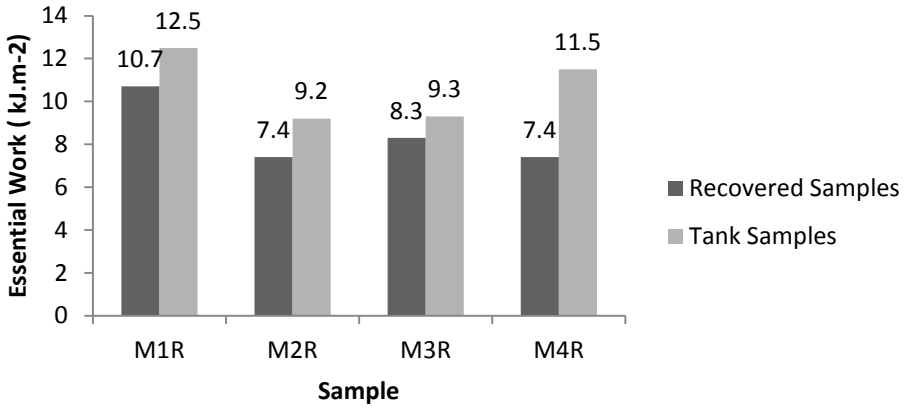

Figure 31. The essential work of fracture of straight and recovered MTO samples

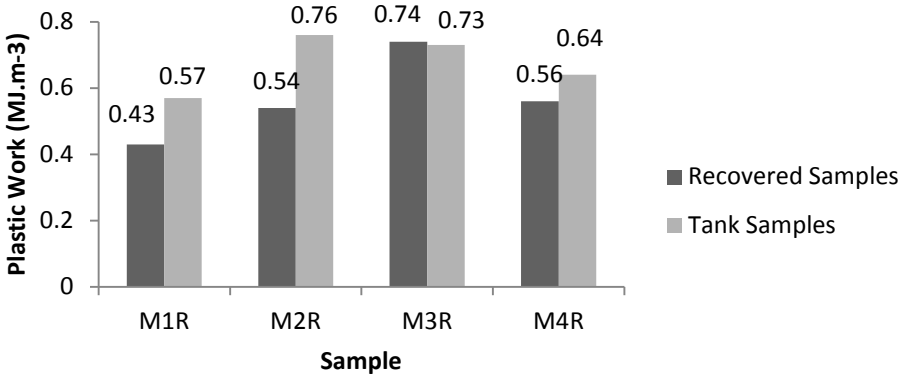

Figure 32. Plastic Work of fracture of straight and recovered asphalt sample

The main purpose of this study was to compare the properties of the asphalt binder samples recovered from the field with their corresponding tank samples. It is quite evident from the above Figures 31 and 32 that the recovered samples performed more poorly as compared to their corresponding tank samples both in terms of essential and plastic work of fracture. For instance, M1R with the w_e of 10.7 and w_p of 0.43 shows low strain tolerance relative to its tank sample M5T with w_e of 12.5 and w_p of 0.57. Similarly, M2R with w_e of 7.4 and w_p of 0.54 shows low strain tolerance when compared to its tank sample M6T with w_e of 9.2 and w_p of 0.76. The other recovered samples M3R and M4R show a similar trend when compared to their corresponding tank samples M7T and M8T, respectively. Thus, the recovered binders are more sensitive to the pavement distresses as compared to their corresponding tank samples due to their low essential and plastic work of fracture. In terms of EWF, M1R has the highest strain tolerance among the recovered samples with a w_e of 10.7. Similarly, M5T exhibits highest strain tolerance among tank samples in terms of EWF with a value of 12.5. In terms of plastic work of fracture, M3R and M6T have the highest strain tolerance among recovered and tank samples with the values of 0.74 and 0.76 respectively.

LS 299 DENT test protocol introduce another parameter called a critical crack tip opening displacement (CTOD). It is calculated by dividing the specific essential work of fracture with the net section stress corresponding to 5 mm ligament. It gives "a measure of strain tolerance in the ductile state under the conditions of severe confinement" [31]. This parameter is expected to provide better correlation with the field performance at the time of ductile failure in asphalt pavement when the binder and mastic are highly confined between the course aggregate particles. This parameter is used as specification criteria for assessing Ontario's asphalt pavement in their resistance towards fatigue cracking. Higher CTOD values are desired as they provide "more room for the fibril for stretching before failure occurs" [72]. MTO sets lower limits on CTOD values based on the low temperature grades of asphalt binders. PG -28 should have a CTOD of at least 15 mm, PG -34 should have at least 20mm and PG-40 should have a CTOD of 40 mm [71]. The following Figure 33 provides a clear picture of the strain tolerance of recovered and tank asphalt samples in terms of their CTOD values.

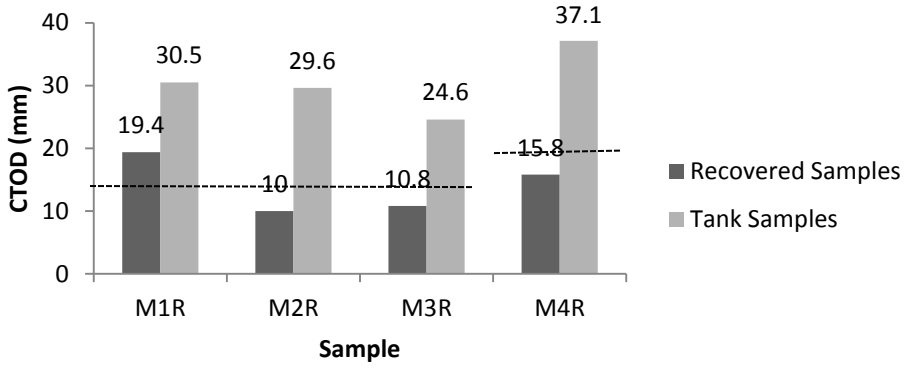

Figure 33. CTOD values of the recovered and the straight asphalt samples.

In the above figure 33, both black dotted lines correspond to the Ministry imposed CTOD limits of 20 and 15 mm for low temperature grades of -28^{o}C and -34^{o}C, respectively. The above diagram clearly demonstrates that the recovered binder samples perform very poorly as compared to their tank samples. Except M1R, all other recovered binder samples poorly fail DENT test as their CTOD values are falling below the Ministry imposed limits. Even M1R is barely passing this test with a value of 19.4 being very close to its corresponding Ministry imposed limit of 15 mm. Thus, all recovered samples have very low strain tolerance meaning that they are highly sensitive to the premature cracking as they fail to meet even minimum criteria regarding their performance under a ductile state. On the contrary, it can be easily seen that tank asphalt samples behave very well in terms of their performance. It can be clearly seen that CTOD of all tank samples are above their corresponding Ministry imposed limits. Thus these samples are highly resistant to premature cracking due to the higher CTOD values above the Ministry imposed limits.

4.1.2 DENT test Analysis of 11 contract samples

4.1.2.1 Analysis at 15^{o}C

The following Figure 34 shows the load displacement diagram of 11 contract samples.

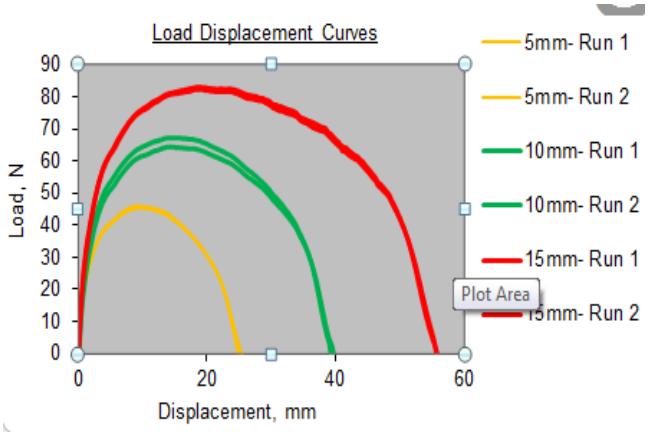

D1 Load Displacement Diagram

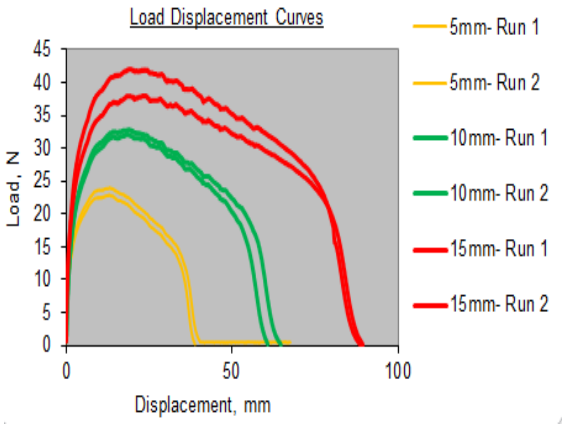

D2 Load Displacement Diagram

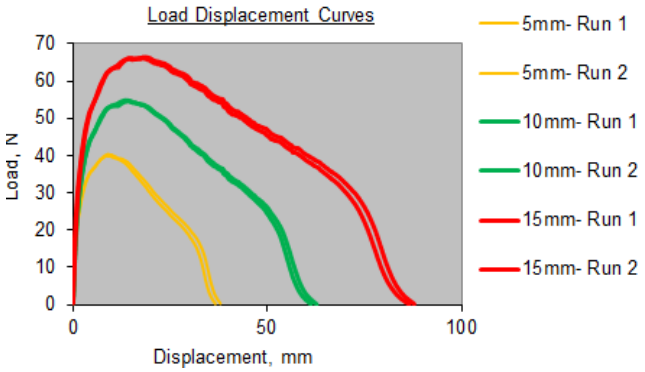

D3 Load-Displacement Diagram

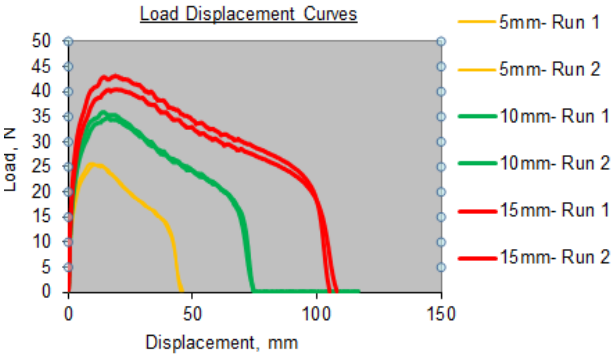

D4 Load Displacement Diagram

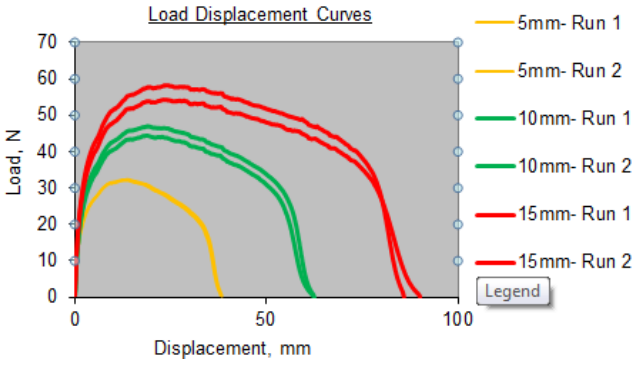

D5 Load Displacement Diagram

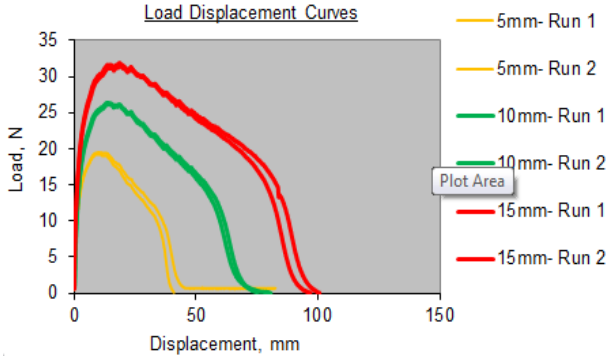

D7 Load Displacement Diagram

Figure 34. Load Displacement Diagrams of six contract samples

It is quite evident from the above load displacement diagrams that sample specimens show similar behavior in terms of necking, yielding and tearing processes as we move in the diagram from ligament to ligament [7]. However, this behavior is different if we compare samples. It is also apparent from the above diagrams that samples yielded fully prior to failure, which is evident from a sudden drop in the load at the end of the test. The following Figure 35 shows the comparison of the essential work of fracture among the contract samples

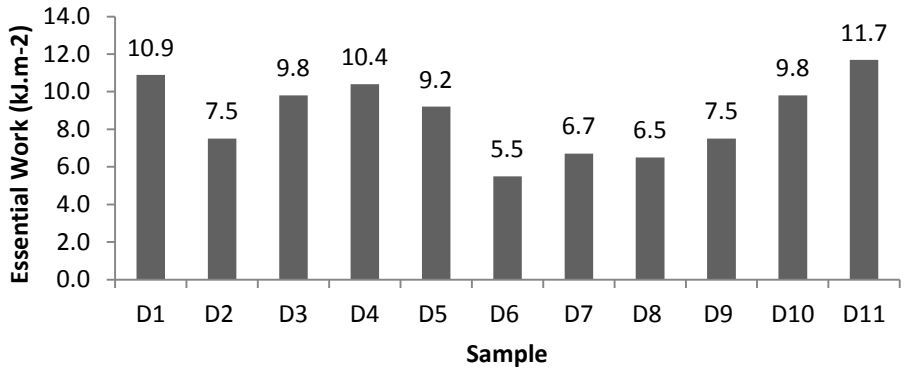

Figure 35. Comparison of essential work of fracture at 15^{o}C.

The essential of fracture gives a measure of energy required to pull apart a tiny fibril of material in a confined state [73]. It is a material property that is independent of the geometry of the specimen as mentioned previously. Sample D11 shows the highest strain tolerance among the contract samples in terms of the essential work of fracture with a value of 11.7. Sample D6 ranks lowest among the contract samples in terms of essential work of fracture with a value of 5.5. The following Figure 36 shows the comparison of the plastic work of fracture at 15^{o}C.

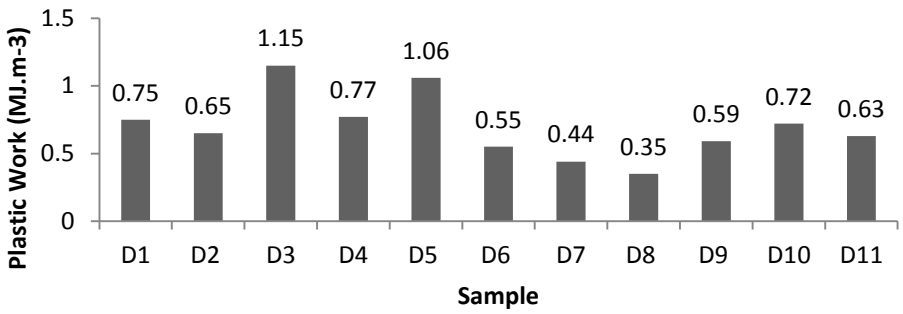

Figure 36. Comparison of the plastic work of fracture at 15^{o}C

The plastic work of fracture is not a material property and thus is related to the mixture design, air voids and binder content. The asphalt mixtures rich in binder content will show higher strain tolerance in terms of plastic work of fracture [71]. As mentioned previously, it is generally expected that samples with both higher essential and plastic work provide good resistance to fatigue and low temperature cracking. If this criteria is considered to rank the asphalt binders due to their performance in terms of both essential and plastic work of fracture, D3 and D5 are the best performing samples with an essential work of fracture values of 9.8 and 9.2, respectively and the plastic work of fracture values of 1.05 and 1.06, respectively. Under this new criteria, D6 and D8 are the least performing samples with the essential work of 5.5 and 6.8 and the plastic work of fracture of 0.55 and 0.35.

However, CTOD provides a clearer picture of asphalt binders strain tolerance, as it gives "a measure of strain tolerance in the ductile state under the conditions of severe confinement" [31]. Figure 37 shows the CTOD comparison at 15^{o}C. These values are also assessed against MTO's imposed CTOD limits.

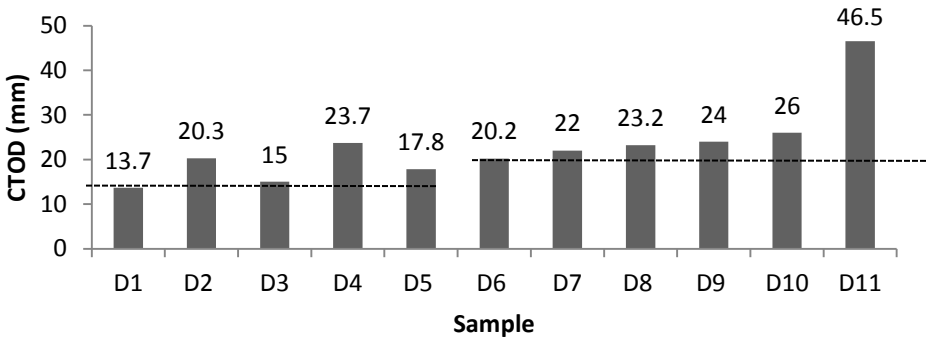

Figure 37. CTOD comparisons at 15^{o}C

In the above diagram, the both black dotted lines correspond to the Ministry imposed limits of 15 mm and 20 mm. Samples from D1 to D5 have a low temperature grade of -28^{o}C and thus will be assessed against 15 mm CTOD limit and samples from D6 to D11 have a low temperature grade of -34^{o}C and thus will be assessed against CTOD limit of 20 mm. It is evident that the first 5 samples pass the DENT test except D1, which fails with CTOD of 13.7 mm. This value is below the Ministry imposed limit of 15mm. Among these first 5 samples, D4 has the highest CTOD value of 23.7 mm. We can clearly see that sample D3 just barely passes the test with a CTOD of exactly 15 mm. Among the last 6 samples, D11 has the highest value of 46.5 mm. In fact this is the highest value among all samples. This performance can be due to the possible polymer modification as indicated from its performance grade -34P, which gives it an added elasticity. All other samples in -34 grade group pass the test; however they have CTOD values very close to the ministry imposed limit of 20 mm.

4.1.2.2 Analysis at 20°C

The following Figure 38 show load displacement curves at 20°C.

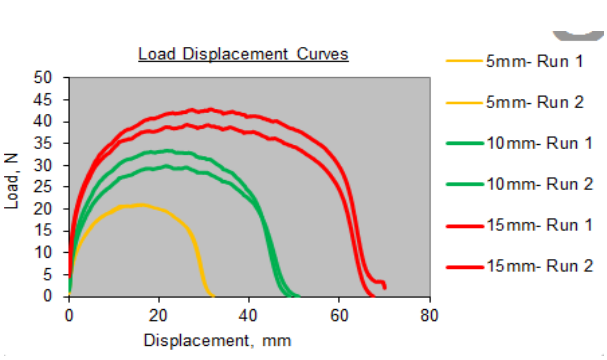

D1 Load Displacement Diagram

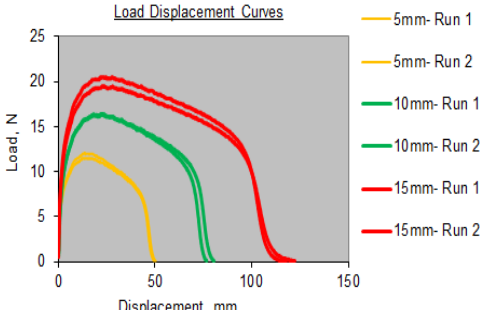

D2 Load Displacement Diagram

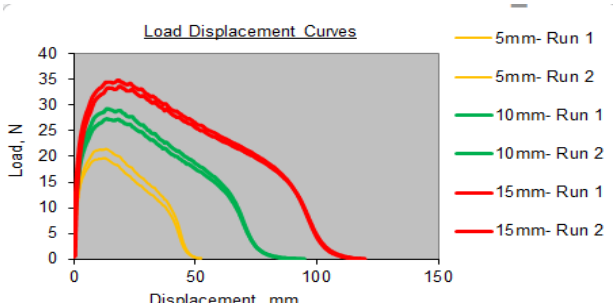

D3 Load Displacement Diagram

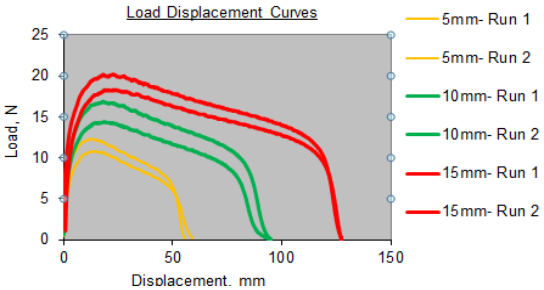

D4 Load Displacement Diagram

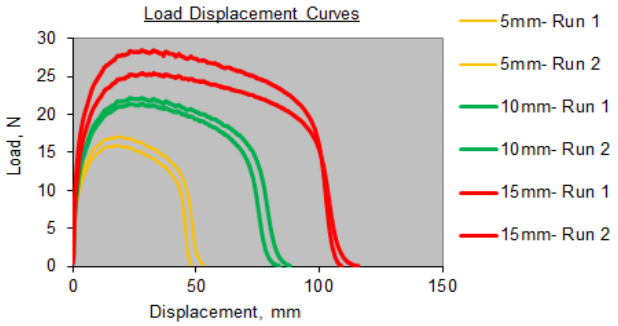

D5 Load Displacement Diagram

Figure 38. Load Displace Diagrams of 5 Contract Samples

The above load displacement curves show a self-similar behavior as individual ligament curves follow a similar pattern in terms of necking, yielding and tearing processes. However, this behavior varies significantly among samples. These samples yield fully prior to failure as indicated by a sudden drop of load at the end of each process [7]. The following Figure 39 and 40 shows the comparison of the essential and plastic work of fracture at 20^{o}C.

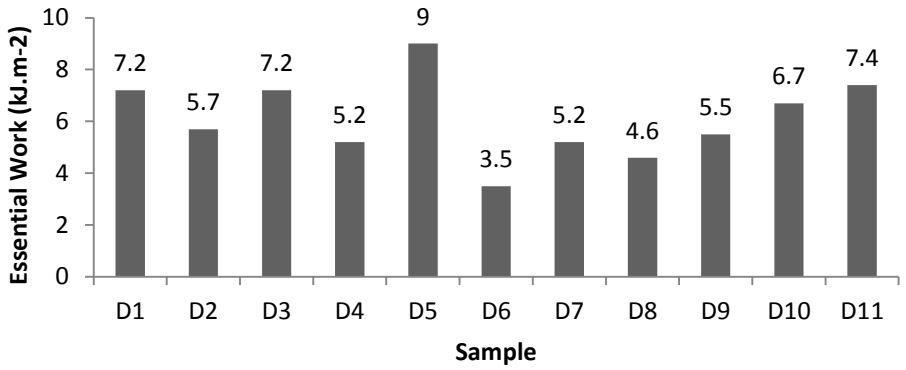

Figure 39. The essential work comparison at 20^{o}C.

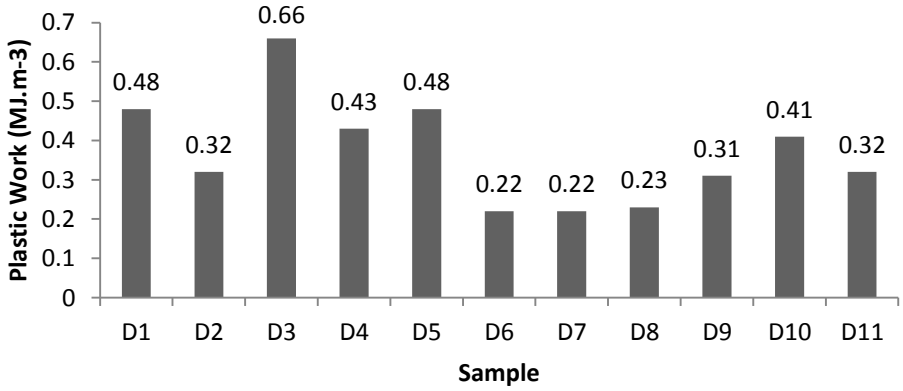

Figure 40. The plastic work comparison at 20^{o}C.

From Figure 39, it is quite evident, that sample D5 ranks highest in terms of the essential work of fracture followed by samples D1, D3 and D11 with the values of 7.2, 7.2 and 7.4 mm; whereas, D6 ranks lowest with the essential work of 3.5. In terms of plastic work of fracture, D3 ranks highest followed by D1 and D5 with 0.48. D6 and D7 have lowest strain tolerance in terms of plastic work with the values of 0.22. As mentioned before that it is generally expected for the samples with higher values of both essential and plastic work of fracture to provide better resistance to fatigue. It is quite evident from both figures that samples D1, D3 and D5 seem to fulfill these criteria with the higher values of both essential and plastic work of fracture. However, it is CTOD value that simulates the actual fatigue phenomenon more effectively, as experienced by the pavements in the field. Figure 41 (below) shows CTOD comparison at 20^{o}C.

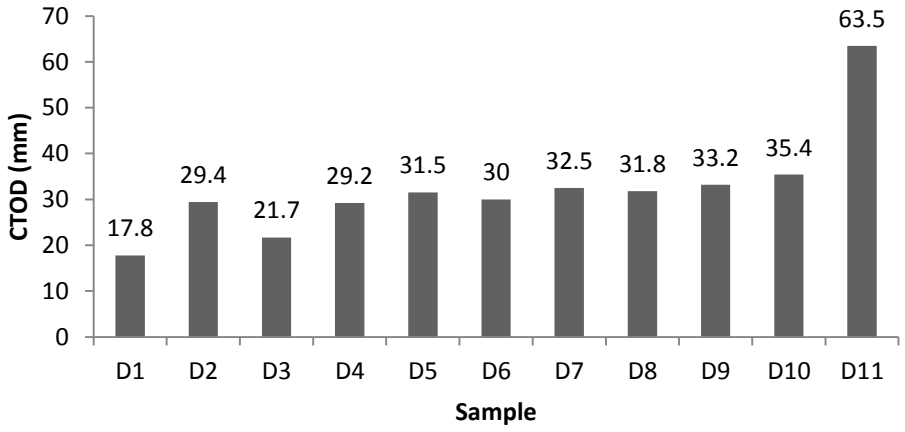

Figure 41. CTOD comparison at 20^{o}C

Figure 41 demonstrates that sample D11 shows a highest strain tolerance with CTOD value of 63.5 mm. This superior performance in ductility can be attributed to its

possible polymer modification as indicated by letter ‘P’ with its low temperature grade. Sample D1 shows a lowest strain tolerance with CTOD value of 17.8 mm.

4.1.2.3 Analysis at 25 ^{o}C

The following figure 42 shows the load displacement curves at 25 ^{o}C. It is quite apparent from the diagram below that the load displacement diagram from the same sample belonging to different ligaments are similar in shape and all specimens yield fully prior to failure except sample D1. This peculiar behavior can be attributed to the irregularities and possible errors during the experimental procedure. Thus, all the underlying assumptions or requirements of EWF models have been fulfilled. This dent analysis involves all samples with a low temperature grade of 28^{o}C.

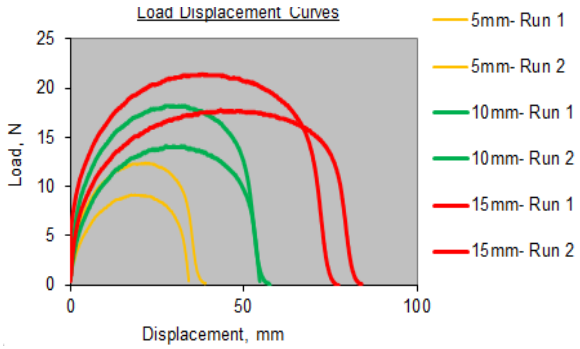

D1 Load Displacement Diagram

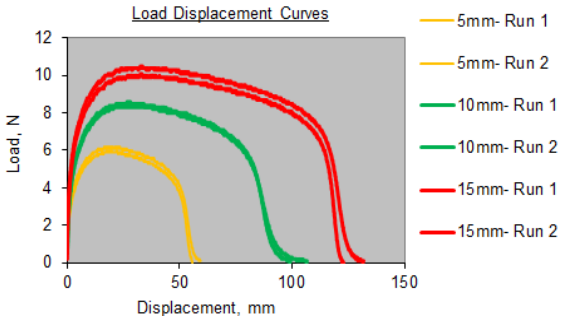

D2 Load Displacement Diagram

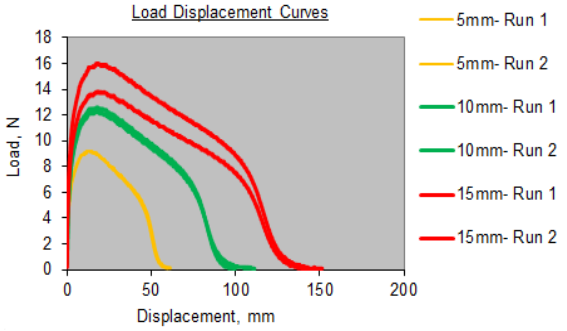

D3 Load Displacement Diagram

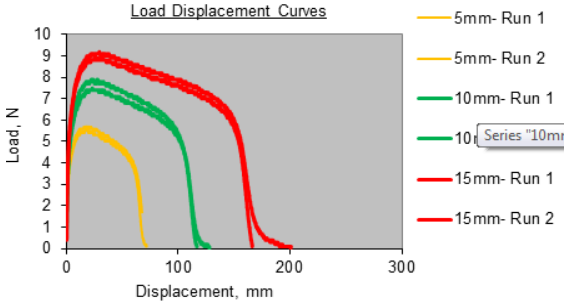

D4 Load Displacement Diagram

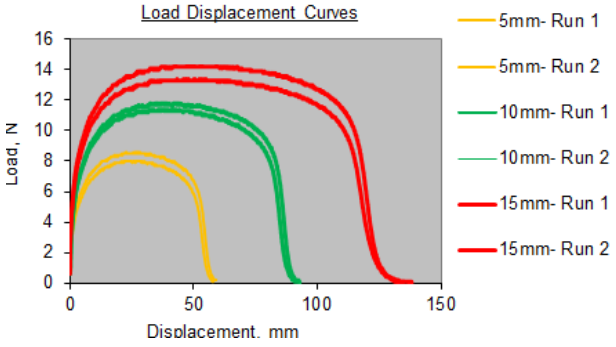

D5 Load Displacement Diagram

Figure 42. Load Displacement Diagram at 25°C

The following Figures 43 and 44 show the comparison of the essential and plastic work fracture at 25^{o}C.

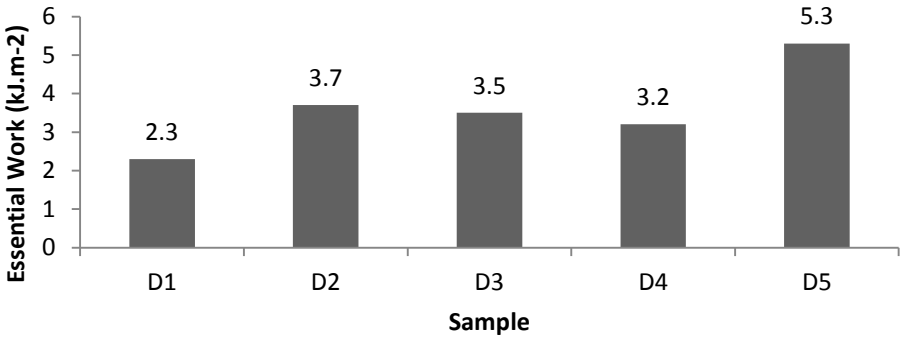

Figure 43. The essential work of fracture at 25^{o}C

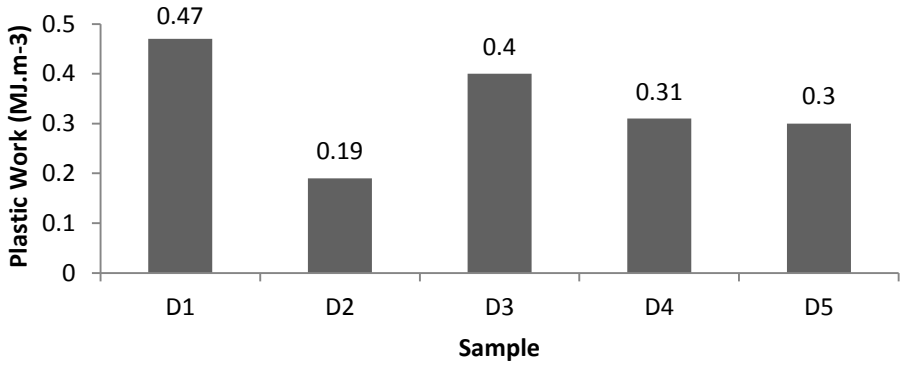

Figure 44. The plastic work of fracture at 25^{o}C

It is quite obvious from the above Figure 43 that the sample D5 shows a highest stain tolerance in terms of the essential work of fracture with a value of 5.3; whereas, D1 shows a least amount of strain tolerance with a value of 2.3. Thus, D5 offers a good resistance to fatigue cracking, whereas D1 is most susceptible to fatigue distress in terms

of the essential work of fracture. In terms of the plastic work of fracture, D1 ranks highest among all samples with a plastic work of fracture of 0.47 and D2 displays the lowest strain tolerance in terms of plastic work of fracture. However, the plastic work fracture is the non-essential term in terms of assessing strain tolerance and the essential work of fracture and CTOD are most relevant in terms of evaluating the resistance of asphalt cement to fatigue distress as experienced by the pavements in the field [74]. The following Figure 45 contains the CTOD comparison at 25^{o}C.

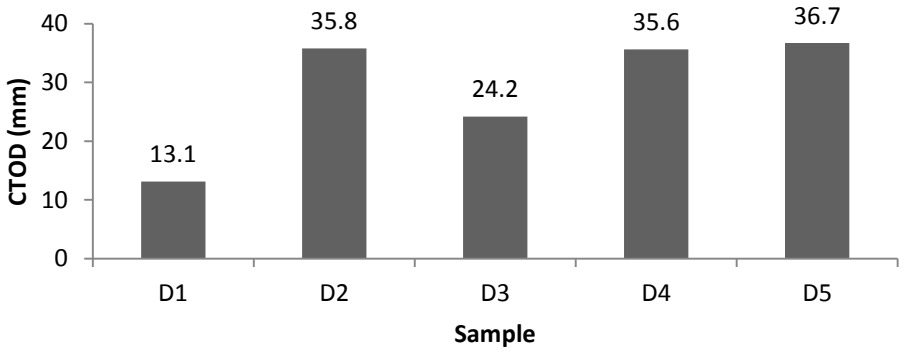

Figure 45. CTOD comparison at 25^{o}C

Samples D5, D4 and D2 show a highest resistance to fatigue cracking with CTOD values of 36.7, 35.6 and 35.8 mm respectively and Sample D1 is most susceptible to fatigue with a lowest CTOD value of 13.1 mm. CTOD offers a more accurate depiction of an actual fatigue distress phenomenon in the field.

4.1.2.3 Analysis at 10^{o}C

The following Figure 46 contains load-displacement diagrams of 3 samples tested at 10°C. This analysis was performed on samples with a lower temperature grade of -34°C

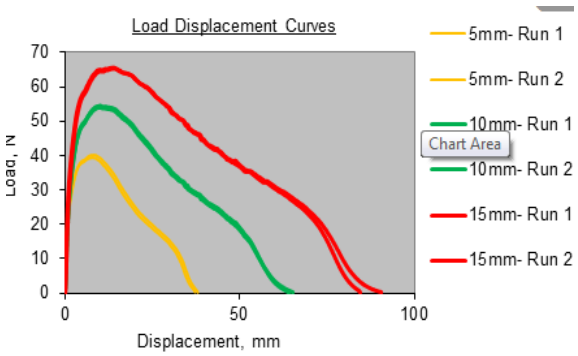

D6 Load Displacement Diagrams

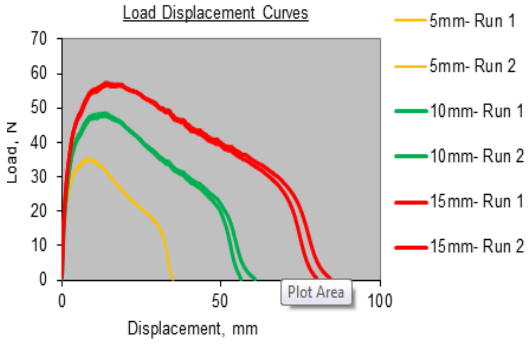

D7 Load Displacement Diagram

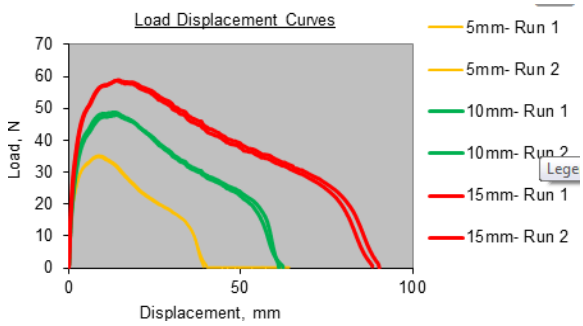

D8 Load Displacement Diagram

Figure 46. Load Displacement Diagrams of 3 samples at 10°C

The above load displacement diagrams of different ligaments from the same sample show a similar behavior yet different from other samples. Each specimen yields fully prior to failure as indicated by the sudden drop in the load at the end of each process. The following Figures 47 and 48 contain the comparison of essential work and the plastic work of fracture at 10°C.

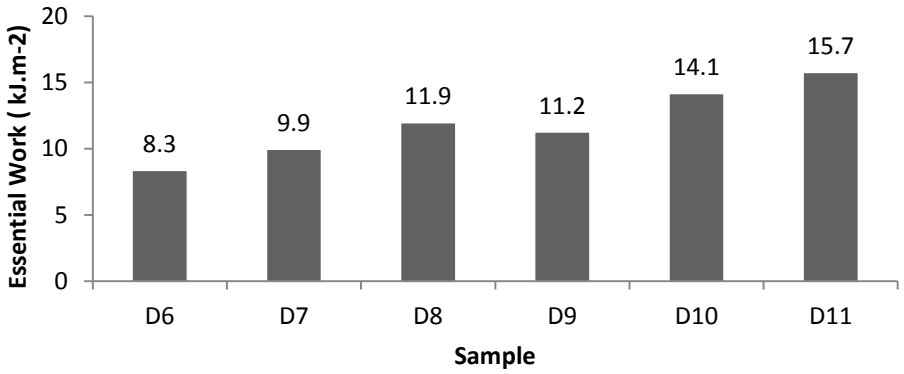

Figure 47. Comparison of the essential work of fracture at 10°C

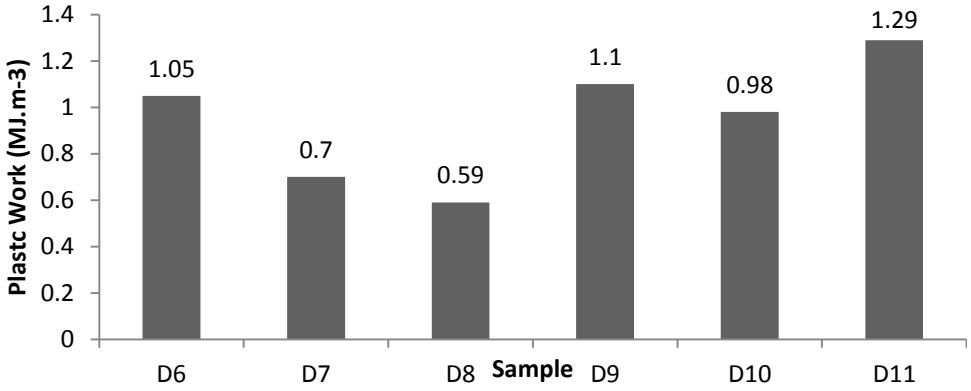

Figure 48. Comparison of the plastic work of fracture at 10°C

Sample D11 displays a highest strain tolerance and a greater ability to resist fatigue cracking in terms of essential work of fracture with a value of 15.7 among all other samples tested at this temperature. Sample D6 displacement showed the worst performance among all samples tested and thus is most susceptible to fatigue distress in terms of essential of fracture. Sample D11 again shows a highest performance in terms of plastic work of fracture with a value of 1.29. This performance of D11 at this temperature

is rather distinct from its performance at other temperatures where we did not observe a high performance in terms of both essential and plastic work of fracture. It thus displays superior characteristics and will offer good resistance to fatigue distress under these conditions with both higher values of essential and plastic work of fracture as expected generally from all asphalt binders [74]. Sample D8 shows worst strain tolerance in terms of plastic work of fracture with a value of 0.59. The following Figure 49 shows the CTOD comparison at 10^{o}C.

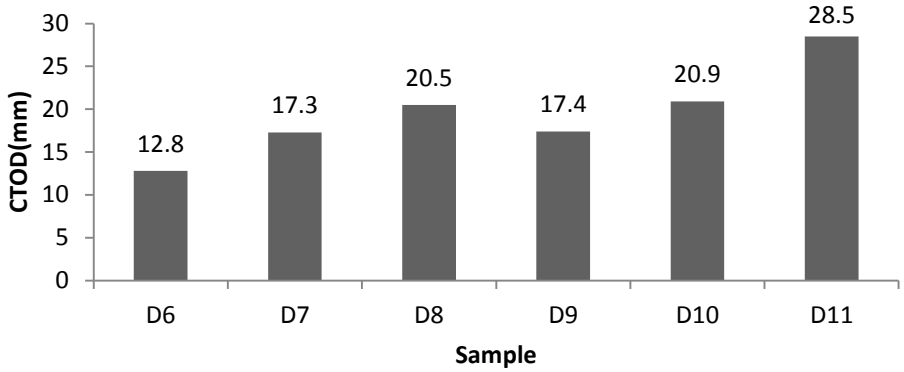

Figure 49. CTOD comparison at 10^{o}C

It is quite evident from Figure 49 above that sample D11 shows best performance in terms of its resistance to fatigue distress with a CTOD value of 28.5. These characteristics can be attributed to its possible polymer modification as indicated by its low temperature performance grade of -34P. The high resistance of this sample to fatigue cracking is not only evident at this temperature but it has been consistently showing highest performance at all other temperatures. Sample D6 shows worst performance in terms of CTOD with a value 12.8 mm. It is thus most susceptible to fatigue distress among all the samples tested at this temperature.

4.1.2.4 CTOD analysis at different temperatures

This section seeks to investigate the application of current CTOD requirements at temperatures other than 15°C, which have been specified in the current LS 299 dent test protocols. For this purpose, the variation of CTOD with temperature was studied to find the correlation between the two variables as shown in the following Figure 50.

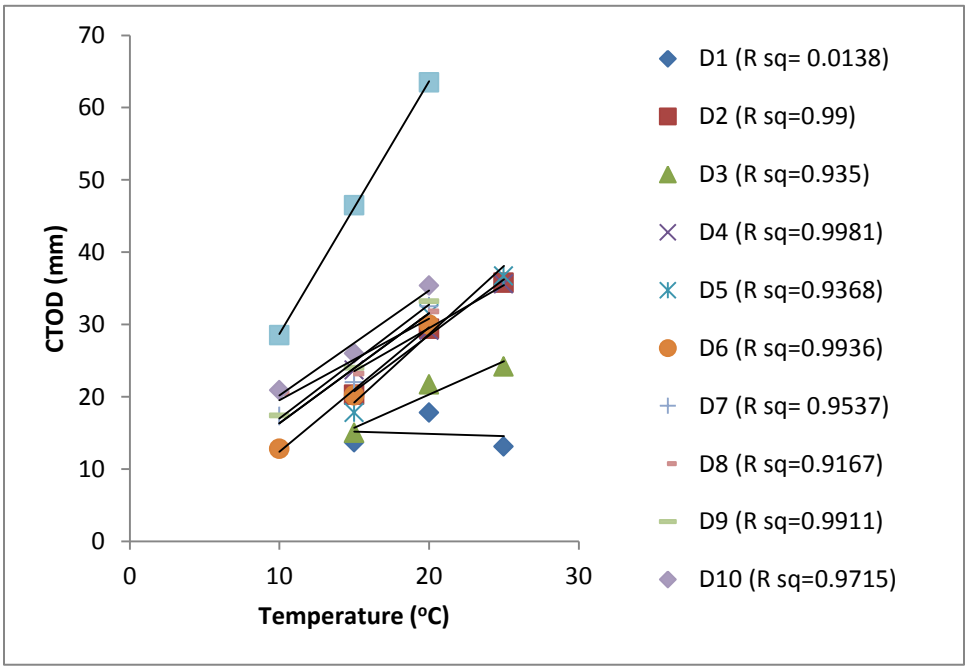

Figure 50 Study of the CTOD (mm) correlation with temperature (°C)

It is quite evident from Figure 50 that samples with the exception of D1 show a strong correlation of CTOD values with temperature as R^2 for all samples except D1 range from 0.9167 for D8 to 0.9997 for D11. D1 has an extremely low R^2 value 0.0138. This

deviation from a strong relationship between CTOD and temperature can be due to the experimental errors and imperfection such as error in sample preparation, inadequate conditioning time or to preparation of binder itself with the addition of modifiers that have a detrimental effect on the viscoelastic behavior of asphalt binder. In the light of these facts, it is quite evident that the current CTOD requirements at $15^{o}C$ can be applied at other temperatures.

4.2 XRF Analysis

The presence of trace metals such as zinc and molybdenum in asphalt binders is a strong indicator of the existence of the waste engine oil. Commercial engine oils contain zinc dialkylthiophosphate, "which is a universal anti-wear additive used in commercial engine oils" [Hesp, WEO detection in asphalt]. Molybdenum di sulphide is used in commercial engine oils. These compounds eventually make up their way in the residue from the re-refining of waste engine oil. This material is used as an extender in asphalt pavements. XRF has proven to an effective tool in the detection of these metals in asphalt binders. Since the emergence of Superpave grading system in North-America, several publications and patents have introduced cheaper and inexpensive ways of increasing the grade span of asphalt pavements through the addition of chemical agents such as waste engine oil (WEO) [69]. The work of the majority of these chemical agents is targeted towards the creation of gel- type binders with a reduction in the solubility of asphaltenes in a maltenes continuous phase. The binders produced from such methods as a result are "characterized by low stiffness, high zero shear viscosity, significant degrees of non-Newtonian flow and delayed elasticity" [Hesp etal. waste engine oil residue in asphalt

cement]. The use of WEO is the most cost-effective and a cheaper way to increase the asphalt grade span. However, the research has shown that with an increase in the engine oil, the binders with high levels of asphaltene content, become highly susceptible to physical and chemical hardening and binders produced this way tend to crack prematurely and excessively. This can be reflected in a grade loss of close to or over 6^{o}C in EBBR and significant decrease in ductility in terms of the loss of CTOD levels below the ministry imposed limits in DENT test results.

4.2.1 XRF analysis of 8 recovered and straight asphalt samples

The following Figures 51 and 52 show the levels of zinc and molybdenum in both recovered and straight asphalt binder samples. Zinc and molybdenum counts were determined for all samples and then expressed as a percentage of the average of the levels from two engine oil brands.

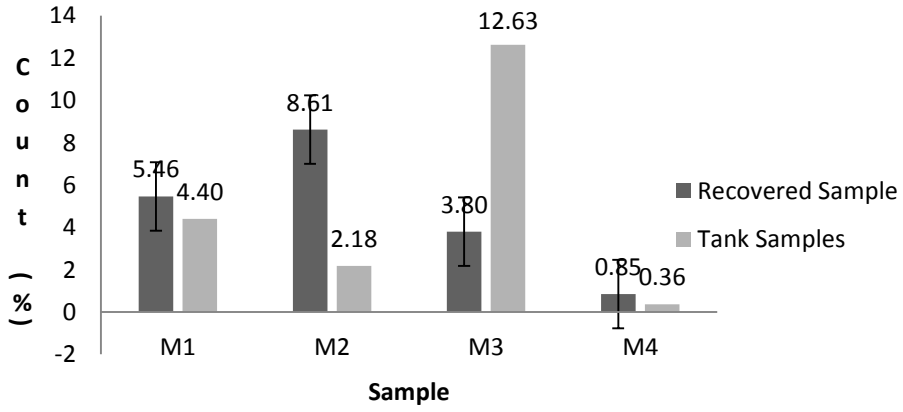

Figure 51. Zinc levels in both recovered and straight asphalt samples

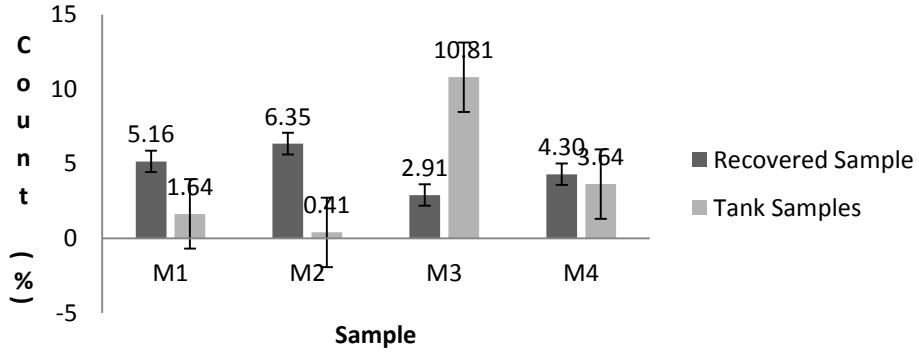

Figure 52. Molybdenum levels in recovered and straight samples

It is clearly evident from the above Figure 51 and 52, that the waste engine oil has been used in these MTO samples. This in turn has shown its detrimental effects in EBBR and DENT test results in the form of low temperature cracking and physical hardening. Due to these levels of zinc and molybdenum, we can see a poor performance of recovered binders in DENT test analysis with a CTOD levels falling below the ministry imposed limits except M1R. Even M1R has CTOD of 19.4, which is very close to ministry imposed limit of 15 mm as evident in Figure 34. Similarly, in EBBR results, we can see losses ranging from 3.7 to 10^{o}C in recovered binder as shown in the Figure in EBBR section. This is a clear evidence of premature, fatigue cracking and physical hardening. Thus the recovered binders are unable to relax their thermal stresses. When we look at the relative levels of zinc and molybdenum in recovered vs tank asphalt samples, we can see

that the recovered binders have a high levels of zinc and molybdenum then their tank samples except the M3R and M5T pair. Thus, the tank samples are not really reflective of the samples in the field. This could be attributed to the unknown changes, processes or events happened during construction.

4.2.2 XRF analysis of 11 contract samples

XRF analysis was performed on these samples to investigate the possible presence of waste engine oil. Again, zinc and molybdenum levels were determined from individual XRF spectrum for each sample at 8.64 KeV and 17.48 KeV respectively. These numbers were then converted to the percentage of zinc and molybdenum levels in a 100% engine oil sample. Following Figures 53 and 54 show the levels of zinc and molybdenum in the 11 contract samples respectively.

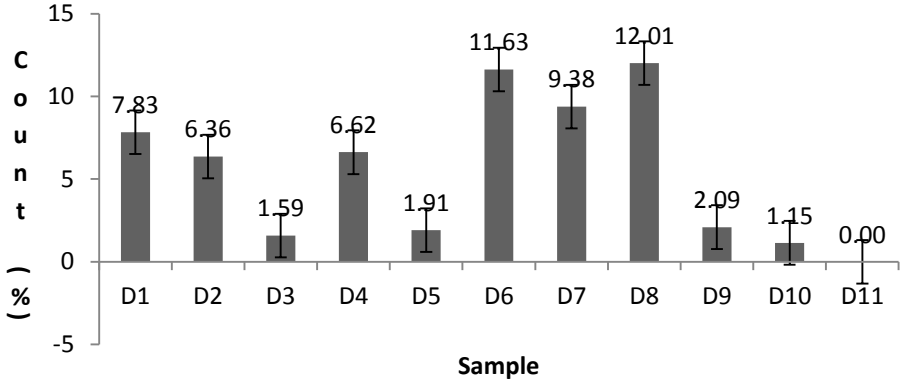

Figure 53. Zinc levels in 11 contract samples

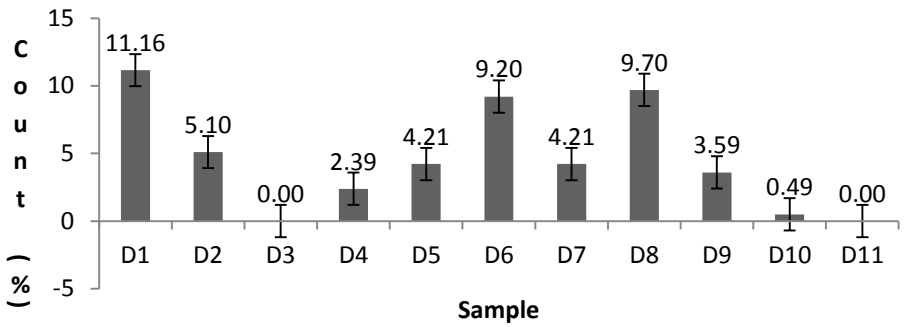

Figure 54. Molybdenum levels in 11 contract samples.

It is quite evident from the above Figures 53 and 54 that sample D1 contains high content of WEO with about 7.83% zinc and 11.16% molybdenum. These levels are likely responsible for the poor performance of this sample in the DENT test analysis. This amount of waste engine oil has probably caused excessive physical and chemical hardening which is why it consistently showed poor performance with lowest CTOD level at all temperatures among all samples. On the other hand, sample D11 shows no content of either zinc or molybdenum and thus consistently shows a good performance in terms of its resistance to fatigue cracking at all temperatures with highest CTOD levels. Samples D6 and D8 have also been found to contain considerably high levels of zinc and molybdenum with about 12% and 9% respectively, which is why they barely pass the DENT test at 15^{o}C with CTOD levels of 20.2 and 23.2 mm. These values are very close to the Ministry imposed limit of 20 mm for these samples. Samples D4 with lower levels of zinc and molybdenum also show a good performance in terms of their resistance to fatigue cracking especially within its performance grade of -28^{o}C with CTOD values about 23.7 mm.

4.3 FTIR Analysis

FTIR spectroscopy is an effective tool to investigate the level of oxidative (chemical) hardening in asphalt binders through the detection of carbonyls and sulfoxides at the wavenumber of 1760 cm^{-1}-1665 cm^{-1} and 1070 cm^{-1}- 985 cm^{-1} respectively. Carbonyl functional group is an immediate product of oxidation and thus a strong indicator of oxidative hardening. Sulfoxides are another product of oxidation however sulfoxides do not harden the asphalt. FTIR is also an effective tool to determine the level of polymer modifier such Styrene Butadiene Styrene (SBS) by looking at styrene and butadiene levels in asphalt cement. SBS is a common asphalt modifier, which is known to enhance the elasticity of asphalt to prevent rutting and cohesive failure[71]. This technique can also be used to determine the level of waste engine oil through the detection of Poly Iso Butylene. It is a dispersant found in high concentrations in recycle engine oil. These peaks were integrated between their respective wavenumbers to determine the area under the peaks. This peak area was then expressed as a percentage of CH_2 peak area. CH_2 was used as an internal standard.

4.3.1 FTIR Analysis of 8 recovered and straight asphalt samples

The FTIR analysis for both recovered and straight asphalt samples did not any presence of carbonyl except samples M2R and M3R with the indices of 0.181 and 0.578 %. The following Figure 55 shows the level of sulfoxides in the recovered and straight asphalt samples.

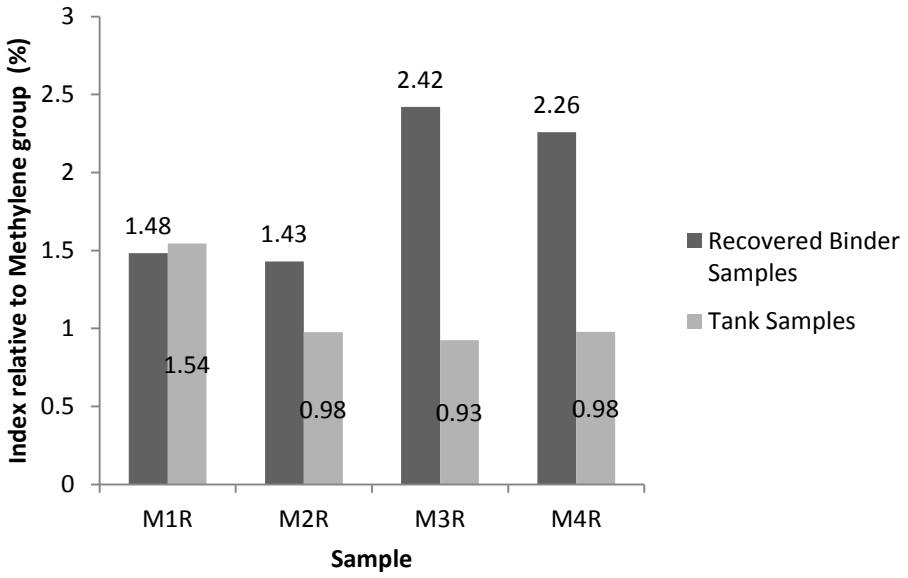

Figure 55. Sulfoxides levels in recovered and straight asphalt Samples

It is quite evident from FTIR results that carbonyl was only detected in samples M2R and M3R. This carbonyl formed as a result of the addition of both engine oil and 20% recycled asphalt as shown in the mix design of the recovered samples. As a result of these carbonyl levels, we see the evidence of physical hardening and low temperature cracking in both M3R and M2R in the form of 72 hours grade loss of 3.7 ^{o}C and 9.1^{o}C respectively in EBBR and the substantial loss of ductility with CTODs of 10 mm and 10.8 mm respectively, which is below the Ministry imposed limit of 15 mm. This same performance is reflected in the results of corresponding tank samples of M6T and M7T with 72 hr grade losses of 4.3^{o}C and 2.7^{o}C as compared to their corresponding recovered samples M2R and M3R. The tank samples also perform well in terms of ductility with CTODS of 29.6 and 24.6. These values are above the Ministry imposed limits of 15 ^{o}C. The other two recovered samples show similar performance in terms of hardness and

ductility with 72 hrs grade loss of 5.6 ^{o}C and 5 ^{o}C respectively. These samples have CTODs of 19.4 and 15.8 repectively. M1R just barely passes the DENT test with CTOD very close to the ministry imposed limit of 15 ^{o}C. M4R fails DENT test with a CTOD of 15.8, which is below the Ministry imposed limit of 20 ^{o}C. Despite these results, no carbonyl levels were detected in these two samples even though they also contained 20% recycled asphalt. The root cause behind this result needs to be further investigated as oxidative hardening is a complex phenomenon, which is still not fully understood. Figure 55 shows sulfoxide levels in both recovered and tank asphalt samples. As evident from Figure 55 above, the recovered samples contain greater level of sulfoxides as compared to the tank samples except the M1R and M5T pair, where the sulfoxide levels in recovered and tank sample are very close with % count of 1.48 and 1.54 respectively. The greater level of sulfoxides in the recovered samples is a sign of greater extent of oxidation in the pavement in the field however sulfoxides are a secondary product of oxidation and they do not harden the asphalt. Figure 56 and 57 shows levels of styrene and butadiene in both recovered and tank asphalt samples. Higher levels of styrene and butadiene in tank asphalts samples as shown in Figures 56 and 57 are clear indication of higher levels of SBS in tank samples as compared to the recovered samples. The effect of these levels can be clearly seen in terms superior ductility and greater resistance to low temperature cracking in tank samples as evident from EBBR and dent test results. These effects can also be clearly seen from the raw force displacement diagrams of tank sample versus recovered samples as tank samples were able to stretch to greater displacement as compared to the samples as SBS is known to enhance elasticity and prevent cohesive failure.

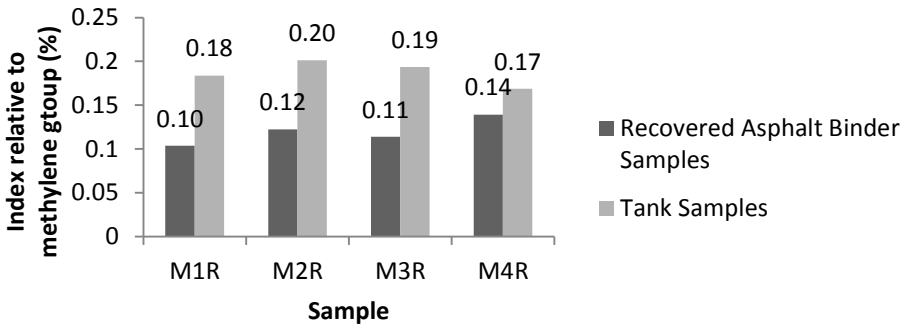

Figure 56. Styrene levels in recovered and tank samples

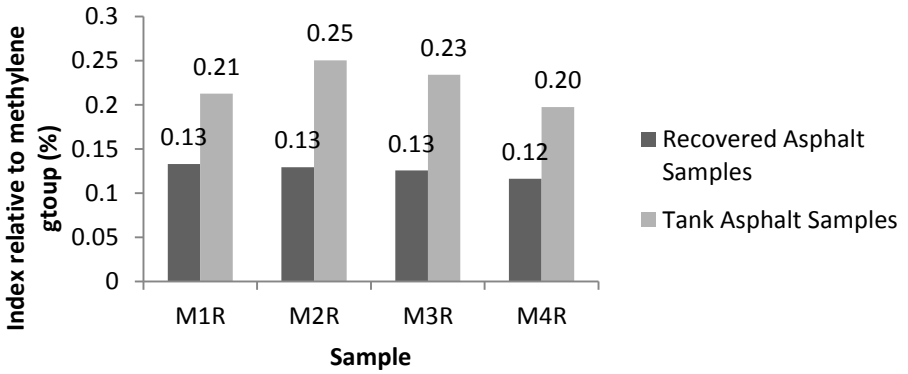

Figure 57. Butadiene levels in recovered and tank samples

However, lower levels of SBS in recovered samples can be explained by the fact that it is quite possible that in the presence recycled asphalt and WEO, the SBS begins to degrade or ages, which in turn is reflected in relatively lower levels in recovered samples. Figure 58 below shows levels of polyisobutylene (PIB) in recovered and tank asphalt samples.

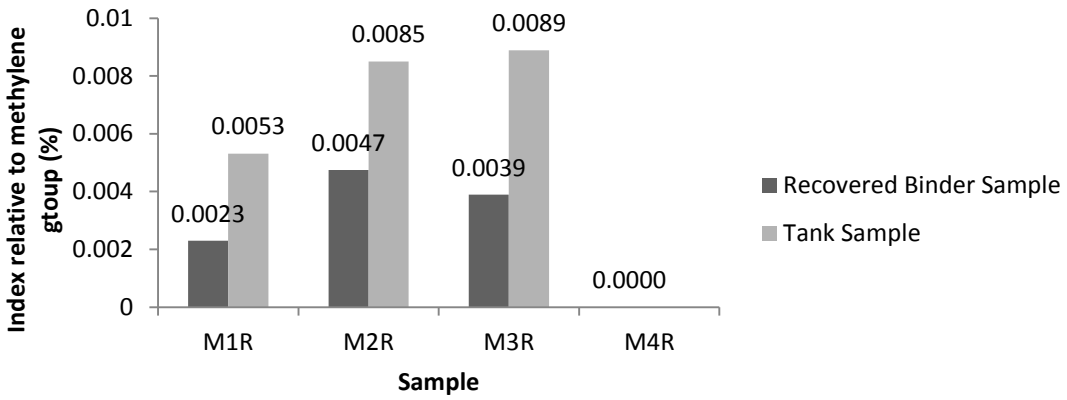

Figure 58. Polyisobutylene (PIB) levels in recovered and tank asphalt sample

The levels of PIB in both recovered and tank asphalt samples except M4R and M8T is a further confirmation of the addition WEO in these samples. The relatively lower levels of PIB in recovered samples can be explained by the fact that PIB sticks very strongly to the aggregate therefore not all of it can be obtained in the binder during the recovery process. The presence of WEO and 20% recycled asphalt seems to have an added adverse effect on the performance of these samples in the field. This is quite evident from both DENT test and EBBR results.

4.3.2 FTIR Analysis of 11 Contract Samples

FTIR analysis was performed on these samples investigate the extent of hardening, polymer modification and the possible presence of engine oil in these samples. Peak area for each functional group was calculated at the respective wavenumbers belonging to each functional group. The peak areas were then converted to a percentage of CH_2 group,

which is used as an internal standard. The following Figure 59 represents carbonyl levels in these samples.

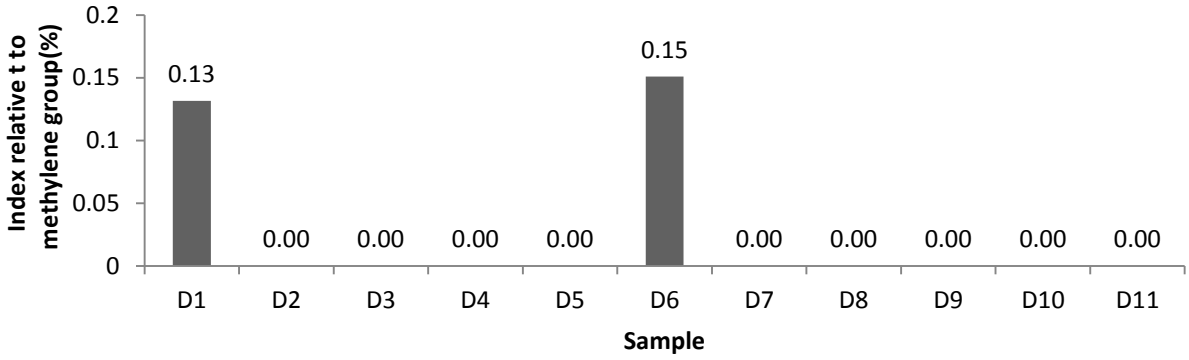

Figure 59. Carbonyl levels in 11 contract samples

It is quite evident from the above Figure 59 that sample D1 and sample D6 show relatively high levels of carbonyl group with a percentage of 0.13 and 0.15 respectively. These levels are strong indication of oxidative and chemical hardening in these samples and are therefore reflected in the poor performance of these samples within their respective performance grades in the DENT test with a CTOD of 13.7 mm for D1 and 20.2mm for D6. All other samples show no levels of carbonyl. The following Figure 60 shows sulfoxide levels for these contract samples.

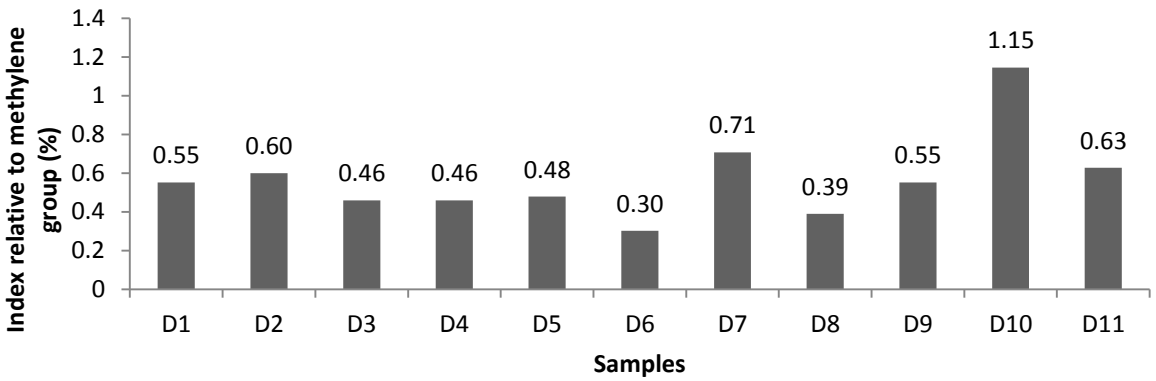

Figure 60. Sulfoxide levels in 11 contract samples.

It is quite evident from above Figure 60, that all sample contain considerable proportion of sulfoxides, which is another indication of oxidation process happening in these samples. However, sulfoxide is a secondary product of oxidation and thus does not harden the asphalt. The following Figure 61 represents level of aromatics in these contract samples.

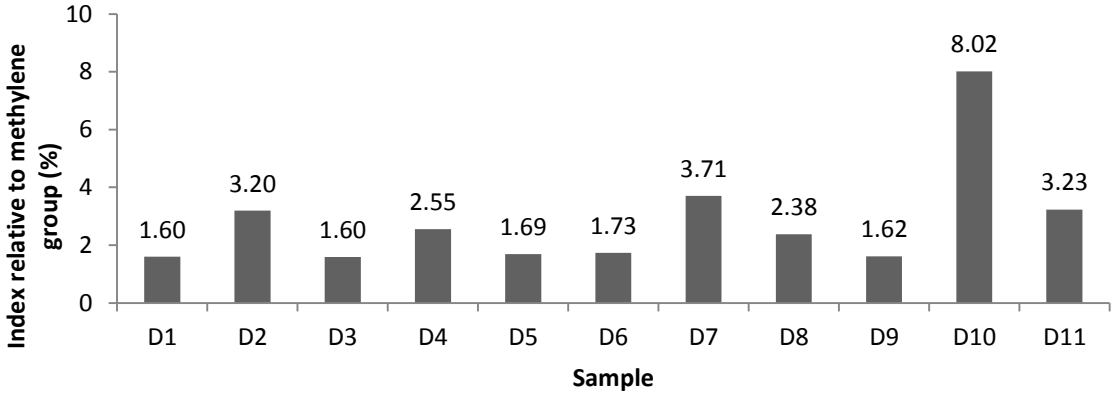

Figure 61. Aromatic content in 11 contract samples.

High aromatic levels in asphalt are seen as a positive indicator in terms of pavement performance in the field. These aromatics are the lowest molecular weight naphthenic aromatic compounds in asphalt [39]. They make up a major portion of the dispersion

medium for peptised asphaltenes. It is quite apparent from the above figure that sample D1 and D6 contain relatively lower proportion of aromatics with a percentage of 1.60 and 1.73 respectively. These levels are probably responsible for oxidative hardening in these samples due to the precipitation of asphaltenes from a continuous maltene phase as a result of the addition of WEO. Sample D11 contains relatively higher aromatic content, which is responsible for its superior performance in the dent test analysis. Sample D10 however, shows the highest aromatic content, which is why, it can be ranked second to sample D11 in terms of good performance in the dent test result at 15^{o}C with a CTOD of 26m. The following Figures 62 and 63 contain butadiene and styrene levels of these contract samples.

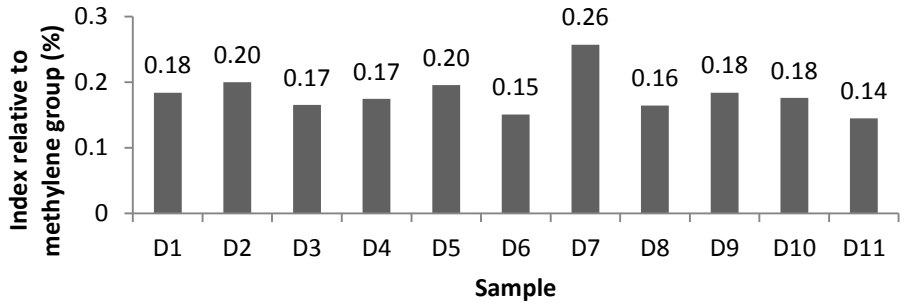

Figure 62. Butadiene content in 11 contract samples.

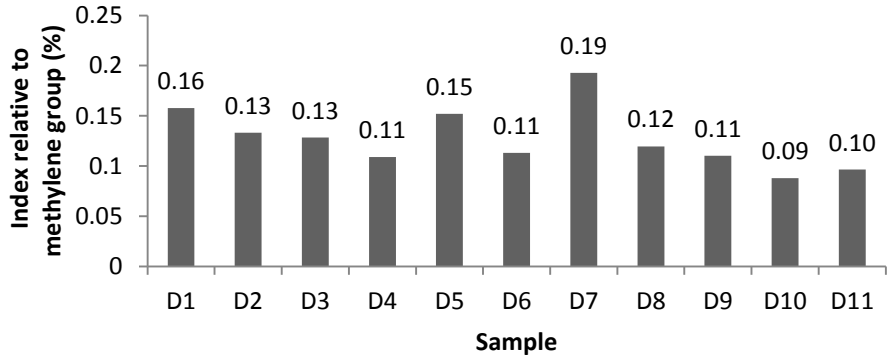

Figure 63. Styrene content in 11 contract samples.

It is quite evident from the above Figures 62 and 63 that there is a strong indication of SBS based polymer modifications in all samples. D11 shows lowest amount with butadiene content of 0.14% and styrene content of 0.1 %. Sample D7 shows the highest amount of SBS with a butadiene content of 0.26% and styrene content of 0.19%. Sample D1 shows unexpected result with a relatively higher content of SBS then D11 with both styrene and butadiene content 0.18 and 0.16%. It is quite possible that in the presence of WEO, the polymer probably degraded and was failed to achieve desired elasticity as expected from this modifier. There is no indication of polyisobutylene in any of these samples, which would have further substantiated the existence of WEO in these samples. Currently, PIB is widely used as a dispersant is engine oils. However, it is quite possible that WEO present in these samples possibly contained olefins based copolymers as viscosity modifier instead of PIB [76].

4.4 EBBR Analysis

All samples were conditioned at 10^{o}C and 20^{o}C temperatures warmer than the minimum temperature grade for 1h, 24 h and 72 h and then tested at 10^{o}C and 16^{o}C warmer than the minimum temperature grade as per LS 308 extended bending beam rheometry protocols[77]. Limiting temperature grades were determined according to ASHTO M320 protocols by selecting the temperatures where m-(60s) = 0.3 and creep stiffness at 60 s reached 300 MPa. Then the warmer temperature among the two is selected to obtain the lower temperature grade. The grade losses (i.e. the temperature difference between the 1 hr and 72hr temperature grade) were also determined according to LS308 protocols.

The recovered samples M1R to M3R and straight asphalt samples M5T to M7T were conditioned at -8^{o}C and -18^{o}C and then tested at -12^{o}C and -18^{o}C after 1 h, 24 h and 72h. The samples M4R and M8T were conditioned at -14^{o}C and -24^{o}C and then tested at -24^{o}C and -18^{o}C after 1 h, 24 h and 72 h as per LS 308 protocols. Table 4.1 below contains the summary of the results.

Table 4.1 Summary of EBBR results

Sample	**Actual temperature grade**	**1 h Grade**	**72 h Grade**	**Grade Loss**
M1R	64-28	-34.5	-28.9	5.6
M2R	64-28	-33.4	-24.3	9.1
M3R	64-28	-31.2	-26.8	3.7
M4R	58-34	-35.5	-30.5	5
M5T	64-28	-32.8	-32	0.8
M6T	64-28	-36.2	-32	4.3
M7T	64-28	-34.9	-32.5	2.4
M8T	58-34	-37	-32.9	2.7

The LS 308 1 h and 72 h grades are further illustrated in the following Figures 64 and 65.

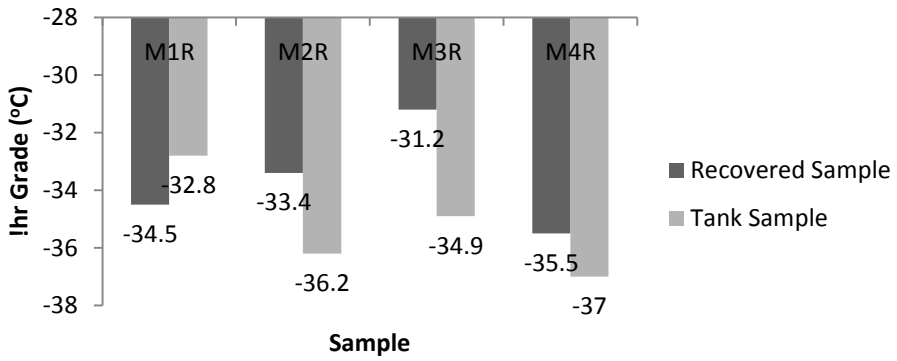

Figure 64. 1 h grade comparison of recovered and straight asphalt samples.

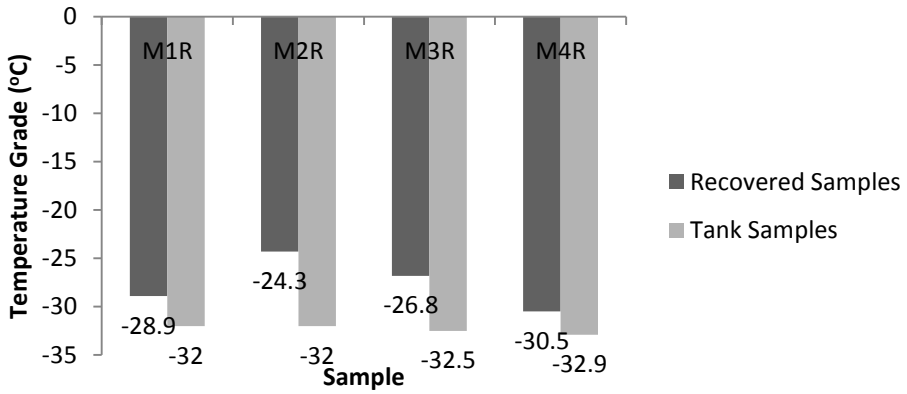

Figure 65. 72 h grade comparison of recovered and straight asphalt samples.

It is quite apparent from above Figure 64 that all recovered and tank asphalt sample seem to pass EBBR test. In fact the all samples have 1 hr grades above the minimum temperature grades thus they are showing a good resistance to the effects of low temperature. However, after 72 hours, their performance seems to be affected significantly after prolonged exposure to low temperatures. It is because, asphalt pavements cool for several weeks and months before their structure is affected by cold weather during the months of January, February and March [31]. It is during this period of extended conditioning that poor quality asphalt pavements consolidate their wax/ asphaltene structure and thereby lose their ability to relax thermal stresses. Therefore, a 1

hour conditioning time that was specified in a conventional BBR method, is insufficient to truly simulate low temperature behavior of the binder as experienced by pavements in the field. The performance of recovered samples is significantly affected as compared to the tank samples. For instance, M2R, M3R and M4R have limiting temperatures of about 3.7^{o}C, 1.2^{o}C and 3.5^{o}C warmer than their minimum temperature grade. Thus, these pavements would not be able to function in areas where the winter temperatures fall below the minimum temperature grade of these samples. In comparison to these recovered samples, straight asphalt samples such as M6T and M7T perform much better than their corresponding recovered samples M2R and M3R. These samples have limiting grades of 4^{o}C and 4.5^{o}C lower than their minimum grade thus they would be able to offer good to resistance low temperature cracking in areas where winter temperatures fall below the minimum temperature grade of theses samples. In case of M8T, the limiting temperature grade is about 1.1^{o}C warmer than its minimum temperature grade -34, which is comparatively better performance as compared to M4R with 3.5^{o}C difference between it 72 h grade and its minimum temperature grade. The sample M8T would also not be able resist the low temperature as its 72 h grade is warmer than its minimum temperature grade. In case of M1R and M5T, a better performance is displayed as compared to other samples because the limiting temperatures of theses samples are 0.9^{o}C and 4^{o}C lower than their minimum temperature grade of -28^{o}C. Thus, as a whole, the signs of low temperature cracking are more apparent in the recovered samples as compared to their corresponding tank samples. This difference in performance is due to the combined effect of the addition of WEO and 20% recycled asphalt in these samples as discussed

previously in FTIR section. The following Figure 66 shows a grade loss comparison between the recovered and straight asphalt samples.

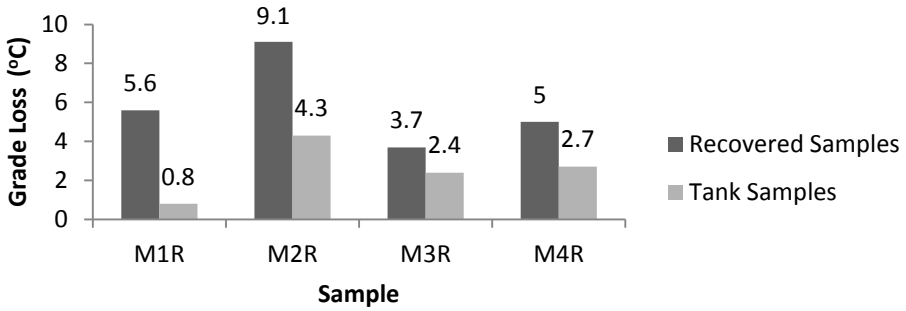

Figure 66. Grade loss comparison between recovered and straight asphalt samples.

Figure 66 above shows a more pronounced effect of low temperature cracking in recovered samples as compared to the tank samples. The grade loss here can be considered to be an ability of the asphalt pavement to relax thermal stresses upon repeated exposure to low temperatures. The recovered samples seem to be adversely affected as grade losses range from 3.7^{o}C to 9.1^{o}C.

These values are very significant as the intended confidence seem to be reduced significant from 98% to more than 50% in case of M3R and to below 0 in case of M2R. On the contrary, tank samples perform much better as the grade losses are within the 6^{o}C range. This difference in performance is due to the addition of negative modifiers such WEO and recycled asphalt, which seem to accelerate the hardening process by reducing the solubility of asphaltenes in a continuous maltene phase, which results in a pavement with less flexibility and reduced ability to relax thermal stresses.

4.5 DSR Analysis

4.5.1 High Temperature Grades

The high temperature grades of recovered and straight asphalt samples were determined according to standard DSR protocols. These grades assess the ability of the asphalt binders to resist rutting. The DSR uses the elastic portion of the complex modulus G*/sin δ to evaluate the high temperature performance grade of the asphalt samples. In order to have a good performance, this elastic portion of complex modulus should be maximized. Thus a minimum value of 1 KPa is specified for unaged samples and 2.2 KPa is specified for RTFO/recovered asphalt samples. For tank samples, the high temperature grades for both unaged and RTFO aged samples were evaluated and warmer temperature between the two grades was selected as a high temperature grade. Figure 67 shows the comparison of the performance of recovered and straight asphalt samples. It is clearly evident from the following figure that the recovered binders are showing a better performance at high temperatures as they show higher temperature grades relative to their corresponding straight asphalt. This means that these binder samples will be able to perform better in high temperature climatic regions. This performance can be attributed partly to addition of 20% reclaimed asphalt (RAP), which gives an added elasticity to these samples and thus they attain better resistance to rutting at higher temperatures.

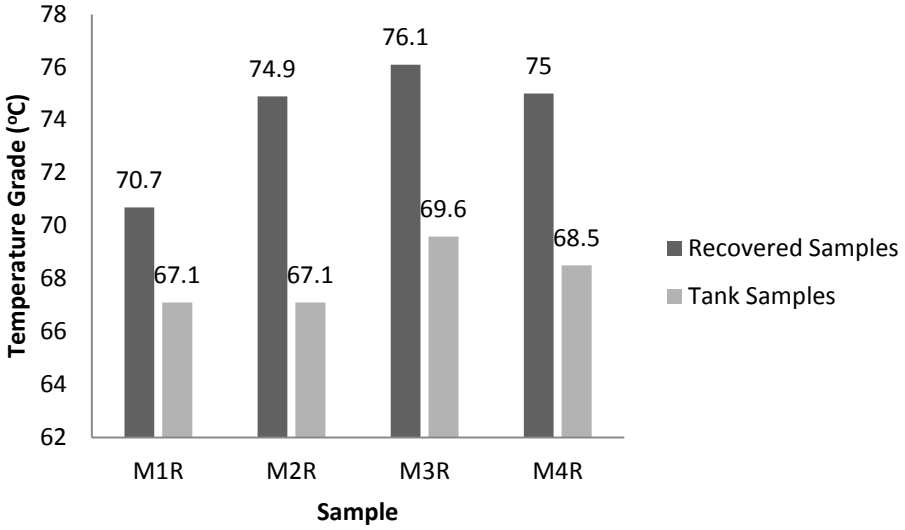

Figure 67. High Temperature Grades of recovered and straight asphalt samples.

4.5.2 Intermediate Temperature Grades

The intermediate temperature grades were also determined according to standard DSR protocols. These grades assess the ability of the asphalt samples to resist fatigue cracking. In this case, the viscous portion of complex modulus "G^*. sin δ " is used to evaluate intermediate temperature grades. This viscous portion of complex modulus should be minimized in order to have a good performance at intermediate temperatures. Therefore, a maximum limit of 5000 KPa was specified for this grading procedure. Figure 68 shows intermediate temperature grades of the recovered and straight asphalt samples. It is clearly evident from the following figure that that the recovered samples are performing better than the tank samples as they have higher intermediate grades then the tank samples. This shows that at intermediate temperatures these samples would still have viscous component to resist fatigue cracking. However, DSR intermediate grading procedure does not correlate well with the fatigue distress phenomenon as experienced by

the pavements in the field. That is why, DENT test was introduced as an improvement over DSR intermediate grading procedure as it provides better correlation with an actual fatigue distress phenomenon in the field in the form of an approximate crack tip opening displacement (CTOD).

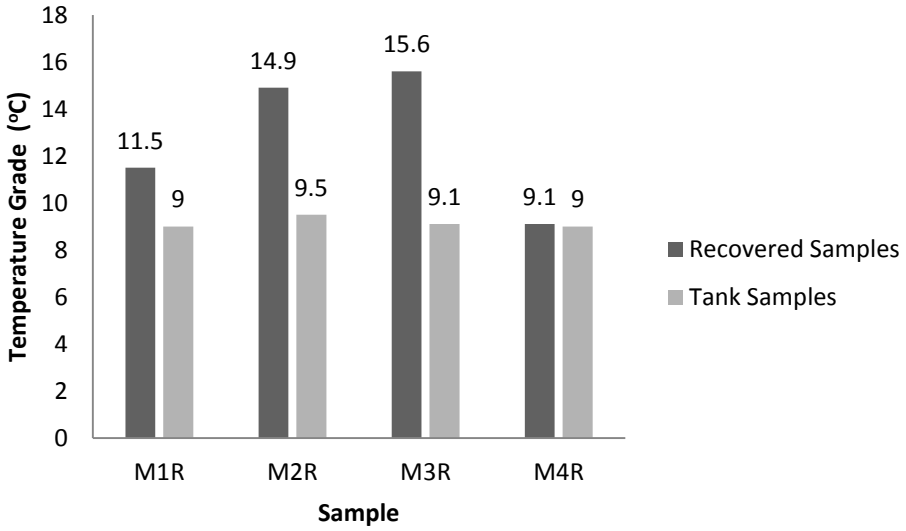

Figure 68. Intermediate Temperature Grades of recovered and straight asphalt samples.

4.5.3 Black Space Diagrams

A Black space diagram is a useful tool in understanding the rheological behavior of asphalt samples. It helps in distinguishing a binder with a homogeneous composition from a heterogeneous one with multiple phases. It uses a plot of the logarithm of stiffness vs phase angle. A Black space diagram, which has a smooth and continuous progression of curves corresponding to different temperatures, is said to be rheologically simple and thus homogenous. On the contrary, a Black space diagram with discontinuities among curves and anomalous behavior corresponds to a binder with heterogeneous composition

and multiple phases. The following Figures 69 to 76 contain the black space diagram of recovered and straight asphalt samples at both high and intermediate temperatures.

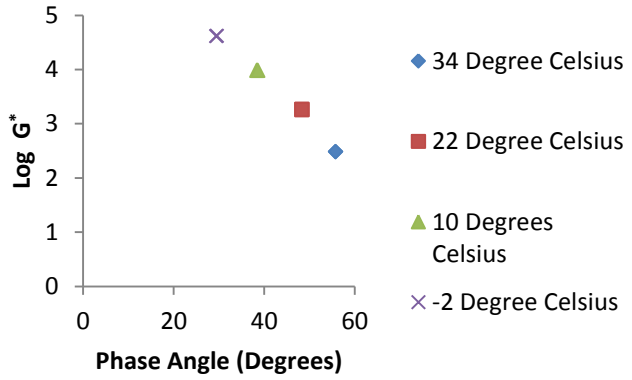

Figure 69(a). M1R Black Space Diagram at intermediate.

temperatures

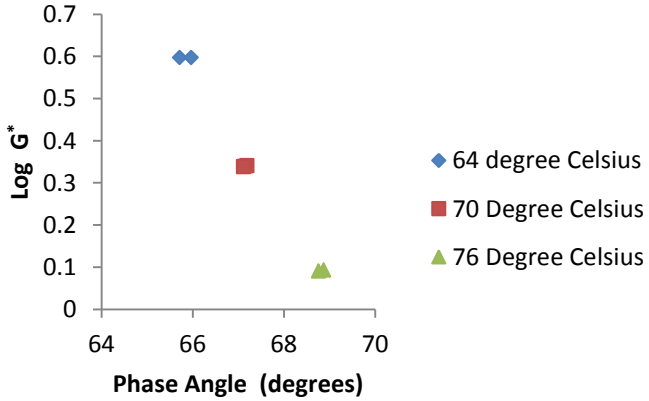

Figure 69(b). M1R Black Space Diagram at high temperatures.

Figure 69 M1R Black Space Diagrams.

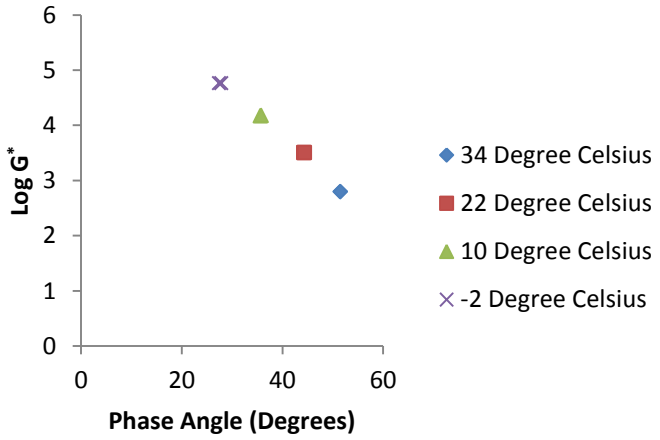

Figure 70(a). M2R Black Space Diagram at Intermediate temperatures.

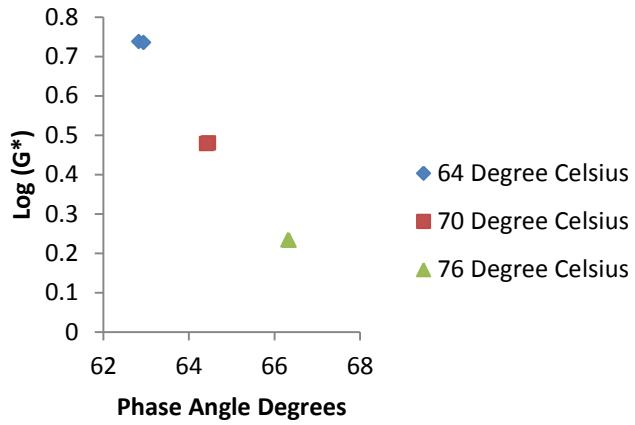

Figure 70(b). M2R Black Space Diagram at high temperatures.

Figure 70 M2R Black Space Diagrams.

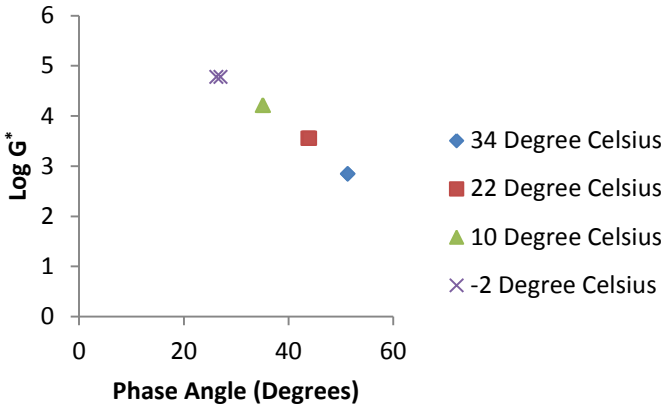

Figure 71(a). M3R Black Space Diagram at Intermediate Temperatures.

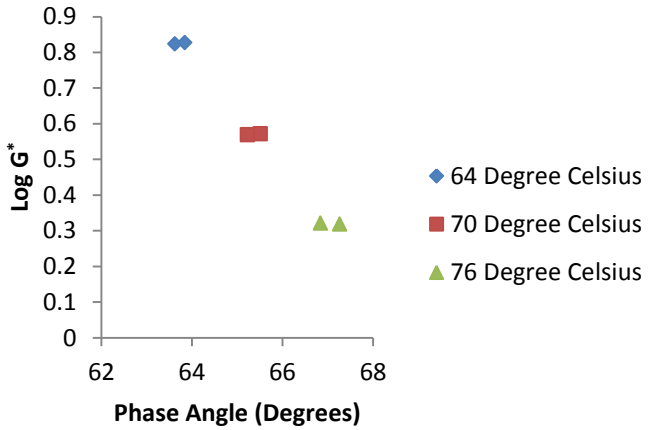

Figure 71(b). M3R Black Space Diagram at High Temperatures.

Figure 71. M3R Black Space Diagrams.

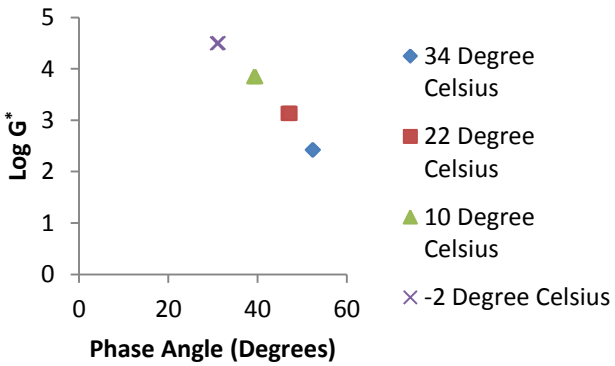

Figure 72(a). M4R Black Space Diagram at Intermediate Temperatures.

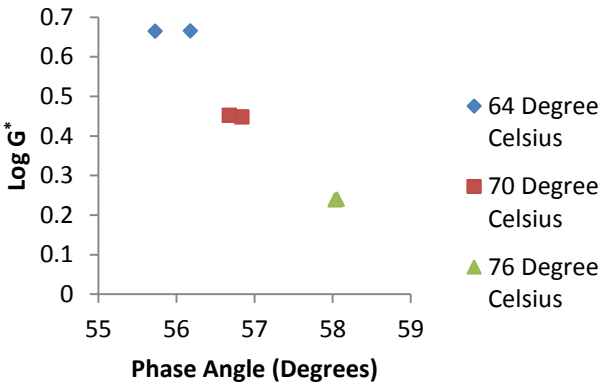

Figure 72(b). M4R Black Space Diagram at High Temperatures.

Figure 72. M4R Black Space Diagrams.

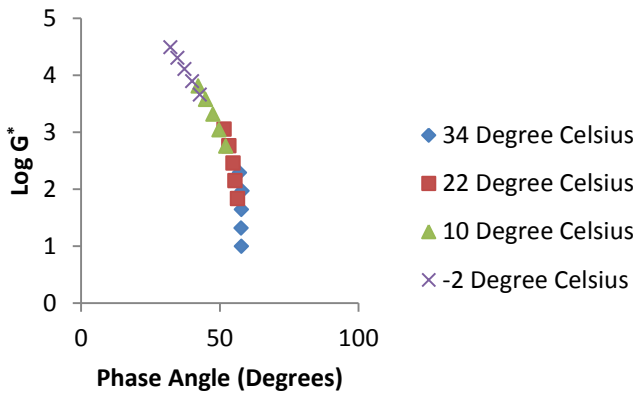

Figure 73(a). M5T Black Space Diagram at Intermediate Temperatures.

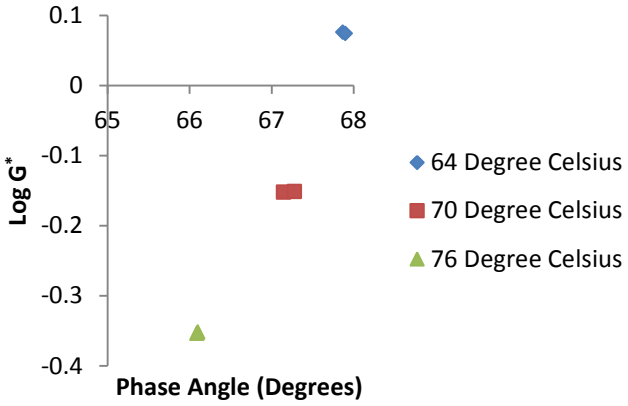

Figure 73(b). M5T Black Space Diagram at High Temperatures.

Figure 73. M5T Black Space Diagrams.

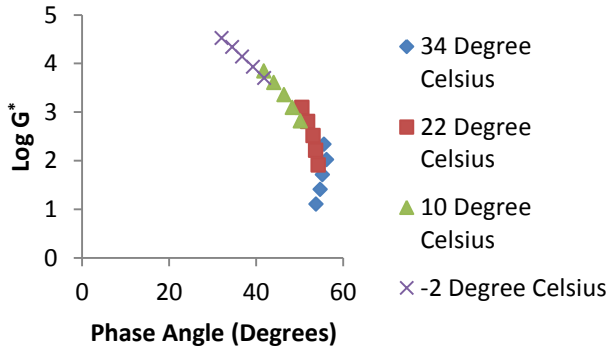

Figure 74(a). M6T Black Space Diagram at Intermediate Temperatures.

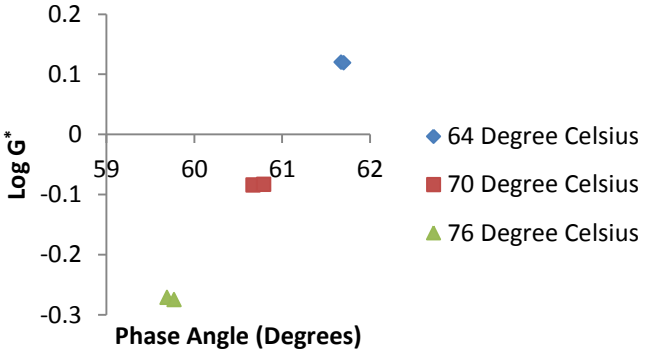

Figure 74(b). M6T Black Space Diagram at High Temperatures.

Figure 74. M6T Black Space Diagrams.

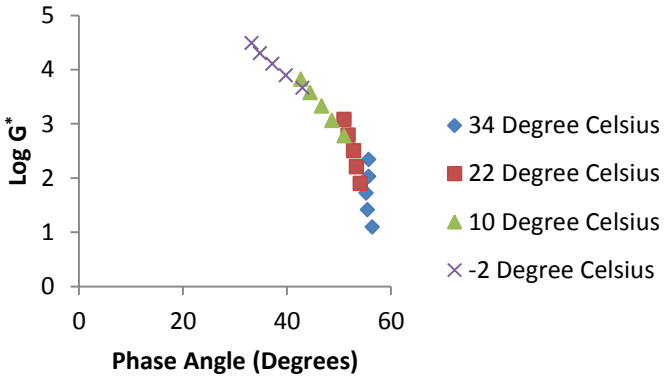

Figure 75(a). M7T Black Space Diagram at Intermediate Temperatures.

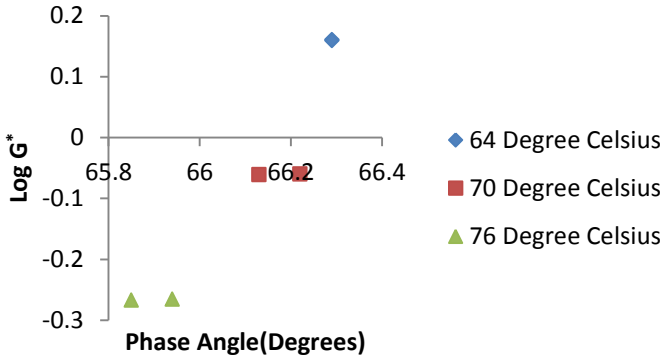

Figure 75(b). M7T Black Space Diagram at High Temperatures.

Figure 75. M7T Black Space Diagrams.

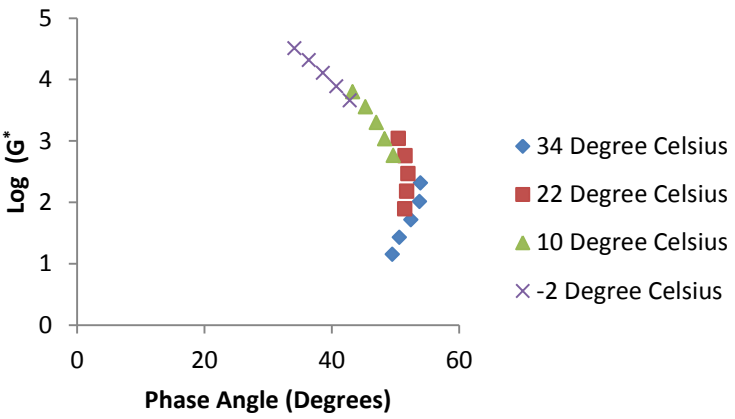

Figure 76(a). M8T Black Space Diagram at Intermediate Temperatures.

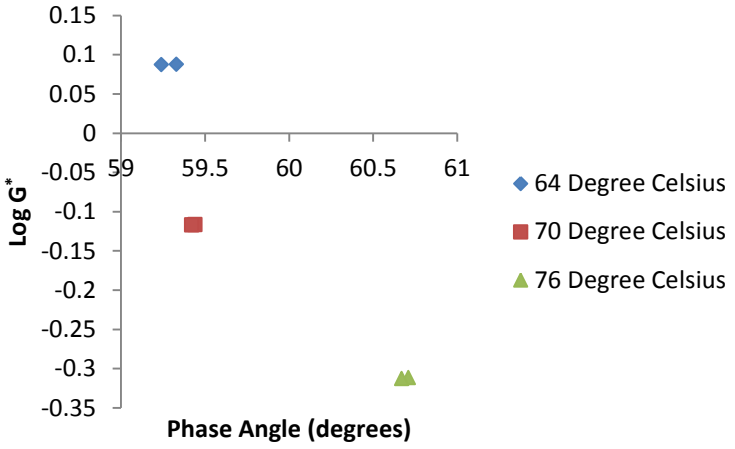

Figure 76(b). M8T Black Space Diagram at High Temperatures.

Figure 76. M8T Black Space Diagrams.

From the above diagrams, It is clearly evident that the tank samples are rheologically complex or heterogeneous with multiple phases due to the discontinuity in progression among curves corresponding to different temperatures. This heterogeneity is due to the addition of WEO in asphalt samples as WEO is known to cause precipitation of asphaltenes from a continuous maltenes phase.

4.6 Case Study of a Local Kingston Road

This section includes a case study from a local road in Kingston, Ontario. The asphalt mix sample of this road was received on January 2016. The asphalt binder from the mix sample was then recovered and tested for its ability to resist thermal and fatigue cracking through EBBR and DENT test respectively. Both tests revealed shocking results regarding the ability of the binder to withstand fatigue and thermal stress. The following Figure 77 includes force- displacement diagrams of the ligaments of this sample under the DENT test.

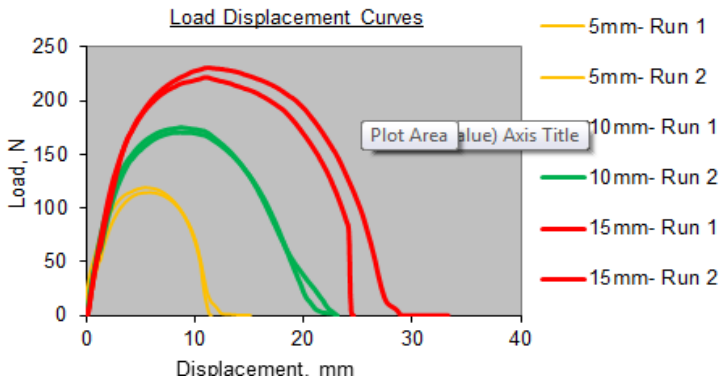

Figure 77. Load Displacement Diagram of a local Kingston road.

It is quite evident from the above load displacement diagrams that the binder shows poor performance in terms of ductility. In fact of one of the ligaments does not even yield fully and shows a brittle failure as evident from an immediate drop in the load prior to the end of the test. This sample with a low-temperature grade of -28^{o}C was tested against a

Ministry imposed 15mm CTOD limit. The sample showed poor performance with a CTOD of 5.6 mm. Sample also performs poorly in EBBR with a 72hr limiting grade of -16^{o}C, which is 12^{o}C warmer than its low temperature grade of -28^{o}C. This pavement would not be able to withstand the effect of low temperature as the average low air temperature around the Kingston area -27.8^{o}C as obtained from long term pavement performance binding (LTPP Bind) software. The sample also displays a grade loss of about 8^{o}C in 72 hrs. This in turn shows its reduced ability to relax its thermal stresses under repeated temperature drop t below -28^{o}C. The extent of this damage can be further revealed from the following pictures taken at the affected location.

Figure 78. Evidence of Low Temperature cracking in the field.

Figure 79. Evidence of Fatigue Temperature cracking in the field.

It is quite apparent from the above Figures 78 and 79 that the pavement has gone through extensive thermal and fatigue distress as evident from transverse cracks and cracks displaying aligator like pattern in the above Figures 78 and 79. In fact, there is a mix of both low temperature and fatigue distress in several areas along the road. This pattern can be seen over a stretch of 5 km along this road. Sample needs to be further tested though XRF and FTIR procedures to determine the possible root causes behind this failure.

Chapter 5

Summaries, Conclusion and Recommendations

5.1 Summaries and Conclusions

Based on the theoretical background and detailed findings presented in this thesis, following conclusions can be drawn

- All contract samples tested at 15^{o}C passed the DENT test except sample D1, which consistently showed poor performance at all temperatures. Sample D11 displayed superior characteristics in terms of its resistance to fatigue cracking at all temperatures. All samples showed strong correlation of CTOD with temperature. Thus, current CTOD requirement in LS 299 dent test protocols can be used at other temperatures.
- All recovered samples displayed poor performance in terms of their ability to withstand thermal and fatigue distress relative to their corresponding straight asphalt as evident in dent test and EBBR results.
- XRF and FTIR testing of all asphalt binders, indicated the presence of waste engine oil to be the root cause of failure in asphalt pavements as a result of physical and chemical hardening through the detection of carbonyl and polyisobutylene in FTIR and zinc and molybdenum levels in XRF.
- DSR high and intermediate temperature grading showed superior performance of recovered binder samples. The superior performance at high temperatures can be

attributed to the addition of RAP, which gives added elasticity to the binder at high temperatures and thus a superior resistance to rutting. The DSR intermediate grading results do not correlate well with an actual fatigue distress phenomenon in the field. Therefore, dent test is recommended as it gives a clearer picture in the form of approximate crack tip opening displacement (CTOD).

- Study of the local Kingston road showed extensive signs of damage through fatigue and thermal distress as evident from dent test, EBBR results and the field pictures. Therefore, the underlying causes need to be investigated through XRF and FTIR.

5.2 Recommendations

In the light of above findings, the following actions are recommended.

- The use of waste engine oil and recycled asphalt (RAP) in asphalt pavements should be avoided.
- The existing DENT test CTOD requirements should be extended to temperatures other than 15^{o}C.

References

[1] Robertson WD. “Using the SHRP Specification to Select Asphalt Binders for Low TemperatureService”, Proceedings, Canadian Technical Asphalt Association, 40, 170-195 (1995).

[2] Kandhal PS, Dongré R, Malone MS. “Prediction of Low-Temperature Cracking of Pennsylvania Project Using Superpave Specifications”, Journal, Association of Asphalt Paving Technologists, 65,491-531 (1996).

[3] Button JW, Hastings CP. “How Well Can New Binder Tests Predict Cracking?”, Proceedings, Canadian Technical Asphalt Association, 43, 48-72 (1998).

[4] Anderson K, Christison J, Bai B, Johnston C, Quinn T, McCullough D. “Temperature and Thermal Contraction Measurements as Related to the Development of Low Temperature Cracking on the Lamont Test Road.”, Proceedings, Canadian Technical Asphalt Association, 43, 16-47 (1998).

[5] Anderson K, Christinson T, Johnston C. Low Temperature Pavement Performance: An Evaluation using C-SHRP Test Road Data, Transportation Association of Canada, Ottawa, Ontario (1999).

[6] Gavin J, Dunn L, Juhasz M. “The Lamont Test Road – Twelve Years of Performance Monitoring”, Proceedings, Canadian Technical Asphalt Association, 48, 355-376 (2003).

[7] Andriescu A, Hesp SAM, Youtcheff JS. “Essential and Plastic Works of Ductile Fracture in Asphalt Binders”, Transportation Research Record 1875, Bituminous Binders 2004, Transportation Research Board, National Research Council, Washington, D.C., 1-8 (2004).

[8] Andriescu A, Iliuta S, Hesp SAM, Youtcheff JS. “Essential and Plastic Works of Ductile Fracture in Asphalt Binders and Mixtures”, Proceedings, Canadian Technical Asphalt Association, 49, 93-121 (2004).

[9] Iliuta S, Andriescu A, Hesp SAM, Tam KK. “Improved Approach to Low-Temperature and Fatigue Fracture Performance Grading of Asphalt Cements”, Proceedings, Canadian Technical Asphalt Association, 49, 123-158 (2004).

[10] Yee P, Aida B, Hesp SAM, Marks P, Tam KK. “Analysis of Three Premature Pavement Failures”, Transportation Research Record 1962, Bituminous Materials and Non bituminous Components of Bituminous Paving Mixtures, Transportation Research Board, National Research Council, Washington, D.C., 44-51 (2006).

[11] Zhao MO, Hesp SAM. “Performance Grading of the Lamont, Alberta C-SHRP Pavement Trial Binders”, International Journal of Pavement Engineering, 7(3), 199-211 (2006).

[12] Hesp SAM, Iliuta S, Shirokoff JW. “Reversible Aging in Asphalt Binders”, Energy & Fuels, 21(2), 1112-1121 (2007).

[13] Bodley T, Andriescu A, Hesp SAM, Tam KK. “Comparison between Binder and Hot Mix Asphalt Properties and Early Top-Down Wheel Path Cracking in a Northern Ontario Pavement Trial”, Journal, Association of Asphalt Paving Technologists, 76, 345-390 (2007).

[14] Hesp SAM, Soleimani A, Subramani S, Marks P, Philips T, Smith D, Tam KK. “Asphalt Pavement Cracking: Analysis of Extraordinary Life Cycle Variability in Eastern and Northeastern Ontario”, International Journal of Pavement Engineering, 10 (3), 209-227 (2009).

[15] LTPPBind®, Version 2.1, Superpave® Binder Selection Program, Developed by Pavement Systems LLC, Bethesda, Maryland, July 1, 1999.

[16] Van der Poel C. “A General System Describing the Viscoelastic Properties of Bitumens and Their Relation to Routine Test Data”, Journal of Applied Chemistry, 4, 221-236 (1954).

[17] Van der Poel C. “Time and Temperature Effects on the Deformation of Asphaltic Bitumens and Bitumen-Mineral Mixtures”, Journal of the Society of Plastics Engineering, Sept., 47-53 (1955).

[18] Heukelom W. “Observations on the Rheology and Fracture of Bitumens and Asphalt Mixes”, Proceedings, Association of Asphalt Paving Technologists, 36, 359-397 (1966).

[19] Hills JF, Brien D. “The Fracture of Bitumens and Asphalt Mixes by Temperature-Induced Stresses”, Proceedings, Association of Asphalt Paving Technologists, 35, 292-309 (1966).

[20] McLeod NW. “Transverse Pavement Cracking Related to Hardness of the Asphalt Cement”, Proceedings, Canadian Technical Asphalt Association, 13, 5-95 (1968).

[21] Heukelom W. “A Bitumen Test Data Chart for Showing the Effect of Temperature on the Mechanical Behavior of Asphaltic Bitumens”, Journal of the Institute of Petroleum, 55, 404-417 (1969).

[22] Fromm HJ, Phang WA. “Temperature Susceptibility Control in Asphalt Cement Specifications”, Report IR 35, Department of Highways, Toronto, Ontario (1970).

[23] Readshaw EE. “Asphalt Specifications in British Columbia for Low Temperature Performance”, Proceedings, Association of Asphalt Paving Technologists, 42, 562-581 (1972).

[24] Hills JF. “Predicting the Fracture of Asphalt Mixes by Thermal Stresses”, Institute of Petroleum, 74-014 (1974).

[25] Deme IJ, Young FD. “Ste. Anne Test Road Revisited Twenty Years Later” Proceedings, Canadian Technical Asphalt Association, 32, 254-283 (1987).

[26] Anderson DA, Kennedy TW. “Development of SHRP Binder Specification”, Journal, Association of Asphalt Paving Technologists, 62, 481-507 (1993).

[27] American Association of State Highway and Transportation Officials (AASHTO) M320. “Standard Specification for Performance-Graded Asphalt Binder”, Standard Specifications for Transportation Materials and Methods of Sampling and Testing, Part 1B, Washington, D.C. (2002).

[28] Baskin CM. Proceedings of the American Society for Testing and Materials, 35(II), 576-579. (1935).

[29] Shields BP, Anderson KO. “Some Aspects of Transverse Cracking in Asphalt Pavements” Proceedings, Canadian Technical Asphalt Association, 9, 209-226 (1964).

[30] Rader LF, Ochalek RT. “Proposed Method for Testing the Physical Properties of Asphalt Paving Mixtures at Low Temperatures”, Symposium on the Science of Asphalt in Construction, Division of Petroleum Chemistry, American Chemical Society, Los Angeles, D126-D135 (1971).

[31] Hesp, S. A. M., Genin, S. N., Scafe, D., Shurvell, H. F., & Subramani, S. Five Year Performance Review of a Northern Ontario Pavement Trial: Validation of Ontario’s Double-Edge-Notched Tension (DENT) and Extended Bending Beam Rheometer (BBR) Test

Methods. Canadian Technical Asphalt Association Proceedings Of The Annual Conference, *54*, 99–126. (2009)

[32] Abraham, Herbert (1938). *Asphalts and Allied Substances: Their Occurrence, Modes of Production, Uses in the Arts, and Methods of Testing* (4th ed.). New York: D. Van Nostrand Co. (1938).

[33] Performance Graded Asphalt Binder Specification and Testing. Asphalt Institute. Superpave Series no 1 (SP-1). Revised 2003.

[34] Anja Sörensen and Bodo Wichert "Asphalt and Bitumen" in Ullmann's Encyclopedia of Industrial Chemistry Wiley-VCH, Weinheim, 2009.

[35] ACPA. Differences Between Concrete and Asphalt Pavement. Retrieved from http://overlays.acpa.org/Concrete_Pavement/Technical/Fundamentals/Differences_Between_Concrete_and_Asphalt.asp . Accessed 5th May, 2016.

[36] Pavement Interactive. http://www.pavementinteractive.org/article/deflection/ Accessed 6th May, 2016.

[37] Pavement Design. http://www.myasphaltpavingproject.com/design/pavement-design/. Accessed 7th May, 2016.

[38] Kett, Irving, Andrew, William. Asphalt Materials and Mix Design Manual. Technology and Engineering. Dec 2nd, 2012.

[39] Read, J., Whiteoak, D., In the Shell Bitumen Handbook, Fifth edition; Hunter, R. N., Ed.; Thomas Telford: London, **2003**

[40] Pavement Interactive. http://www.pavementinteractive.org/article/materialsasphalt. Accessed 8th May, 2016.

[41] Superpave Mix Design. Asphalt Institute. Superpave Series no 2 (SP-2). Revised 2003.

[42] Lu, X., Isacsson, U., *Effect of ageing on bitumen chemistry and rheology*, Construction and Building materials, 15-22, 16, **2002**.

[43] Bahia, H.U., Anderson DA. *Glass transition behaviour and physical hardening of asphalt binders*. J Assoc Asphalt Paving Technol, 93-129, 62, **1993**

[44] Petersen, J.C., *Chemical composition of asphalt as related to asphalt durability*: state of the art. Transport. Res. Record, 13-30, 999, **1984**

[45] Traxler, R.N., Coombs, C.E., *Proceedings of the Fortieth Annual Meeting, American Society for Testing Materials*, New York City, NY, 549**,** 37(II), **1937**.

[46] Struik, L.C.E., *Physical Aging in Amorphous Polymers and other Material*, Elsevier Scientific Publishing Co. Amsterdam, **1978**.

[47] Sigurdur, E. (2013). Failure Modes in Pavements Pavement conditions Type of failure modes, (March), 1–12.

[48] 5 Gallon Big A Alligator Asphalt Repair Patch For Sale _ Asphalt Sealcoating Direct. https://www.asphaltsealcoatingdirect.com/products/big-a-alligator-asphalt-repair-5-gallon. Accessed 4th June, 2016.

[49] Pothole Repair _ Buckeye Asphalt Paving Co. http://www.buckeyepaving.com/pothole-repair.html. Accessed 6th June, 2016.

[50] Distress Identification Manual for LTPP (Fourth Revised Edition). US Department of Transportation Federal Highway Administration Research and Technology. http://www.fhwa.dot.gov/publications/research/infrastructure/pavements/ltpp/reports/03031/03.cfm. Accessed 15th June, 2016.

[51] Moisture Susceptibility. Pavement Interactive. http://www.pavementinteractive.org/article/moisture-susceptibility/. Accessed 20th June, 2016

[52] Bending Beam Rheometer _ Pavement Interactive. Retrieved from http://www.pavementinteractive.org/article/bending-beam-rheometer/. Accessed 21st June, 2016

[53] Laboratory-Pavement Materials; *Penetration of Bituminous Materials, School of Civil and Structural Engineering*, Nanyang Technological University, **2002**.

[54] Penetration Grading _ Pavement Interactive. http://www.pavementinteractive.org/article/Penetration-grading/. Accessed 21st June, 2016

[55] Specification, S. Softening Point of Bitumen (Ring-and-Ball Apparatus), 43850–43855. (1993)

[56] Softening Point _ Pavement Interactive. http://www.pavementinteractive.org/article/softening-point/ . Accessed 21st June, 2016.

[57] Absolute Viscosity _ Pavement Interactive. http://www.pavementinteractive.org/article/absolute-viscosity/. Accessed 22nd June, 2016

[58] American Society for Testing and Materials (ASTM).. *Annual Book of ASTM Standards, Volume 04.03, Road and Paving Materials; Vehicle-Pavement Systems*. ASTM International. West Conshohocken, PA. (2003)

[59] Viscosity Grading _ Pavement Interactive. http://www.pavementinteractive.org/article/viscosity-grading/. Accessed 23rd June, 2016

[60] Roberts, F.L.; Kandhal, P.S.; Brown, E.R.; Lee, D.Y. and Kennedy, T.W. . *Hot Mix Asphalt Materials, Mixture Design, and Construction*. National Asphalt Pavement Association Education Foundation. Lanham, (1996)

[61] Rolling Thin Film Oven _ Pavement Interactive. http://www.pavementinteractive.org/article/rolling-thin-film-oven/. Accessed 23rd June, 2016

[62] Pressure aging Vessel _ Pavement Interactive. http://www.pavementinteractive.org/article/pressure-aging-vessel/. Accessed 24th June, 2016

[63] Dynamic Shear Rheometer _ Pavement Interactive. http://www.pavementinteractive.org/article/dynamic-shear-rheometer/. Accessed 24th June, 2016

[64] Bending Beam Rheometer _ Pavement Interactive. http://www.pavementinteractive.org/article/bending-beam-rheometer/. Accessed 25th June, 2016

[65] Stuart RE300 Rotary Evaporator. http://www.keison.co.uk/stuart_re300rotaryevaporator.shtml. Accessed 1st July, 2016

[66] ABM Asfalt- & Betontechniek B. http://www.abmbv.nl/en/catalog/articlegroup/594086/pav-pressure-aging-vessel. Accessed 5th July, 2016.

[67] Soleiman A. *Use of dynamic phase angle and complex modulus for the low temperature performance grading of asphalt cement*, M.Sc. Thesis, Department of Chemistry, Queen's University, Kingston , Canada, 2009

[68] News _ Hesp Research Group _ Asphalt Science and Engineering at Queen's University _ Kingston, Ontario, Canada. http://www.hespresearchgroup.ca/news.html. . Accessed 15th, 2016.

[69] Hesp, S. A. M., & Shurvell, H. F. (2012). Waste engine oil residue in asphalt cement. *Seventh International Conference on Maintenance and Rehabilitation of Pavements and Technological Control*. (2012)

[70] Sowah-Kuma, D. Assessment of Low Temperature Cracking in Asphalt Pavement Mixes and Rheological. M.Sc. Thesis, Department of Chemistry, Queen's University, Kingston , Canada. 2015

[71] Agbovi, H. K. Effects of Low Temperatures , Repetitive Stresses and Chemical Aging on Thermal and Fatigue Cracking in Asphalt Cement Pavements on Highway 417, 154. M.Sc. Thesis, Department of Chemistry, Queen's University, Kingston , Canada. 2012

[72] Queen, S. Quality and Durability of Rubberized Asphalt Cement and Warm Rubberized Asphalt Cement. M.Sc. Thesis, Department of Chemistry, Queen's University, Kingston , Canada. 2013

[73] Xu, H., Mcintyre, A., Adhikari, T., & Hesp, S. A. M. Quality and Durability of Warm Rubberized Asphalt Cement in Ontario Transportation Research Board, *750*(3), 26–32. 2013

[74] Ghimire, B. C. Low Temperature Testing of Ontario Hot Mix Asphalt. M.Sc. Thesis, Department of Chemistry, Queen's University, Kingston , Canada. 2015

[75] Hesp, S. A. M. (n.d.). Detection and analysis of waste engine oil (WEO) residues in asphalt cements using X-Ray Fluorescence (XRF) spectroscopy.

[76] Part 1 - Understanding the Fundamentals of Viscosity Modifiers for Automotive Engine Oils. http://pceo.com/ViscosityModifierPart1.html. Accessed August 6th, 2016.

[77] Method of Test for Determination of Performance Grade of Physically Aged Asphalt Cement Using Extended Bending Beam Rheometer (BBR) Method, Ontario Ministry of Transportation, 2016.